ANL-ZPR-491

ZPPR Progress Report: January 1989 through April 1989

Argonne National Laboratory–West, Idaho Falls, Idaho 83403-2528
Operated by The University of Chicago
for the United States Department of Energy Under Contract W-31-109-Eng-38

CONTENTS:

ANL-ZPR-491

ZPPR PROGRESS REPORT: JANUARY 1989 THROUGH APRIL 1989

edited by

P. J. Collins and S. B. Brumbach

Engineering Physics Division
Argonne National Laboratory - West
P.O. Box 2528
Idaho Falls, ID 83403-2528

April 27, 1989

TABLE OF CONTENTS

ZPPR PROGRESS REPORT: JANUARY 1989 THROUGH APRIL 1989

edited by

P. J. Collins and S. B. Brumbach

ABSTRACT

Further results are presented from the large, homogeneous assembly ZPPR-18 in the JUPITER-III program. Reaction rate results are given for ZPPR-18B along with measured gamma ray dose results from ZPPR-18A and 18B. Control rod worth results from the ZPPR-18 assemblies are included.

Calculation models, measured and calculated k-effective values and measured sodium worth values are presented for the ZPPR-19 assemblies of the Io program.

1. PROGRAM STATUS (P. J. Collins and S. B. Brumbach)

Processing of experimental data and analysis has been completed for the large conventional cores of the JUPITER-III program, ZPPR-18 and ZPPR-19. This report contains data for control rod worths in ZPPR-18, reaction rates in ZPPR-18B, gamma ray dose measurements in ZPPR-18 and sodium void reactivities in ZPPR-19B. The data remaining to be reported are reaction rates in ZPPR-18C and ZPPR-19B and control rod worths in ZPPR-19B. These will be included in the next report (ANL-ZPR-492) which is in production at this time.

Experimental data for reactivities and reaction rates in mockups of the nuclear assembly test (ZPPR-20A, 20B and 20F) and the reference flight system (ZPPR-20C) have been issued as "ZPPR-20 Data Sheets". Processing of the reactivities for the flooding experiment (ZPPR-20D) and for the sand-buried experiment (ZPPR-20E) are nearing completion.

A major concern arising from the initial analysis of ZPPR-20 is the underprediction of control rod reactivity worths. Calculations by the MCNP Monte Carlo code give worths lower than experiment by 16%. The experimental worths are directly proportional to the effective source ratio which, in the case of ZPPR-20, must be calculated. A number of transport calculations using the TWODANT code have been made to investigate errors in the source ratios calculated by diffusion theory in xyz geometry. Differences of only 1-2% are indicated for a range of cases. The rz model, with a suitable shielding factor derived for the control rod annulus gives excellent agreement with MCNP results for the rod worths.

A processing code which constructs the input data for the VIM Monte Carlo code directly from the ZPPR experimental data base is operational. The ZPPR assemblies are described in great detail including drawers, cladding of the material plates and air gaps. Initial tests indicate that a value of the source ratio will be obtained to useful accuracy from the Monte Carlo calculations.

2. MEASUREMENT AND CALCULATION OF CONTROL ROD WORTHS IN ZPPR-18A

(D. M. Smith, P. J. Collins, G. L. Grasseschi and F. Nakashima*)

2.1 Introduction

The ZPPR-18 assembly was designed to provide basic physics data for a very large, homogeneous LMR. Of particular interest were spatially sensitive parameters, including control rod worths. The ZPPR-18A configuration contained 24 control rod positions (CRPs) arranged as an inner ring of six, a middle ring of six and an outer ring of twelve. The outer bank is located at the boundary between the inner core and outer core. Because there were distinct zones of plutonium and uranium fuel in the outer core, outer ring CRPs are not all in equivalent environments.

In addition to measurements in the standard CRP locations, the worths of individual rods and pairs of rods were measured as a function of radius along the x-axis of the assembly. These latter measurements were made with respect to fuel. The control locations are given in Fig. 2.1. As shown, all CRPs are two-by-three drawers in size except for the special measurements at x-axis locations in the inner core which are three-by-three drawers in the inner core.

The measurements fall into four basic categories; those with 100% natural B_4C rods, those at various radii along the x-axis, banks and partial banks with 50% natural B_4C rods and half-inserted banks. All measurements were made in the ZPPR-18A subcritical reference (described in ANL-ZPR-485, p 2). This reference loading was rebuilt immediately prior to the control rod experiments, after the x-axis measurements and after the 50% B_4C rod bank measurements. The reactivity was established by inverse kinetics analysis of the power history following a rod drop. The experimental rod worths were measured relative to this reference reactivity by the modified-source-multiplication method using the countrates recorded on a system of

---

*On assignment from the Power Reactor and Nuclear Fuel Development Corporation.

sixty-four in-core fission chambers. All measured values presented here are from the least-squares fitting of reactivity versus detector efficiency in the McCRUNCH code. Adjustments to the calculated effective source ratio after the least squares fitting were small, usually of the order of tenths of a percent and about 1% for some multiple rod patterns.

Various control rod drawers were used. Atom densities corresponding to these control rod and CRP drawers, with axial sections labeled in inches, are given in Table 2.1.

2.2 Measurements with 100% B_4C Rods

The worth of each of the three CR banks was measured for rods containing 100% natural B_4C. Master 603 was used in rods 1 to 6, 7 to 12 and 13, 14, 17, 18, 19, 20, 23 and 24. Master 604 was used in rods 15, 16, 21 and 22. Details of the data processing are given in Table 2.2. The reference reactivity prior to the measurements (loading number 45) was -22.92¢ ± 0.18¢. The 64 detector data for this reference were recorded on data file 42.

2.3 Measurements of Worth vs Radius on the x-axis

A series of thirteen worth measurements was made for single rods and rod pairs along the x-axis. These measurements were made with respect to fuel. Later, the worths of CRPs were measured in the central location (A) and an outer location (F + f). For all locations, the 50% B_4C master 606 was used. The reference reactivity was determined at the end of this measurement sequence and was -25.81¢ ± 0.21¢ (loading number 62, 64-counter data file 59, inverse kinetics file 43). After correcting for temperature, interface gap and ^{241}Pu decay, the difference between reference reactivities in loadings 45 and 62 was 0.30¢. This difference is attributed to material movement in loading and unloading fuel drawers during the x-axis measurements. Details of the data processing are given in Table 2.3.

2.4 Worths of Banks and Partial Banks with 50% B_4C Rods

Worths were measured for twenty-seven configurations which included unique individual rods, whole banks, partial banks and combinations of banks.

The control rod drawer masters assigned to the various locations are given in Table 2.4. The reference reactivity for this measurement sequence was that described above and measured in loading 62 (+25.81¢). A reference reactivity measurement was repeated after this series of measurements and differed from the loading 62 reactivity by only 0.03¢, and continued use of the previous reference is appropriate.

Details of the data processing are given in Table 2.4.

2.5 Worths of Half-Inserted Rod Banks

Worths were also measured for a few configurations with half-inserted rods. All half-inserted rods had their B_4C in half two of the assembly. The drawers used for half-inserted rods were master 608 and contained 787 mm-long (31-inch) columns of natural B_4C in contrast to 508 mm-long (20 inch) columns in drawers used for fully inserted rods. Master 605 was used in CR 24 when CR 24 was fully inserted. The reference reactivity for this measurement is again that from loading 62 (+25.81¢). Details of the data processing are given in Table 2.5.

2.6 Reference Diffusion Calculations and Comparisons with Measurement

The basic calculations were required to provide adjoint fluxes and source-driven real fluxes for each control rod measurement in order to calculate detector efficiencies and effective source ratios for processing the experimental data. For economy, these calculations were made with diffusion theory in xy geometry with cross sections collapsed to six energy groups. The adjoint k-effectives give calculated worths for each case.

This simple calculation model gave excellent predictions of flux distributions relative to those in the reference core. This can be seen in Tables 2.4 and 2.5 where the number of detectors retained in the McCRUNCH processing was close to 60 in almost all cases. The good predictions of detector efficiencies give confidence in the calculated effective source ratios.

The calculations were made with the finite difference path of DIF3D for convenience in the editing codes (local to ZPPR usage) rather than the nodal diffusion path. A mesh spacing of 55 mm (one mesh per ZPPR matrix position) was used. Thus calculated rod worths are closer to transport results than by the nodal method due to mesh size errors.

The six group data were collapsed from an xyz model of the reference core calculated in 21 groups. This model used average compositions for each characteristic drawer master type - in the inner core (single plutonium column types DUM and DUF), in the outer core (plutonium single and double column, uranium single and double column), control positions (CRPs), and each blanket and reflector zone. A second xyz calculation with all even numbered controls rods inserted was used to collapse data for control rods. Data were collapsed individually for each rod in the ring. Thus, in the outer ring, the control rods adjacent to the plutonium section (Numbers 24 and 18) were distinct from those near the uranium section (Numbers 22 and 16). However, cross sections for the odd numbered rods used data collapsed for the even numbered rods.

Effective buckling terms for each drawer type in the reference and for control rods were generated by a method analogous to that used for group collapse. Two xyz calculations in six groups provided axial leakages at the core/axial blanket interface which were matched to group and region dependent DB^2 terms.

Benoist diffusion coefficient modifiers were collapsed from 21 groups to 6 groups using

$$\Sigma D_{ig} \Phi_g / \Sigma D_{homg} \Phi_g$$

with i = x,y,z, D_{homg} the Isotropic diffusion coefficient and summation over the 6 group subsets of the 21 groups.

Although the six group collapse was done with generic master compositions, the xy models used the individual drawer compositions in the loading as for the xyz calculation models described in ANL-ZPR-489, p. 12 et. seq.

Calculated worths are defined as $(k_1-k_2)/(k_1 k_2 \beta)$ with k_1 the k-effective for the subcritical reference, k_2 the k-effective for the case with control rods inserted and β = 0.0037855, the calculated β-effective for ZPPR-18A (ANL-ZPR-489, p. 49). The k-effective calculated for the subcritical reference xy model was 0.989333.

Five measurements were made for patterns of half-inserted control rods (Table 2.5). In the xy models these rods were represented with control rods and CRP compositions and bucklings combined with 50% volume fractions. The McCRUNCH processing was carried out in two steps. First, the processing was done with the half-one detectors and half-two detectors separately. This gave average biases of 1.023 for the reactivity predicted by the half-two detectors and 0.977 for the half-one detectors compared with the mean of all detectors. In the second stage, the efficiencies for half-two detectors were adjusted by a factor 0.977 and those for the half-one detectors by 1.023. This produced an adequate fit to the experiment countrates with over 50 detectors being retained in the data processing (Table 2.5). The calculated rod worths were overpredicted by about 5% relative to the results for the rods fully inserted due to underestimation of boron shielding with the 50% density rods in the model. Three-dimensional calculations will be needed to improve these results.

2.6.1 Control Rods Along the X-axis

A series of control rod worth measurements was made for positions along the x-axis to provide detail on the accuracy of prediction

of worths as a function of radius and to give rod interaction effects. The rods occupied 3 x 3 matrix positions in the inner core and 2 x 3 matrix positions in the outer core (Figure 2.1). The rod worths were measured relative to fuel rather than relative to CRPs as in the other measurements. A similar series of measurements was made in the smaller conventional core ZPPR-9 (ZPR-TM-356 p. 2). A comparison of the measured and calculated worths for ZPPR-18A is shown in Table 2.6 and interaction effects are given in Table 2.7.

The results of the analysis are:

(i) The rod worths are predicted most consistently with a mean C/E of 1.104 and standard deviation 0.006. No trend in C/E with radius is apparent, including rod G which is in the steep flux gradient at the edge of the outer core. The unvarying prediction is consistent with the analysis of fission rate distributions (ANL-ZPR-489) and contrasts with results in the smaller conventional cores of the Jupiter-I series.

(ii) The worths of CRPs relative to fuel are overpredicted by 20%. A large overprediction is always obtained by diffusion calculations and has been shown to be due to overprediction of axial leakage in the sodium channels. Note that in the present case the axial leakage errors are contained in the CRP buckling terms which were calculated from an xyz diffusion model.

(iii) The C/Es for control rod worths relative to fuel are higher than those relative to CRPs by about 3%. This is shown in the last two lines of Table 2.6 where experimental and calculated worths are given relative to CRPs. All other control rod worths in ZPPR-18A were made in the CRP positions of the reference loading. As will be seen, the C/E results relative to CRPs of 1.064 (CR A) and 1.0770 (CRs F + f) are consistent with other results for inner ring rods and outer ring rods near the plutonium sector.

(iv) Interaction effects are usually defined as the percent change in the combined rod worth relative to the sum of the

individual worths. These interactions are well calculated by the simple diffusion model (table 2.7). The interaction effects for ZPPR-18A in percent appear to be smaller than in ZPPR-9. For example, the interaction for the pair of outer ring control rods relative to fuel in ZPPR-9 (rods 13, 19 in ZPPR-9 numbering scheme) is 27% while that for rods E + e in ZPPR-18B is 17%. However, a better comparison is made by normalizing the interaction percent to the worth of a single rod, as is shown in the fourth column of Table 2.7. Since the rods in ZPPR-9 have about twice the worth of those in ZPPR-18A, the normalized interactions for the pair of outer ring rods are 15% $\$^{-1}$ in ZPPR-9 and 21% $\$^{-1}$ in ZPPR-18A.

2.6.2 Worths of Control Rod Banks and Constituent Rods

These data have been selected to show the analysis of the principal rod banks and of single rods, pairs of rods, and quartets of rods in the banks. The single rods were measured in each of the positions with 60° symmetry in the banks. Sets of two and four rods were measured at positions in the outer bank adjacent to the plutonium sector and adjacent to the uranium sector to provide data on the azimuthal predictions in the outer ring which could be calculated by refined methods using one-eighth core symmetry. Differences in accuracy of prediction of rods near the two sectors have an impact on the utilization of the complete rod bank worths for an all-plutonium fueled core.

Results in the following tables are given a descriptive label for ease of comprehension. The full description of the measurement can be found in Tables 2.3 to 2.5 by means of the data file numbers. Single rod positions are indicated by the angle relative to the positive x-axis. Note that the statistical uncertainties for the measurement are between 0.1% and 0.2%. This is the standard by which to compare the relative accuracies of predictions.

The analysis of rods in the individual banks is given in Table 2.8. A number of interesting conclusions result:

(i) The rod worths in the inner ring are predicted with remarkable consistency. The 100% B_4C rod bank has a C/E which is marginally higher than the standard 50/50 B_4C/Na rod.

(ii) In the middle ring, CR 11 at the y-axis has a C/E lower than that of CR 12 near the x-axis by 1.8%. This difference is attributed to underpredictions of fluxes near the uranium sector relative to prediction near the plutonium sector.

(iii) In the outer ring, rods adjacent to the uranium sector have a C/E lower by 5% to 6% than those adjacent to the plutonium section (compare results for CR 22 and CR 24, pairs of rods and quartets of rods). This difference is consistent with analysis of fission rates at the y- and x- axes (ANL-ZPR-489, p. 50). The average of the C/Es for rods 21, 23, and 24 is 1.042 and consistent with the C/Es for 12 outer ring rods (1.041) and for 6 outer ring rods (1.039). This result shows that the C/E bias for the banks (1.04) should not be applied to an all plutonium core. However, the consistent C/Es for the banks and single rods show that the bias factors could be taken from the results of measurements near the plutonium sectors.

(iv) The difference of 1.5% between C/Es for CRs 15 and 16 and for rods 15, 16, 21, and 22 is evidence of a tilt between the top and bottom of the ZPPR matrix. As shown in detail in ZPPR-13 experiments, the reactor halves are in contact at the top of the assembly and separated by about 1 mm at the bottom. Control rods 15 and 16 were positioned at the lower part of the assembly where fuel is separated and measured worths are thus lower than at the top. The difference between CRs 15 and 16 and CRs 21 and 22 was measured in ZPPR-19B.

(v) The worths of the banks of 100% B_4C rods are calculated with biases similar to those for the 50% B_4C rod banks (Table 2.8).

2.6.3 Rod Bank Combinations and Interactions

Three measurements were made of combinations of complete control rod banks. The results are given in Table 2.9. The worths of the individual rod banks from Table 2.8 are also included for comparison.

Small negative interactions are found for adjacent rod banks, -2% for IR + MR and -4% for MR + OR. A large interaction of 32% occurs between the more widely spaced inner and outer banks. In this case, the worth of inserting the inner bank when the outer bank is already inserted in the core is $11.28 which is 58% greater than the worth of the inner bank alone.

These interaction effects are adequately predicted by the simple diffusion calculations.

2.6.4 Rod Bank Combinations with Missing Rods

Measurements were made for combinations of two rod banks with a rod missing from each bank in turn. The missing rod in each case was one nearest to the plutonium sectors. These results are given in Table 2.10. The results for the complete rod banks (Table 2.9) are also included for comparison. The C/E values for each of the three sets are consistent within 0.4% but these results are not a sensitive test of calculation.

By subtracting these results one can deduce the worth of the missing control rods. This is important in evaluation of rod run-out or stuck rod effects. This analysis is given in Table 2.11. Comparisons are made with the single rod worth and the worth of the rod within its bank. Note that the statistical uncertainties, which are shown in the table, may be relatively large due to subtraction of two worths of similar magnitude.

The worths of single rods vary considerably due to interaction effects between rods in a ring and interaction effects between rod banks. The worth of a rod in the inner ring is reduced in comparison

with the isolated rod due to a negative interaction between rods in the ring and further reduced if the middle ring is also inserted. However, the worth is increased by 60% when the outer bank rods are inserted.

A strong positive interaction exists in the middle ring because of the wide separation of the rods and the single rod worth is enhanced by 77%. The worth is further enhanced to about a factor of 2 greater when the inner ring bank is present but the increase in worth is only 46% when the neighboring outer bank is inserted. Interaction effects in the outer ring gave an increase in the single rod worth of 12% but insertion of the inner ring enhances the single rod worth by 180%.

These effects are quite well calculated as can be seen by comparing the relative C/E results for each rod group.

2.6.5 Half Inserted Rods

The present calculations are aimed at data reduction and do not provide good comparisons with experiment. Improvements would require three-dimensional calculations or derivation of appropriate rod shielding factors and buckling terms for use in the xy model. For completeness, however, the results for these cases are recorded in Table 2.12.

The consistency among the C/E results in Table 2.12 is quite remarkable, although the sample model results in biases which are 6-9% higher than those for the fully inserted rods.

The worth of control rod 24 is 0.784$ with 6 inner ring and 11 outer ring rods half inserted (Table 2.5, Files 93 and 94). This compares with the worth of 1.479$ with the same rods fully inserted and the worth of 0.514$ when inserted alone (Table 2.11).

2.6.6 Three-dimensional Diffusion and Transport Calculations

A series of three-dimensional calculations with 21 group cross sections was made for selected cases exhibiting one-eighth core

symmetry in order to provide refined results for comparison with data in other cores. The cases chosen were the three complete rod banks, both with 100% B_4C rods and with the 50/50 B_4C/Na reference rods, plus the two groups of four rods adjacent to the plutonium sector and adjacent to the uranium sector. The latter cases were of particular interest because of the different accuracies of prediction found for rods near the two sectors. These differences clearly have an impact on the use of the outer rod bank with analysis for extrapolation to an all plutonium fueled core. Most effective use of the data may require a full sensitivity analyses.

Three dimension diffusion calculations were made using the nodal diffusion and nodal transport solutions. The xy mesh in the nodal solutions was constrained by the ZPPR geometry to 55 mm but coarse node spacings of 100-150 mm were used in the z dimension. The k-effective values are recorded in Table 2.13 and Table 2.14 compares the C/E results for the two methods.

Transport corrections, relative to the nodal diffusion, are close to -3% for the inner and middle ring rods and -1.5% for the outer ring rod bank. Different transport corrections are calculated for the outer ring rods adjacent to the plutonium sector (-0.8%) and for the rods adjacent to the uranium sector (-2.5%). The simple xy calculations give results within about 2% of those from the xyz transport values. This result is typical of the compensation of course mesh and transport errors found in conventional cores, but effects of group collapse and axial buckling approximations have not been explored for ZPPR-18.

The xyz calculations show about 2% higher C/E values for the 100% B_4C rods than for the reference B_4C/Na rods. This is attributed to heterogeneity effects in the B_4C/Na rods which has not been treated in the calculations.

The xyz calculation confirms the lower C/E for rods adjacent to the uranium sector than adjacent to the plutonium sector (5% lower by diffusion, 6% lower by transport). This difference clearly affects the C/E for the outer ring bank and possibly the middle ring bank. This

result appears to be consistent with the analysis of foil reaction rate data. The bias factor developed for an all-plutonium loaded core would need to take account of this effect.

TABLE 2.1 Atom Densities for the Control Rods in ZPPR-18
(atoms/barn-cm)

Isotopes	Control Position Master 601 0-20	Control Position Master 601 20-31	Control Position Master 601 31-36	Control Position Master 602 0-20	Control Position Master 602 20-31	Control Position Master 602 31-36
B0	0.0	0.0	0.0	0.0	0.0	0.0
B1	0.0	0.0	0.0	0.0	0.0	0.0
C	0.0000308	0.0000309	0.0000447	0.0000307	0.0000309	0.0000447
O	0.0000013	0.0000013	0.0000013	0.0000013	0.0000013	0.0000013
Na	0.0182904	0.0184405	0.0179925	0.0182904	0.0184405	0.0179925
Si	0.0001649	0.0001649	0.0001705	0.0001645	0.0001649	0.0001705
Al	0.0000047	0.0000049	0.0000048	0.0000047	0.0000049	0.0000048
Mn	0.0002433	0.0002443	0.0002511	0.0002430	0.0002443	0.0002511
Cr	0.0029568	0.0029657	0.0030388	0.0029514	0.0029657	0.0030388
Fe	0.0104374	0.0104697	0.0110018	0.0104182	0.0104697	0.0110018
Ni	0.0013247	0.0013281	0.0013586	0.0013223	0.0013281	0.0013586
Cu	0.0000354	0.0000353	0.0000370	0.0000353	0.0000353	0.0000370
Mo	0.0000174	0.0000174	0.0000183	0.0000173	0.0000174	0.0000183
P	0.0000040	0.0000040	0.0000042	0.0000040	0.0000040	0.0000042
S	0.0000012	0.0000012	0.0000013	0.0000012	0.0000012	0.0000013
Cl	0.0000006	0.0000006	0.0000006	0.0000006	0.0000006	0.0000006
Ca	0.0000042	0.0000042	0.0000041	0.0000042	0.0000042	0.0000041
Co	0.0000038	0.0000037	0.0000043	0.0000038	0.0000037	0.0000043

TABLE 2.1 (Contd)

Isotopes	Control Rod Master 603 0-20	Control Rod Master 603 20-31	Control Rod Master 603 31-36	Control Rod Master 604 0-20	Control Rod Master 604 20-31	Control Rod Master 604 31-36
B0	0.0153857	0.0	0.0	0.0152058	0.0	0.0
B1	0.0623918	0.0	0.0	0.0616654	0.0	0.0
C	0.0199484	0.0000309	0.0000447	0.0098260	0.0000309	0.0000447
O	0.0000781	0.0000013	0.0000013	0.0000651	0.0000013	0.0000013
Na	0.0	0.0181363	0.0179925	0.0	0.0181363	0.0179925
Si	0.0002321	0.0001651	0.0001705	0.0001961	0.0001651	0.0001705
Al	0.0000026	0.0000043	0.0000048	0.0000012	0.0000043	0.0000048
Mn	0.0002144	0.0002432	0.0002512	0.0001950	0.0002432	0.0002512
Cr	0.0025322	0.0029562	0.0030388	0.0022743	0.0029562	0.0030388
Fe	0.0090962	0.0104363	0.0110018	0.0082314	0.0104363	0.0110018
Ni	0.0011231	0.0013233	0.0013586	0.0009914	0.0013233	0.0013586
Cu	0.0000322	0.0000357	0.0000370	0.0000309	0.0000357	0.0000370
Mo	0.0000161	0.0000174	0.0000183	0.0000155	0.0000174	0.0000183
P	0.0000040	0.0000040	0.0000042	0.0000040	0.0000040	0.0000042
S	0.0000012	0.0000012	0.0000013	0.0000012	0.0000012	0.0000013
Cl	0.0	0.0000006	0.0000006	0.0	0.0000006	0.0000006
Ca	0.0	0.0000042	0.0000041	0.0	0.0000042	0.0000041
Co	0.0000038	0.0000037	0.0000043	0.0000038	0.0000037	0.0000043

TABLE 2.1 (Contd)

Isotopes	Control Rod Master 605 0-20	Control Rod Master 605 20-31	Control Rod Master 605 31-36	Control Rod Master 606 0-20	Control Rod Master 606 20-31	Control Rod Master 606 31-36
B0	0.0071583	0.0	0.0	0.0085434	0.0	0.0
B1	0.0290256	0.0	0.0	0.0346512	0.0	0.0
C	0.0094051	0.0000309	0.0000447	0.0110453	0.0000309	0.0000447
O	0.0000006	0.0000013	0.0000013	0.0000787	0.0000013	0.0000013
Na	0.0087470	0.0181363	0.0179925	0.0087470	0.0181363	0.0179925
Si	0.0002035	0.0001651	0.0001705	0.0001999	0.0001651	0.0001705
Al	0.0000054	0.0000043	0.0000048	0.0000033	0.0000043	0.0000048
Mn	0.0002605	0.0002432	0.0002512	0.0002198	0.0002432	0.0002512
Cr	0.0031765	0.0029562	0.0030388	0.0026312	0.0029562	0.0030388
Fe	0.0112393	0.0104363	0.0110018	0.0094141	0.0104363	0.0110018
Ni	0.0014421	0.0013233	0.0013586	0.0011628	0.0013233	0.0013586
Cu	0.0000361	0.0000357	0.0000370	0.0000336	0.0000357	0.0000370
Mo	0.0000178	0.0000174	0.0000183	0.0000167	0.0000174	0.0000183
P	0.0000040	0.0000040	0.0000042	0.0000040	0.0000040	0.0000042
S	0.0000012	0.0000012	0.0000013	0.0000012	0.0000012	0.0000013
Cl	0.0000003	0.0000006	0.0000006	0.0000003	0.0000006	0.0000006
Ca	0.0000020	0.0000042	0.0000041	0.0000020	0.0000042	0.0000041
Co	0.0000038	0.0000037	0.0000043	0.0000038	0.0000037	0.0000043

TABLE 2.1 (Contd)

Isotopes	Control Rod Master 607 0-20	Control Rod Master 607 20-31	Control Rod Master 607 31-36	Control Rod Master 608 0-20	Control Rod Master 608 20-31	Control Rod Master 608 31-36
B0	0.0071436	0.0	0.0	0.0071583	0.0072759	0.0
B1	0.0289671	0.0	0.0	0.0290256	0.0295024	0.0
C	0.0093870	0.0000309	0.0000447	0.0094051	0.0095480	0.0000479
O	0.0000006	0.0000013	0.0000013	0.0000006	0.0000068	0.0000013
Na	0.0087470	0.0181363	0.0179925	0.0087470	0.0087131	0.0175023
Si	0.0002043	0.0001651	0.0001705	0.0002035	0.0002034	0.0001905
Al	0.0000051	0.0000043	0.0000048	0.0000054	0.0000048	0.0000060
Mn	0.0002613	0.0002432	0.0002512	0.0002605	0.0002578	0.0002692
Cr	0.0031882	0.0029562	0.0030388	0.0031765	0.0031389	0.0032725
Fe	0.0112792	0.0104363	0.0110018	0.0112393	0.0111169	0.0118247
Ni	0.0014482	0.0013233	0.0013586	0.0014421	0.0014216	0.0014830
Cu	0.0000361	0.0000357	0.0000370	0.0000361	0.0000359	0.0000384
Mo	0.0000178	0.0000174	0.0000183	0.0000178	0.0000177	0.0000189
P	0.0000040	0.0000040	0.0000042	0.0000040	0.0000040	0.0000050
S	0.0000012	0.0000012	0.0000013	0.0000012	0.0000012	0.0000013
Cl	0.0000003	0.0000006	0.0000006	0.0000003	0.0000003	0.0000006
Ca	0.0000020	0.0000042	0.0000041	0.0000020	0.0000020	0.0000040
Co	0.0000038	0.0000037	0.0000043	0.0000038	0.0000037	0.0000051

TABLE 2.2 Data Processing for ZPPR-18A 100% Natural B_4C Control Rod Measurements

Control Rods	Reactor Loading Number	Data File Number	Number of FCs	X^2	Source Ratio	Measured Worth, $	Statistical Uncertainty, %	Total Uncertainty, %
1-6	46	43	61	1.279	1.0036	8.444	0.152	0.869
7-12	47	44	60	1.340	0.9851	7.997	0.136	0.868
13-24	48	45	61	1.472	0.8521	7.408	0.146	1.029

TABLE 2.3 Data Processing for Control Rods on the X-Axis in ZPPR-18A

Control Rods	Reactor Loading Number	Data File Number	Number of FCs	χ^2	Source Ratio	Measured Worth, $	Statistical Uncertainty, %	Total Uncertainty, %
A	49	46	64	1.438	1.0153	2.224	0.111	0.873
B	50	47	63	1.295	0.9994	1.985	0.0973	0.873
B+b	51	48	63	1.469	1.0128	3.982	0.108	0.866
C	52	49	64	1.418	0.9732	1.575	0.0958	0.876
C+c	53	50	64	1.445	0.9945	3.805	0.133	0.871
D	54	51	64	1.190	0.9614	1.198	0.0968	0.882
D+d	55	52	63	1.054	0.9601	2.951	0.0999	0.869
E	56	53	63	1.133	0.9645	0.809	0.0809	0.894
E+e	57	54	63	1.470	0.9471	1.892	0.104	0.874
F	58	55	64	1.112	0.9761	0.532	0.101	0.919
F+f	59	56	64	1.470	0.9578	1.178	0.0930	0.885
G	60	57	64	0.865	0.9872	0.282	0.113	0.990
G+g	61	58	64	1.277	0.9744	0.591	0.108	0.916
CRP A	91	88	64	1.436	1.0019	0.496	0.118	0.928
CRP F+f	92	89	64	1.034	0.9877	0.359	0.139	0.957

TABLE 2.4 Data Processing for ZPPR-18A 50% Natural B_4C Control Rod Bank Measurements

Control Rod Pattern	Drawer Master	Reactor Loading Number	Data File Number	Number of FCs	χ^2	Source Ratio	Measured Worth, $	Statistical Uncertainty, %	Total Uncertainty, %
6	606	63	60	64	1.094	1.0000	1.286	0.0937	0.881
5	606	64	61	63	1.299	1.0024	1.204	0.0880	0.882
12	606	65	62	63	1.334	0.9840	0.842	0.0875	0.894
11	606	66	63	63	1.169	0.9924	0.737	0.0927	0.900
21	606	67	64	64	1.362	0.9944	0.407	0.116	0.945
23	606	68	65	64	1.306	0.9881	0.470	0.113	0.932
24	606	69	66	63	1.235	0.9814	0.514	0.123	0.925
14,18,20,24	605								
16,22	607	70	67	63	0.974	0.9533	3.050	0.0825	0.872
13,14,17,18,19,20,23,24	605								
15,16,21,22	604	71	68	61	1.475	0.9013	5.745	0.117	0.916
13,14,17,18,19,20,23	605								
15,16,21,22	607	72	69	61	1.287	0.9140	5.176	0.113	0.892
13,14,17,18,19,23	605								
15,16,21,22	607	73	70	57	1.359	0.8970	10.979	0.155	0.923
and 7-12	606								
13,14,17,18,19,20,23,24	605								
15,16,21,22	607	74	71	59	1.464	0.8766	10.221	0.200	0.977
and 7-11	606								
13,14,17,18,19,23,24	605								
15,16,21,22	607	75	72	59	1.361	0.8790	11.458	0.141	0.960
and 7-12	606								
13,14,17,18,19,20,23,24	605								
15,16,21,22	607	76	73	58	1.514	0.9837	14.996	0.179	0.874
and 1-5	606								

TABLE 2.4 (contd)

Control Rod Pattern	Drawer Master	Reactor Loading Number	Data File Number	Number of FCs	χ^2	Source Ratio	Measured Worth, $	Statistical Uncertainty, %	Total Uncertainty, %
13,14,17,18,19,20,23,24 15,16,21,22 and 1-6	605 607 606	77	74	57	1.472	1.0048	17.026	0.188	0.875
13,14,17,18,19,20,23 15,16,21,22 and 1-6	605 607 606	78	75	59	1.468	0.9919	15.547	0.151	0.868
1-6	606	79	76	61	1.179	1.0174	7.119	0.135	0.867
1-5	606	80	77	62	1.288	1.0113	5.958	0.130	0.867
1-5 and 7-12	606 605	81	78	59	1.486	1.0093	11.980	0.163	0.870
1-6 and 7-11	606 605	82	79	61	1.494	0.9827	11.472	0.155	0.870
1-6 and 7-12	606 605	83	80	59	1.523	1.0113	13.114	0.181	0.873
7-11	606	84	81	63	1.122	0.9735	4.772	0.100	0.866
7-12	606	85	82	62	1.308	0.9909	6.264	0.120	0.866
13,24	606	86	83	63	1.274	0.9571	0.910	0.127	0.897
13,18,19,24	606	87	84	63	1.316	0.9344	2.180	0.103	0.878
15,16	606	88	85	63	1.216	0.9845	0.705	0.108	0.906
15,16,21,22	606	89	86	63	0.839	0.9826	1.593	0.0834	0.877

TABLE 2.5 Data Processing for Half Inserted 50% B_4C Control Rods in ZPPR-18A

Control Rods	Reactor Loading Number	Data File Number	Number of FCs	χ^2	Source Ratio	Measured Worth, $	Statistical Uncertainty, %	Total Uncertainty, %
1-6	94	91	59	1.354	1.0217	3.912	0.163	0.877
1-6 and 13-22,24	95	92	57	1.388	1.0023	7.874	0.188	0.877
1-6 and 13-23	96	93	57	1.508	1.0042	7.793	0.162	0.872
1-6 and 13-23 and 24 Full In	97	94	56	1.481	0.9981	8.577	0.155	0.870
1-6 and 13-24	98	95	54	1.501	1.0032	8.278	0.158	0.871

TABLE 2.6 Worths of Control Rods on the X-axis

Data File	Control Rods	Measured Worth, $	Calculated Worth, $	C/E
46	A	2.224	2.444	1.099
47	B	1.985	2.183	1.100
48	B+b	3.982	4.382	1.101
49	C	1.575	1.742	1.106
50	C+c	3.805	4.208	1.106
51	D	1.198	1.317	1.099
52	D+d	2.951	3.277	1.110
53	E	0.809	0.896	1.108
54	E+e	1.892	2.116	1.118
55	F	0.532	0.585	1.100
56	F+f	1.178	1.301	1.104
57	G	0.282	0.309	1.096
58	G+g	0.591	0.654	1.107
88	CRP A	0.496	0.606	1.222
89	CRP F+f	0.359	0.425	1.184
Relative to CRPs				
46, 48	A	1.728	1.838	1.064
56, 89	F+f	0.819	0.876	1.070

TABLE 2.7 Interaction Effects for Control Rods Along the X-Axis

Control Rods	Separation cm	Interaction %	Normalized Interaction % $^{-1}$[a]	Calculated Interaction %
B,b	66.3	0.30	0.15	0.37
C,c	132.6	20.8	13.2	20.8
D,d	187.8	23.2	19.3	24.4
E,e	243.1	16.9	20.9	18.1
F,f	270.7	10.7	20.1	11.2
G,g	303.8	4.8	17.0	5.8

[a]Interaction % divided by the worth of a single rod.

TABLE 2.8 Worths of Control Rods in the Three Banks

Data File	Control Rods	Measured Worth, $	Calculated Worth, $	C/E
	Inner Ring (IR)			
60	CR6 (30°)	1.286	1.372	1.067
61	CR5 (90°, y-axis)	1.204	1.282	1.065
77	5 IR (CR6 out)	5.958	6.345	1.065
76	6 IR	7.119	7.580	1.065
43	6 IR 100% B_4C Rods	8.444	9.027	1.069
	Middle Ring (MR)			
62	CR12 (30°)	0.842	0.897	1.065
63	CR11 (90°, y-axis)	0.737	0.772	1.047
81	5 MR (CR12 out)	4.772	5.013	1.051
82	6 MR	6.264	6.551	1.046
44	6 MR 100% B_4C Rods	7.997	8.382	1.048
	Outer Ring (OR)			
66	CR24 (15°)	0.514	0.552	1.074
65	CR23 (45°)	0.470	0.487	1.036
64	CR21 (105°)	0.407	0.414	1.017
69	11 OR (CR24 out)	5.176	5.377	1.039
70	12 OR	5.745	5.988	1.042
67	6 OR (even numbered)	3.050	3.169	1.039
45	12 OR 100% B_4C Rods	7.408	7.822	1.056
83	2 OR Near Pu Sector (CRs 13, 24)	0.910	0.982	1.079
84	4 OR Near Pu Sector (CRs 13, 18, 19, 24)	2.180	2.352	1.079
85	2 OR Near U Sector (CRs 15, 16)	0.705	0.731	1.037
86	4 OR Near U Sector (CRs 15, 16, 21, 22)	1.593	1.628	1.022

TABLE 2.9 Worths of Rod Bank Combinations and Interaction Effects

File	Control Rods	Measured Worth, $	Calculated Worth, $	C/E
80	6 IR + 6 MR	13.114	13.814	1.053
76	6 IR	7.119	7.580	1.065
82	6 MR	6.264	6.551	1.046
	Sum 6 IR, 6MR	13.383	14.131	1.056
	Interaction	-2.0%	-2.2%	
74	6 IR + 12 OR	17.026	17.574	1.032
76	6 IR	7.119	7.580	1.065
70	12 OR	5.745	5.988	1.042
	Sum 6 IR, 12 OR	12.864	13.568	1.055
	Interaction	+32%	+30%	
72	6 MR + 12 OR	11.458	12.030	1.050
82	6 MR	6.264	6.551	1.046
70	12 OR	5.745	5.988	1.042
	Sum 6 MR, 12 OR	12.009	12.539	1.044
	Interaction	-4.6%	-4.1%	

TABLE 2.10 Worths of Rod Bank Combinations with Missing Rods

File	Control Rods	Measured Worth, $	Calculated Worth, $	C/E
78	5 IR + 6 MR	11.980	12.587	1.051
79	6 IR + 5 MR	11.472	12.100	1.055
80	6 IR + 6 MR	13.114	13.814	1.053
73	5 IR + 12 OR	14.996	15.501	1.034
75	6 IR + 11 OR	15.547	16.095	1.035
74	6 IR + 12 OR	17.026	17.574	1.032
71	5 MR + 12 OR	10.221	10.742	1.051
70	6 MR + 11 OR	10.979	11.460	1.044
72	6 MR + 12 OR	11.458	12.030	1.050

TABLE 2.11 Variations in the Worth of a Single Control Rod

Control Rod	Rods in Core	Measured Worth, $	Statistical Uncertainty, %	Calculated Worth, $	C/E
CR6 (Inner Ring)	None	1.286	0.1	1.372	1.067
	5 IR	1.161	1.1	1.235	1.064
	5 IR + 6 MR	1.134	2.7	1.227	1.082
	5 IR + 12 OR	2.030	2.1	2.073	1.021
CR12 (Middle Ring)	None	0.842	0.1	0.897	1.065
	5 MR	1.492	0.6	1.538	1.031
	6 IR + 5 MR	1.642	1.8	1.714	1.044
	5 MR + 12 OR	1.237	2.1	1.288	1.041
CR24 (Outer Ring)	None	0.514	0.1	0.552	1.074
	11 OR	0.569	1.6	0.611	1.074
	6 IR + 11 OR	1.479	2.7	1.479	1.000
	6 MR + 11 OR	0.479	4.9	0.570	1.190

TABLE 2.12 Worths of Half-Inserted Control Rods

Data File	Control Rods	Measured Worth, $	Calculated Worth, $	C/E
91	6 IR	3.912	4.395	1.123
95	6 IR + 12 OR	8.278	9.304	1.124
92	6 IR + 11 OR (CR23 out)	7.874	8.834	1.122
93	6 IR + 11 OR (CR24 out)	7.793	8.748	1.123
94	6 IR + 11 OR + CR24 full in	8.577	9.595	1.119

TABLE 2.13 Three-dimensional Calculations of Rod Worths in ZPPR-18A

Control Rods	Nodal Diffusion keff	Nodal Diffusion Worth $	Nodal Transport keff	Nodal Transport Worth $	Transport Correction, %
Subcritical Reference	0.989782	-	0.991872	-	
6 IR 100% B_4C	0.956750	9.213	0.959626	8.948	-2.9
6 MR 100% B_4C	0.958681	8.657	0.961517	8.407	-2.9
12 OR 100% B_4C	0.961627	7.813	0.964024	7.693	-1.5
6 IR	0.962207	7.648	0.964952	7.429	-2.9
6 MR	0.965714	6.651	0.968345	6.470	-2.7
12 OR	0.968157	5.961	0.970465	5.874	-1.5
4 OR Pu Sector	0.981229	2.326	0.983354	2.307	-0.8
4 OR U Sector	0.983795	1.624	0.986010	1.583	-2.5

TABLE 2.14 Diffusion and Transport Results for Rod Worths in ZPPR-18A

Control Rods	Measured Worth, $	Nodal Diffusion C/E	Nodal Transport C/E
6 IR 100% B_4C	8.444	1.091	1.060
6 MR 100% B_4C	7.997	1.083	1.051
12 OR 100% B_4C	7.408	1.055	1.038
6 IR	7.119	1.074	1.044
6 MR	6.264	1.062	1.033
12 OR	5.745	1.038	1.022
4 OR Pu Sector	2.180	1.067	1.058
4 OR U Sector	1.593	1.019	0.994

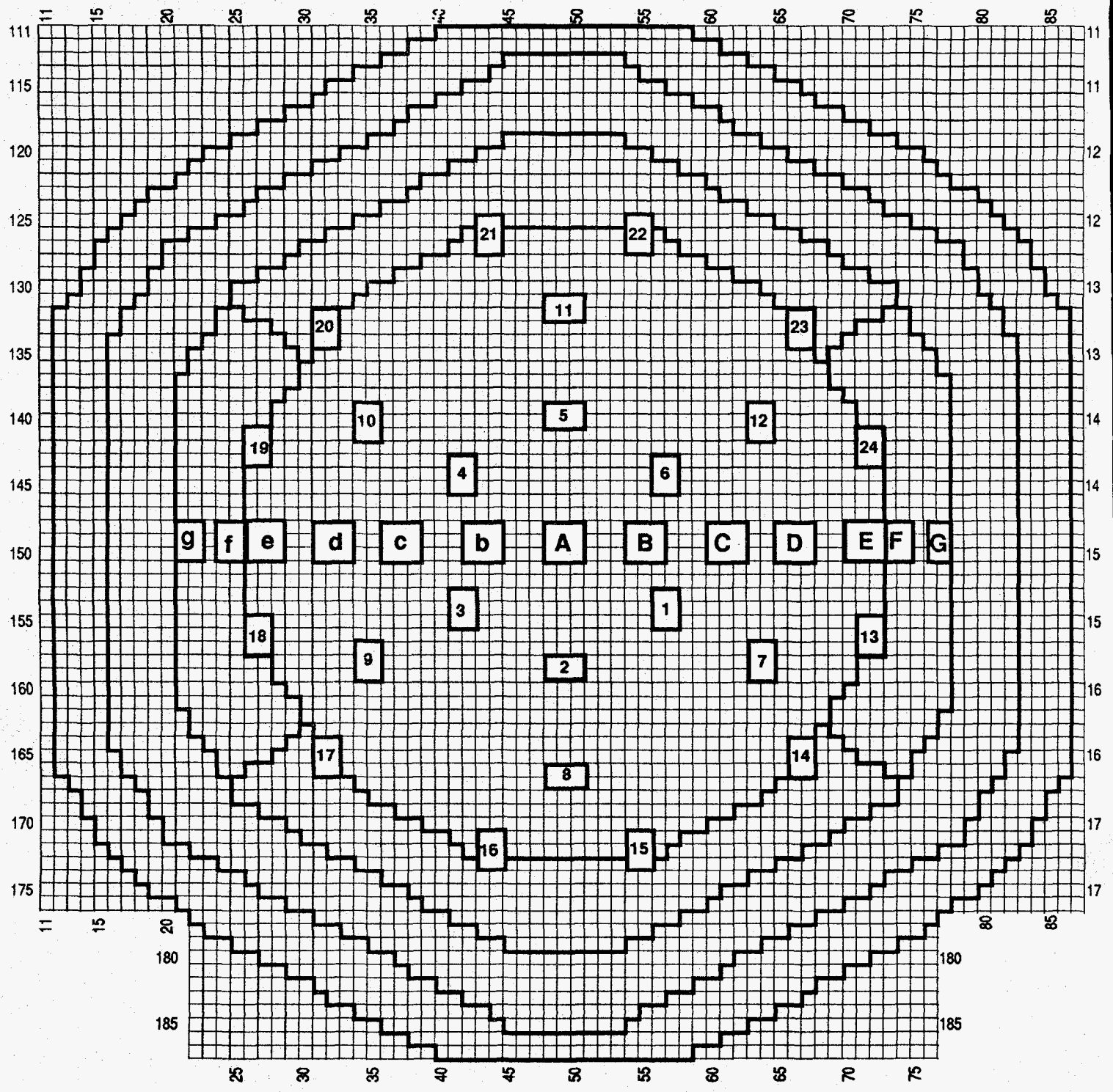

Figure 2.1 Control Rod Locations in ZPPR-18

3. THE CONTROL ROD WORTH MEASUREMENT IN ZPPR-18B

(F. Nakashima* and P. J. Collins)

ZPPR-18B was critical with the inner bank of six control rods and the outer bank of twelve rods half inserted. The raison d'être of 18B was to measure reaction rate distributions (Section 4) but the opportunity was taken to measure the worth of inserting the middle bank of control rods. This measurement provides a test of calculating the shutdown reactivity of the secondary control bank with the primary rods near the beginning-of-cycle position.

The reference for the measurement was the ZPPR-18B subcritical loading described in ANL-ZPR-485, p. 15. The control rod measurement was made on December 4, 1987 in reactor run 95, loading 106. Fission chamber countrates and other operational data were recorded on ZPPR-18 64 detector file 104. The reactivity of the subcritical reference was -32.5¢ (1σ = 0.28¢) and countrate data were recorded on file 102.

The middle bank control rods were constructed with drawer master 606 and compositions are given in Section 2, Table 1 of this report.

The calculation of detector efficiencies and source ratio used a 6 group xy diffusion model for ZPPR-18B. The control positions with half-inserted rods in the reference core used a mixture of control rod and CRP compositions and bucklings, with the buckling terms taken from the ZPPR-18A control rod calculation. The calculation for the reference core was adjusted to 0.990600 (close to the k-effective for ZPPR-18A with this model) by using a mixture of 34% control rod and 66% CRP in the inner and outer bank positions. Then, inserting the middle ring rods (at full density) gave a k-effective of 0.966521 and a calculated worth of 6.604$ using a β-effective of 0.3801%.

*On assignment from the Power Reactor and Nuclear Fuel Development Corporation.

The data processing for this measurement is shown in Table 3.1. Results for all four methods used in the McCRUNCH code are compared: (i) using all 64 fission chambers, (ii) rejecting detectors which predict reactivities greater than 3.6 standard deviation from the mean, (iii) least squares fit of reactivity versus efficiency, and (iv) least squares fit with adjustment to the calculated source ratio. The fit to the experimental countrates is excellent with no more than four detectors being rejected. This gives confidence in the simple calculation model used and in the source ratio. The preferred reactivity worth is taken from the last case, i.e., 6.181$ which has an acceptable value of chi-square and yields a total uncertainty of 0.92%.

The ratio of calculation to experiment using the xy diffusion model is 1.068 which compares with 1.046 for the worth of the middle bank in ZPPR-18A.

TABLE 3.1 Data Processing for the Measurement of the Worth of the Middle Bank of Control Rods in ZPPR-18B

	Mean using all Detectors	Mean with Rejection >3.6σ	Least Squares Fit (LSFIT)	LSFIT with Adjusted Source Ratio
Number of Detectors	64	60	63	63
Reduced chi-square	5.95	1.78	1.28	1.28
Source Ratio	0.9977	0.9977	0.9977	0.9974
Worth, $	6.175	6.157	6.183	6.181
Statistical Uncertainty, 1σ,%	0.20	0.17	0.10	0.10
Correlated Uncertainty, 1σ,%	0.92	0.92	0.92	0.92
Total Uncertainty 1σ,%	0.94	0.93	0.92	0.92

4. MEASUREMENTS AND ANALYSIS OF REACTION RATES IN ZPPR-18B (P. J. Collins, J. M. Gasidlo, D. W. Maddison, and G. L. Grasseschi)

4.1 Introduction

ZPPR-18B was a simulation of a large conventional LMR design with the primary rod banks - 6 inner ring and 12 outer ring - half inserted. Reaction rate distributions were measured in detail in order to compare the accuracy of predictions with those for ZPPR-18A in which no control rods were inserted.

The reactor zones in ZPPR-18B were identical to those in ZPPR-18A. The reactivity of the inserted control rods was compensated by increasing enrichments in the inner and outer core regions. Enrichment changes were approximately uniform within each zone but an additional increase in enrichment was made in the uranium-fuel zones in the outer core in order to improve the power distributions. A detailed description of ZPPR-18B is given in ANL-ZPR-485 p. 15.

This report contains the experimental "cell-averaged" reaction rate data, together with the analysis using ENDF/B-V.2 cross sections and an xyz nodal transport calculation consistent with that used for ZPPR-18A. The basic foil data and the cell-average/foil adjustment factors will be given in a subsequent section.

4.2 Description of the Measurements

Measurements in ZPPR-18B were made in both halves of the core in order to follow the effects of the half-inserted control rods on the fission rates. Two irradiations were necessary to handle the large number of foils. In addition, the in-cell measurements, using multiple foils in selected cells, were made in ZPPR-18B to provide data for deriving the experimental cell-average/foil factors.

The first irradiation was made in loading 112, reactor run 102, on December 10, 1987. Eight ZPPR operating control rods, in matrix 135-67 and

symmetric positions, were inserted to a depth of 42.8 cm from the midplane and had an average worth of 6.08¢ during the irradiation. The second irradiation was made in loading 115, Run 105 on December 15, 1987 and the shim rods were inserted 43.2 cm from the midplane with a worth of 5.83¢.

A set of ten ^{235}U foils were irradiated in the same locations in each irradiation. The average ratio of the corresponding countrates was 1.0008 with a standard deviation of the distribution of 0.0020. The detailed comparison will be given with the basic data report. This agreement enabled the data from the two irradiations to be combined into one set without further adjustment.

Statistical uncertainties in the measured reaction rates were essentially the same as for ZPPR-18A - around 0.7% for the three non-threshold reactions in the core regions and 1.5% to 2.5% for fission in ^{238}U. Foil techniques are described in ANL-82-38 and calibrations were consistent with these used throughout ZPPR-17 and ZPPR-18 as described in ANL-87-5.

Reaction rate distributions were measured in the same positions as in ZPPR-18A, but extended to both halves of the reactor:

(i) Radial distributions along the x-axis at + 5 cm, - 5 cm, + 28 cm, and - 28 cm from the midplane.

(ii) A radial distribution along the y-axis for ^{235}U fission only.

(iii) Radial distributions at 15° to the x-axis, passing through an outer ring CRP (half-1) and outer ring control rod (half-2) at ± 5 cm and ± 28 cm.

(iv) Radial distributions at 30° to the x-axis, passing through an inner-ring control rod and a middle-ring CRP. These measurements were made in half-2 only at Z = -5 cm and -28 cm.

(v) Axial distributions at the core center (matrix 1,249-49), in the inner core (matrix 1,249-64), in the outer core (matrix 1,249-75) and adjacent to an inner bank CRP/control rod (matrix 1,246-57).

A total of 895 reaction rate values were measured. The number of plutonium foils was limited. As for ZPPR-18A, these were used for full radial traverses along the x-axis, at 15° to the x-axis and in an axial traverse at the core center. However, in ZPPR-18B the plutonium foils were used only in half-2 for radial distributions (control rod half) and were made in both halves for the axial distribution at the core center. In general, ^{235}U fission was measured in corresponding locations in both halves but, apart from the axial distributions, ^{238}U capture and fission were measured only in half-2. Thus, the detailed mapping of the core fission distributions is available only for ^{235}U fission.

The foil locations in the xy plane are shown in ANL-ZPR-489, p. 57 for ZPPR-18A. The foil types shown in the figure correspond to those in half-2 of ZPPR-18B as noted above.

4.3 Calculation Methods

Calculations were made with the cross sections processed for ZPPR-18A using the "buckling-recycle" method (ANL-ZPR-489, p. 12). The data were not reprocessed for ZPPR-18B. The calculations used 21 group cross sections in an xyz model with the nodal transport path of DIF3D and included anisotropic transport cross sections. The model required a full-z representation and, because of storage limitations on the IBM computer at the time, it was necessary to use the cubic polynomial approximation rather than the quartic polynomials which are normally used. (A subsequent run using the CRAY computer gave an increase in k-effective of 0.035% using the quartic approximation rather than the cubic). The calculation model is given in ANL-ZPR-489, p. 26.

The shim rods were inserted in the model to a depth of 43.3 cm from the midplane and used special boron carbide cross sections appropriate

to homogenizing the shim blades over the matrix area. The k-effectives were 0.994140 with shim rods inserted and 0.994524 with shim rods withdrawn (cubic polynomial approximation), giving a reactivity of 10.2¢. This compares rather poorly with the measured worth of 6¢ (Section 2). The error is supposed to be due to the experimental control rods in half-2 being immediately adjacent to the shim rods so that the data homogenized over the matrix area is a poor representation of the actual shim blade location. However, since the experimental rods have a much larger worth than the partly inserted shim blades (about 1$ for 4 half-inserted outer ring rods) it is assumed that mispredictions of the shim rod worth have a negligible effect on the calculated reaction rate distributions.

Calculated reaction rates were interpolated to the foil positions of the measurements using a quadratic fit to the node-average values.

4.4 Experimental Reaction Rates and Comparison with Calculation

The reaction rate results are given in Tables 4.1 to 4.14. The data are organized into distributions along the axes, at 15° and 30° to the x-axis and into axial distributions. As for ZPPR-18A (ANL-ZPR-489, p. 50 et seq.), reactor zones are indicated by IC, OC, RB, AB in an obvious notation and the single column drawer types are distinguished by SF (drawers with Fe_2O_3 adjacent to fuel) and by SM (depleted uranium metal adjacent to fuel).

Experimental reaction rates are given in units of 10^{-18} reactions per atom per second at a reactor power of approximately 1 watt. In the analysis, calculations are normalized to give a mean C/E of unity for the 78 measurements of fission in ^{239}Pu which were made along the x-axis and at 15° to the axis at z = -5 cm and for an axial distribution at the core center.

Predictions of reaction rate distributions are similar to those in ZPPR-18A, except for positions in the vicinity of inserted control rods:

(i) Radial distributions along the x-axis and at 15° and 30° are well predicted. In the inner core, the C/E values are

constant within the uncertainties. The non-threshold reaction rates in the outer core have, on average, a lower C/E by 0.5% to 1% than in the inner core. Measured results for ^{235}U fission at 15° to the x-axis and at four axial heights are shown in Fig. 4.1.

(ii) Fission rates along the y-axis show a decreasing C/E with radius and are predicted 5% low in the outer core uranium sector relative to the core center (Table 4.4).

(iii) Fission rates in ^{239}Pu and ^{235}U have C/E values 1% higher in the SM drawers than in the SF drawers.

(iv) Reaction rates in half-two of the assembly (negative z in the tables) intersect an outer ring control rod in the 15° distributions (Tables 4.5, 4.6 and 4.7) and intersect an inner ring control rod in the 30° distributions (Table 4.8). The C/E values for ^{239}Pu and ^{235}U are 1-3% higher in drawers near to the rods than elsewhere.

(v) Axial distributions are well predicted in the core regions with standard deviations of the C/E distributions close to the statistical uncertainties (Tables 4.9 to 4.14). In the axial blankets, the C/Es increase with penetration indicating errors in predicting effects of the steel axial reflector. Calculated and measured results for the axial ^{235}U fission distribution near the core center are shown in Fig. 4.2.

(vi) Axial fission rates adjacent to a half-inserted control rod in the inner ring (matrix 246,146-57) are given in Table 4.14 and illustrated in Fig. 4.3. The average C/E results in the core are in good agreement -- 1.000 (S.D. = 0.007) adjacent to the control rod and 0.995 (S.D. = 0.011) adjacent to the CRP. The predictions in the axial blanket are a few percent different to those in positions removed from the control rod position.

The radial reaction rate analysis for ^{235}U fission is summarized in Figs. 4.4 to 4.7. These figures show the mean C/E results for groups of 3 to 4 adjacent locations at 5 cm and 28 cm above and below the midplane. Table 4.15 gives the mean C/E results for the inner and outer core at the same axial heights. Results for the distributions at the x-axis, 15° and 30°, have been combined in the table. In the all-CRP half (z = +5 cm and +28 cm), the standard deviations are rather larger than statistics. The mean C/E results are 0.5% to 1% higher in the control rod half. This table also shows slightly lower C/E values in the outer core relative to the inner core.

4.5 Reaction Rate Ratios

Reaction rate ratios relative to ^{239}Pu fission are given in Tables 4.16 to 4.18. The experimental values shown are simply the ratios at the respective foil locations and have not been interpolated to a common location.

A summary of the analysis is given in Table 4.19. Results for the ^{235}U fission ratio (F5/F9) and the ^{238}U capture ratio (C8/F9) are consistent among the three distributions. Results for the ^{238}U fission ratio are less consistent between the inner core and the outer core. The mean C/E values compare well with those obtained from analysis of ZPPR-18A as shown below:†

		Mean	Standard Deviation
F5/F9	ZPPR-18B	1.003	0.009
	ZPPR-18A	1.004	0.010
C8/F9	ZPPR-18B	1.042	0.012
	ZPPR-18A	1.046	0.010
F8/F9	ZPPR-18B	1.002	0.024
	ZPPR-18A	0.998	0.023

†The measured results for 238U fission in ZPR-489 have been revised. The corrected values will be published in ANL-ZPR-492.

TABLE 4.1 ZPPR-18B: Radial Reaction Rate Distributions along the x-axis at z = -5.16 cm

		^{239}Pu(n,f)		^{238}U(n,γ)		^{238}U(n,f)	
Matrix	Zone	Exp.	C/E	Exp.	C/E	Exp.	C/E
249 49	IC SF	8.283	0.998	1.1620	1.040	0.1945	1.029
249 50	IC SF	8.295	0.995	1.1680	1.033	0.1966	1.021
249 51	IC SM	8.061	1.011	1.0860	1.040	0.1938	1.027
249 52	IC SF	8.102	0.997	1.1290	1.039	0.1966	1.007
249 53	IC SM	7.842	1.012	1.0480	1.043	0.1952	1.013
249 54	IC SF	7.828	1.003	1.0920	1.038	0.2022	0.999
249 55	IC SM	7.566	1.008	1.0170	1.035	0.1893	1.004
249 56	IC SF	7.474	1.006	1.0620	1.032	0.1840	0.995
249 57	IC SM	7.438	1.003	0.9942	1.042	0.1760	1.031
249 58	IC SF	7.572	0.998	1.0520	1.049	0.1845	1.018
249 59	IC SF	7.581	1.006	1.0550	1.050	0.1923	1.020
249 60	IC SM	7.472	1.016	0.9974	1.051	0.1862	1.016
249 61	IC SF	7.644	0.998	1.0590	1.049	0.1847	1.008
249 62	IC SF	7.639	1.000	1.0700	1.045	0.1863	0.995
249 63	IC SM	7.491	1.009	1.0020	1.048	0.1799	1.017
249 64	IC SF	7.607	0.989	1.0610	1.036	0.1846	0.994
249 65	IC SF	7.433	1.000	1.0280	1.056	0.1816	1.008
249 66	IC SM	7.132	1.010	0.9479	1.053	0.1741	1.011
249 67	IC SF	7.016	0.996	0.9643	1.053	0.1656	1.025
249 68	IC SM	6.640	1.009	0.8831	1.046	0.1583	1.028
249 69	IC SF	6.513	0.991	0.8993	1.038	0.1563	1.011
249 70	IC SM	6.104	1.007	0.8203	1.027	0.1457	1.045
249 71	IC SF	5.899	0.993	0.8084	1.042	0.1447	1.007
249 72	IC SM	5.520	1.003	0.7304	1.035	0.1390	1.006
249 73	OC SF	5.261	1.000	0.7303	1.029	0.1352	1.027
249 74	OC SF	4.905	1.003	0.6656	1.047	0.1338	1.028
249 75	OC D	4.425	0.993	0.5900	1.046	0.1326	0.967
249 76	OC SF	3.808	1.002	0.5308	1.037	0.1042	1.007
249 77	OC SF	3.241	0.988	0.4582	1.057	0.0807	0.932
249 78	RB	--	--	0.3788	1.029	0.0334	1.142
249 79	RB	--	--	0.2990	1.047	0.0198	0.991
249 80	RB	--	--	0.2311	1.051	0.0117	0.922
249 81	RB	--	--	0.1793	1.041	0.0068	0.895
249 82	RB	--	--	0.1496	0.989	0.0036	0.949

TABLE 4.2 ZPPR-18B: Radial ^{235}U Fission Distributions along the x-axis at z = 5.16 cm

Half-1 (CRP Half) z = +5.16 cm				Half-2 (CR Half) z = -5.16 cm			
Matrix	Zone	Exp.	C/E	Matrix	Zone	Exp.	C/E
149 49	IC SF	9.111	0.996	249 49	IC SF	8.791	1.001
149 50	IC SF	9.050	1.003	249 50	IC SF	8.781	1.001
149 51	IC SM	8.833	1.013	249 51	IC SM	8.581	1.009
149 52	IC SF	8.791	1.008	249 52	IC SF	8.566	0.999
149 53	IC SM	8.663	1.006	249 53	IC SM	8.339	1.005
149 54	IC SF	8.633	1.001	249 54	IC SF	8.280	1.000
149 55	IC SM	8.381	1.010	249 55	IC SM	8.020	1.006
149 56	IC SF	8.419	0.998	249 56	IC SF	7.987	0.999
149 57	IC SM	8.269	1.009	249 57	IC SM	7.856	1.010
149 58	IC SF	8.384	1.004	249 58	IC SF	7.990	1.005
149 59	IC SF	8.384	1.002	249 59	IC SF	8.032	1.005
149 60	IC SM	8.241	1.009	249 60	IC SM	7.896	1.018
149 61	IC SF	8.329	1.002	249 61	IC SF	8.103	1.000
149 62	IC SF	8.289	1.008	249 62	IC SF	8.103	1.005
149 63	IC SM	8.163	1.009	249 63	IC SM	8.004	1.006
149 64	IC SF	8.222	0.995	249 64	IC SF	8.047	0.996
149 65	IC SF	8.034	1.005	249 65	IC SF	7.891	1.003
149 66	IC SM	7.680	1.017	249 66	IC SM	7.557	1.013
149 67	IC SF	7.575	0.998	249 67	IC SF	7.401	1.001
149 68	IC SM	7.206	1.005	249 68	IC SM	7.060	1.004
149 69	IC SF	6.985	0.998	249 69	IC SF	6.843	0.995
149 70	IC SM	6.622	1.002	249 70	IC SM	6.470	1.000
149 71	IC SF	6.382	0.992	249 71	IC SF	6.157	1.001
149 72	IC SM	5.980	1.000	249 72	IC SM	5.788	1.005
149 73	OC SF	5.662	1.005	249 73	OC SF	5.554	0.993
149 74	OC SF	5.262	0.998	249 74	OC SF	5.137	0.999
149 75	OC D	4.728	1.001	249 75	OC D	4.675	0.986
149 76	OC SF	4.188	0.990	249 76	OC SF	4.066	0.994
149 77	OC SF	3.629	0.996	249 77	OC SF	3.542	0.995
149 78	RB	3.077	1.011	249 78	RB	3.056	0.993
149 79	RB	2.525	1.002	249 79	RB	2.460	1.004
149 80	RB	2.017	1.002	249 80	RB	1.985	0.996
149 81	RB	1.653	0.997	249 81	RB	1.604	1.005
149 82	RB	1.381	1.067	249 82	RB	1.363	1.058
149 83	RR	--	--	249 83	RR	1.431	1.106

TABLE 4.3 ZPPR-18B: Radial Reaction Rate Distributions along the x-axis at Z = 28.02 cm

		Half-1 z = +28cm		Half-2 z = -28cm					
		$^{235}U(n,f)$		$^{235}U(n,f)$		$^{238}U(n,\gamma)$		$^{238}U(n,f)$	
Matrix	Zone	Exp.	C/E	Exp.	C/E	Exp.	C/E	Exp.	C/E
1,249 49	IC SF	8.025	0.984	6.811	0.996	0.8979	1.038	0.1494	1.013
1,249 50	IC SF	7.971	0.991	6.784	0.998	0.9024	1.031	0.1484	1.023
1,249 51	IC SM	7.793	1.001	6.618	1.005	0.8407	1.031	0.1471	1.020
1,249 52	IC SF	7.809	0.993	6.546	1.001	0.8594	1.046	0.1480	1.007
1,249 53	IC SM	7.694	0.995	6.333	1.008	0.8032	1.037	0.1471	1.007
1,249 54	IC SF	7.761	0.983	6.288	0.996	0.8307	1.035	0.1524	0.989
1,249 55	IC SM	7.552	0.996	6.020	1.008	0.7573	1.047	0.1391	1.014
1,249 56	IC SF	7.586	0.989	5.976	1.001	0.7950	1.036	0.1371	0.988
1,249 57	IC SM	7.460	0.999	5.895	1.010	0.7410	1.051	0.1288	1.044
1,249 58	IC SF	7.537	0.991	6.069	1.000	0.8052	1.037	0.1392	1.006
1,249 59	IC SF	7.421	0.996	6.126	1.004	0.8037	1.051	0.1445	1.019
1,249 60	IC SM	7.209	1.007	6.055	1.020	0.7733	1.042	0.1430	1.000
1,249 61	IC SF	7.286	0.992	6.268	1.002	0.8355	1.033	0.1451	0.977
1,249 62	IC SF	7.283	0.988	6.366	0.998	0.8499	1.027	0.1431	0.992
1,249 63	IC SM	7.109	0.993	6.200	1.018	0.7869	1.045	0.1387	1.015
1,249 64	IC SF	7.093	0.985	6.340	0.994	0.8440	1.025	0.1420	0.996
1,249 65	IC SF	6.958	0.990	6.201	1.005	0.8232	1.040	0.1398	1.012
1,249 66	IC SM	6.612	1.006	6.033	0.999	0.7512	1.046	0.1334	1.019
1,249 67	IC SF	6.517	0.989	5.843	0.997	0.7717	1.036	0.1309	1.000
1,249 68	IC SM	6.234	0.991	5.543	1.004	0.6974	1.040	0.1242	1.009
1,249 69	IC SF	6.052	0.984	5.355	0.995	0.7074	1.033	0.1222	0.993
1,249 70	IC SM	5.701	0.996	5.028	1.003	0.6344	1.036	0.1156	1.008
1,249 71	IC SF	5.487	0.989	4.778	1.002	0.6264	1.046	0.1095	1.014
1,249 72	IC SM	5.128	1.000	4.476	1.007	0.5652	1.035	0.1048	1.014
1,249 73	OC SF	4.922	0.991	4.241	1.005	0.5597	1.039	0.1065	0.990
1,249 74	OC SF	4.560	0.985	3.947	1.003	0.5105	1.055	0.1057	0.987
1,249 75	OC D	4.107	0.984	3.552	1.001	0.4578	1.040	0.1037	0.939
1,249 76	OC SF	3.624	0.975	3.150	0.990	0.4132	1.030	0.0810	0.984
1,249 77	OC SF	3.152	0.977	2.729	0.999	0.3519	1.065	0.0605	0.945
1,249 78	RB	2.647	1.002	2.323	1.014	--	--	--	--
1,249 79	RB	2.193	0.984	1.924	1.000	--	--	--	--
1,249 80	RB	1.716	1.005	1.546	0.998	--	--	--	--
1,249 81	RB	1.417	0.993	1.270	0.994	--	--	--	--
1,249 82	RB	1.205	1.044	1.052	1.077	--	--	--	--

TABLE 4.4 ZPPR-18B: Radial $^{235}U(n,f)$ Distribution along the y-axis at z = -5.16 cm

Matrix	Zone	$^{235}U(n,f)$ Exp.	$^{235}U(n,f)$ C/E
249 49	IC SF	8.791	1.001
248 49	IC SM	--	--
247 49	IC SF	8.628	0.996
246 49	IC SM	8.391	1.005
245 49	IC SF	8.381	0.991
244 49	IC SF	8.137	0.993
243 49	IC SM	7.559	1.018
242 49	IC SF	7.128	1.010
241 49	IC SM	6.072	1.048
	CR		
238 49	IC SF	6.511	1.019
237 49	IC SM	7.157	0.996
236 49	IC SF	7.594	0.978
235 49	IC SF	7.740	0.977
234 49	IC SM	7.617	0.998
233 49	IC SF	7.919	0.978
	CRP		
230 49	IC SM	7.213	0.975
229 49	IC SF	6.744	0.977
228 49	IC SM	6.383	0.974
227 49	IC SF	6.116	0.970
226 49	IC SF	5.790	0.965
225 49	OC UD	5.273	0.959
224 49	OC US	4.890	0.965
223 49	OC UD	4.527	0.941
222 49	OC US	4.000	0.960
221 49	OC US	3.469	0.955
220 49	OC UD	2.948	0.938
219 49	OC US	2.439	0.941

TABLE 4.5 ZPPR-18B: Radial Reaction Rate Distributions at 15° to the x-axis at z = -5.16 cm

		$^{239}Pu(n,f)$		$^{238}U(n,\gamma)$		$^{238}U(n,f)$	
Matrix	Zone	Exp.	C/E	Exp.	C/E	Exp.	C/E
248 50	IC SF	8.278	0.994	1.1610	1.033	0.1988	1.007
248 52	IC SM	7.959	1.010	1.0620	1.044	0.1935	1.021
248 53	IC SF	7.965	0.998	1.0950	1.051	0.1980	1.008
247 54	IC SF	7.652	1.005	1.0620	1.046	0.1915	1.000
247 55	IC SM	--	--	--	--	--	--
247 56	IC SF	7.316	0.994	1.0220	1.036	0.1769	0.983
247 57	IC SF	7.296	0.991	0.9996	1.054	0.1748	0.987
246 57	IC SM	6.823	0.990	0.9026	1.032	0.1571	0.988
246 58	IC SF	6.898	1.013	0.9501	1.069	0.1647	1.001
246 59	IC SM	7.070	1.018	0.9438	1.052	0.1699	1.017
246 60	IC SF	7.383	0.997	1.0180	1.050	0.1758	1.010
245 60	IC SM	7.134	1.011	0.9536	1.047	0.1707	1.022
245 61	IC SF	7.481	0.983	1.0130	1.056	0.1802	1.007
245 62	IC SM	7.287	1.009	0.9783	1.038	0.1779	1.001
244 63	IC SM	7.181	1.007	0.9569	1.046	0.1713	1.007
244 64	IC SF	7.227	0.992	1.0030	1.043	0.1728	0.987
244 65	IC SM	7.020	1.003	0.9297	1.046	0.1633	1.034
244 66	IC SF	6.946	0.994	0.9672	1.038	0.1665	1.009
243 67	IC SF	6.535	1.003	0.9139	1.041	0.1619	0.988
243 68	IC SF	6.307	0.990	0.8749	1.033	0.1532	1.009
243 69	IC SM	5.747	1.003	0.7642	1.036	0.1397	1.003
243 70	IC SM	5.100	1.018	0.7129	1.048	0.1241	0.995
242 70	IC SM CR	4.814	1.028	0.6544	1.045	0.1193	0.991
242 73	OC SF	3.933	1.015	0.5495	1.043	0.1035	0.992
241 73	OC SF	3.924	1.013	0.5529	1.038	0.1026	1.029
241 74	OC SF	3.895	1.011	0.5389	1.043	0.1071	1.009
241 75	OC D	3.684	0.989	0.4998	1.029	0.1118	0.931
241 76	OC SF	3.283	0.988	0.4501	1.034	0.0905	0.992
240 77	OC SF	2.675	0.994	0.3814	1.036	0.0698	0.940
240 78	RB	--	--	0.3053	1.039	0.0288	1.136
240 79	RB	--	--	0.2500	1.020	0.0179	0.927
139 80	RB	--	--	0.1812	1.042	0.0094	0.903
239 81	RB	--	--	0.1386	1.040	0.0059	0.803
239 82	RB	--	--	0.1164	0.977	0.0027	1.006

TABLE 4.6 ZPPR-18B: Radial ^{235}U Fission Distributions at 15° to the x-axis at z = 5.16 cm

Half-1 (CRP Half) z = +5.16 cm				Half-2 (CR Half) z = -5.16 cm			
Matrix	Zone	Exp.	C/E	Matrix	Zone	Exp.	C/E
148 50	IC SF	8.988	1.001	248 50	IC SF	8.644	1.007
148 52	IC SM	8.722	1.011	248 52	IC SM	8.400	1.012
148 53	IC SF	8.697	1.002	248 53	IC SF	8.338	1.003
147 54	IC SF	8.545	0.993	247 54	IC SF	8.069	0.995
147 55	IC SM	8.184	1.015	247 55	IC SM	--	--
147 56	IC SF	8.301	0.993	247 56	IC SF	7.590	0.993
147 57	IC SF	8.227	0.995	247 57	IC SF	7.492	0.999
146 58	IC SF	8.045	1.000	246 58	IC SF	7.139	1.012
146 59	IC SM	7.977	1.011	246 59	IC SM	7.407	1.018
146 60	IC SF	8.129	0.999	246 60	IC SF	7.773	0.997
145 60	IC SM	7.996	1.006	245 60	IC SM	7.541	1.012
145 61	IC SF	8.155	0.990	245 61	IC SF	7.768	1.002
145 62	IC SM	7.997	1.002	245 62	IC SM	7.700	1.010
144 63	IC SM	7.880	1.001	244 63	IC SM	7.626	1.008
144 64	IC SF	7.802	0.999	244 64	IC SF	7.684	0.991
144 65	IC SM	7.550	1.011	244 65	IC SM	7.425	1.004
144 66	IC SF	7.531	0.992	244 66	IC SF	7.325	0.995
143 67	IC SF	7.151	0.994	243 67	IC SF	6.966	0.990
143 68	IC SF	6.911	0.987	243 68	IC SF	6.579	0.995
143 69	IC SM	6.397	1.002	243 69	IC SM	5.988	1.006
143 70	IC SF	6.057	0.990	243 70	IC SF	5.189	1.029
142 70	IC SM	5.957	0.988	242 70	IC SM	5.025	1.032
	CRP			CR			
142 73	OC SF	4.998	0.995	242 73	OC SF	4.027	1.029
141 73	OC SF	4.968	0.987	241 73	OC SF	4.170	1.010
141 74	OC SF	4.570	0.990	241 74	OC SF	4.091	1.007
141 75	OC D	4.142	0.987	241 75	OC D	3.840	0.995
141 76	OC SF	3.602	0.991	241 76	OC SF	3.438	0.987
140 77	OC SF	3.055	0.972	240 77	OC SF	2.904	0.982
140 78	RB	2.571	0.985	240 78	RB	2.492	0.980
140 79	RB	2.060	1.000	240 79	RB	2.047	0.973
139 80	RB	1.591	0.983	239 80	RB	1.561	0.973
139 81	RB	1.256	1.008	239 81	RB	1.251	0.985
139 82	RB	1.068	1.052	239 82	RB	1.043	1.050

TABLE 4.7 ZPPR-18B: Radial Reaction Rate Distributions at 15° to the x-axis at z = 28.02 cm

		Half-1 z = +28cm		Half-2 z = +28cm					
		$^{235}U(n,f)$		$^{235}U(n,f)$		$^{238}U(n,\gamma)$		$^{238}U(n,f)$	
Matrix	Zone	Exp.	C/E	Exp.	C/E	Exp.	C/E	Exp.	C/E
1,248 50	IC SF	--	--	6.689	1.001	0.8839	1.045	0.1520	0.995
1,248 52	IC SM	7.741	0.998	6.427	1.011	0.8082	1.050	0.1460	1.016
1,248 53	IC SF	7.736	0.992	6.320	1.005	0.8340	1.050	0.1459	1.024
1,247 54	IC SF	7.729	0.983	6.029	0.996	0.8066	1.034	0.1416	1.002
1,247 55	IC SM	7.555	1.000	--	--	--	--	--	--
1,247 56	IC SF	7.610	0.999	5.542	0.991	0.7487	1.042	0.1319	0.965
1,247 57	IC SF	7.620	0.991	5.446	1.002	0.7453	1.044	0.1295	0.977
1,246/57	IC SM	7.676	1.001	4.742	0.994	0.6444	1.032	0.1148	0.975
1,246 58	IC SF	7.651	0.981	5.181	1.007	0.7050	1.053	0.1171	1.029
1,246 59	IC SM	7.273	1.004	5.495	1.021	0.7113	1.044	0.1239	1.033
1,246 60	IC SF	--	--	5.836	1.008	--	--	--	--
1,245 60	IC SM	7.100	1.008	5.621	1.027	0.7238	1.045	0.1305	1.026
1,245 61	IC SF	7.113	0.994	5.929	1.009	--	--	--	--
1,245 62	IC SM	6.933	1.001	5.990	1.009	0.7683	1.027	0.1358	1.000
1,244 63	IC SM	6.775	1.004	5.966	1.008	0.7527	1.039	0.1314	1.007
1,244 64	IC SF	6.764	0.991	5.963	1.002	--	--	--	--
1,244 65	IC SM	6.536	1.003	5.818	1.005	0.7291	1.046	0.1296	1.002
1,244 66	IC SF	6.443	0.997	5.716	0.997	--	--	--	--
1,243 67	IC SF	6.280	0.981	5.350	0.999	0.7164	1.031	0.1208	1.009
1,243 68	IC SF	6.071	0.983	5.047	0.993	0.6685	1.038	0.1178	0.992
1,243 69	IC SF	5.795	0.989	4.470	1.011	0.5712	1.045	0.1024	1.021
1,243 70	IC SF	5.666	0.984	3.754	1.027	0.5144	1.058	0.0964	0.937
1,242 70	IC SM	5.631	0.980	3.643	1.018	0.4733	1.041	0.0850	1.009
	CRP/CR								
1,242 73	OC SF	4.908	0.979	2.736	1.028	0.3686	1.060	0.0734	0.982
1,241 73	OC SF	4.789	0.974	2.891	1.006	0.3790	1.043	0.0757	0.985
1,241 74	OC SF	--	--	2.930	1.006	0.3844	1.046	0.0751	1.032
1,241 75	OC D	--	--	2.807	0.996	0.3625	1.037	0.0803	0.940
1,241 76	OC SF	--	--	2.554	0.987	0.3360	1.030	0.0661	0.995
1,240 77	OC SF	--	--	2.200	0.975	0.2873	1.034	0.0516	0.940
140 78	RB	--	--	1.870	0.992	--	--	--	--
140 79	RB	--	--	1.524	0.999	--	--	--	--
139 80	RB	--	--	1.191	0.982	--	--	--	--
139 81	RB	--	--	0.945	1.009	--	--	--	--
139 82	RB	--	--	0.784	1.087	--	--	--	--

TABLE 4.8 ZPPR-18B: Radial Reaction Rate Distributions at 30° to the x-axis

		Half-2 z = -28cm		Half-2 z = -5 cm					
		$^{235}U(n,f)$		$^{235}U(n,f)$		$^{238}U(n,\gamma)$		$^{238}U(n,f)$	
Matrix	Zone	Exp.	C/E	Exp.	C/E	Exp.	C/E	Exp.	C/E
246 54	IC SM	5.691	1.013	7.721	1.010	0.9852	1.042	0.1762	1.023
245 55	IC SM CR	4.717	1.040	6.690	1.044	0.8869	1.050	0.1613	0.968
244 58	IC SM	4.538	1.025	6.446	1.033	0.8405	1.049	0.1425	1.020
243 58	IC SF	4.822	1.014	6.784	1.012	0.8997	1.048	0.1556	0.959
243 59	IC SM	5.283	1.026	7.199	1.017	0.9153	1.043	0.1605	1.017
242 60	IC SM	5.705	1.020	7.491	1.016	0.9515	1.040	0.1682	1.019
242 61	IC SF	5.987	1.000	7.736	0.999	1.0200	1.040	0.1734	0.996
242 62	IC SF	6.103	1.001	7.775	1.004	1.0310	1.034	0.1680	0.994
241 62	IC SF CRP	6.108	1.007	7.814	1.004	1.0470	1.023	0.1631	0.980
240 65	IC SM	5.806	0.998	7.365	1.003	0.9252	1.028	0.1530	0.967
239 65	IC SF	5.704	0.988	7.267	0.994	0.9758	1.018	0.1555	0.973
239 66	IC SM	5.199	1.002	6.765	0.996	0.8518	1.031	0.1509	1.006
238 67	IC SM	4.722	1.001	6.194	1.003	0.7852	1.037	0.1410	1.035
238 68	IC SF	4.609	0.985	6.046	0.994	0.7994	1.035	0.1432	1.005
237 68	IC SM	4.353	0.991	5.737	1.006	0.7431	1.020	0.1383	1.027

TABLE 4.9 ZPPR-18B: Axial Reaction Rate Distributions in Matrix 249-49 (core center)

		^{239}Pu(n,f)		^{235}U(n,f)		^{238}U(n,γ)		^{238}U(n,f)	
Zone	z(mm)	Exp.	C/E	Exp.	C/E	Exp.	C/E	Exp.	C/E
AB	737.4	2.307	1.102	2.307	1.102	0.2689	1.039	0.0071	0.763
AB	686.6	2.611	1.077	2.611	1.077	0.3103	1.068	0.0111	0.908
AB	635.8	3.001	1.043	3.001	1.043	0.3645	1.063	0.0149	1.009
AB	585.0	3.485	1.014	3.485	1.014	0.4326	1.045	0.0243	1.051
AB	534.2	3.939	1.012	3.939	1.012	0.5075	1.029	0.0383	1.028
	Zone Average C/E		1.050		1.050		1.049		0.952
	Standard Deviation		0.039		0.039		0.016		0.119
C SF	483.4	3.882	0.984	4.279	1.020	0.5641	1.060	0.0787	0.932
C SF	432.6	4.495	0.994	4.894	1.011	0.6466	1.051	0.0966	1.006
C SF	380.5	5.188	0.990	5.590	0.999	0.7464	1.028	0.1193	0.996
C SF	356.4	5.424	1.003	5.898	0.996	0.7813	1.034	0.1297	0.990
C SF	280.2	6.351	0.996	6.811	0.996	0.8979	1.038	0.1494	1.013
C SF	229.4	6.904	1.001	7.356	1.004	0.9738	1.042	0.1660	1.004
C SF	178.6	7.403	0.995	7.855	1.000	1.0500	1.028	0.1742	1.022
C SF	127.8	7.786	0.998	8.296	0.998	1.0990	1.035	0.1842	1.021
C SF	77.0	8.138	1.004	8.731	0.997	1.1490	1.040	0.1977	1.001
C SF	50.3	8.283	0.998	8.791	1.001	1.1620	1.040	0.1945	1.029
C SF	26.2	8.461	0.984	8.897	0.997	1.1740	1.037	0.2029	0.995
	Zone Average C/E		0.995		1.002		1.039		1.001
	Standard Deviation		0.007		0.007		0.009		0.026

TABLE 4.10 ZPPR-18B: Axial Reaction Rate Distributions in Matrix 149-49 (core center)

		^{239}Pu(n,f)		^{235}U(n,f)		^{238}U(n,γ)		^{238}U(n,f)	
Zone	z(mm)	Exp.	C/E	Exp.	C/E	Exp.	C/E	Exp.	C/E
IC SF	26.2	8.623	0.981	9.097	0.991	1.1940	1.036	0.2023	1.013
IC SF	50.3	8.488	1.004	9.111	0.996	1.1990	1.039	0.2044	1.010
IC SF	77.0	8.542	1.001	9.097	1.002	1.2070	1.037	0.2065	1.004
IC SF	127.8	8.486	0.984	9.014	0.988	1.1940	1.025	0.2022	1.001
IC SF	178.6	8.260	0.987	8.793	0.990	1.1630	1.027	0.1957	1.008
IC SF	229.4	7.983	0.986	8.453	0.996	1.1160	1.035	0.1914	0.992
IC SF	280.2	7.479	0.983	8.025	0.984	1.0690	1.015	0.1793	0.981
IC SF	356.4	6.657	0.988	7.182	0.991	0.9556	1.023	0.1554	0.996
IC SF	380.5	6.288	0.996	6.882	0.992	0.9059	1.035	0.1461	0.987
IC SF	432.6	5.621	0.988	6.144	1.006	0.8102	1.046	0.1270	0.944
IC SF	483.4	4.954	0.980	5.504	1.014	0.7197	1.060	0.1018	0.904
	Zone Average C/E		0.989		0.995		1.034		0.985
	Standard Deviation		0.008		0.009		0.012		0.033
AB	534.2	--	--	5.207	1.001	0.6647	1.021	0.0514	0.969
AB	585.0	--	--	4.671	1.007	0.5833	1.024	0.0307	1.058
AB	635.8	--	--	4.118	1.031	0.5019	1.037	0.0191	1.009
AB	686.6	--	--	3.624	1.070	0.4296	1.052	0.0123	1.045
AB	737.4	--	--	3.302	1.084	0.3723	1.043	0.0083	0.852
	Zone Average C/E		--		1.039		1.035		0.987
	Standard Deviation		--		0.037		0.013		0.083

TABLE 4.11 ZPPR-18B: Axial ^{235}U Fission Distributions in Matrix 249-64 and 149-64

		Matrix 249-64				Matrix 149-64	
Zone	z(mm)	Exp.	C/E	Zone	z(mm)	Exp.	C/E
AB	737.4	2.233	1.097	AB	737.4	2.861	1.085
AB	686.6	2.498	1.080	AB	686.6	3.185	1.058
AB	635.8	2.908	1.029	AB	635.8	3.638	1.016
AB	585.0	3.350	1.005	AB	585.0	4.075	1.006
AB	534.2	3.765	1.005	AB	534.2	4.545	1.002
	Zone Average C/E		1.043		Zone Average C/E		1.033
	Standard Deviation		0.043		Standard Deviation		0.036
IC SF	483.4	4.062	1.014	AB	483.4	4.812	1.014
IC SF	432.6	4.622	1.006	IC SF	432.6	5.445	0.995
IC SF	381.8	5.263	0.991	IC SF	381.8	5.996	0.998
IC SF	331.0	5.802	0.993	IC SF	331.0	6.605	0.985
IC SF	280.2	6.340	0.994	IC SF	280.2	7.093	0.985
IC SF	229.4	6.793	1.006	IC SF	229.4	7.539	0.991
IC SF	178.6	7.281	0.994	IC SF	178.6	7.832	0.991
IC SF	127.8	7.673	0.989	IC SF	127.8	8.089	0.986
IC SF	77.0	7.922	1.002	IC SF	77.0	8.136	1.007
IC SF	50.3	8.047	0.996	IC SF	50.3	8.222	0.995
IC SF	26.2	8.106	0.993	IC SF	26.2	8.194	0.993
	Zone Average C/E		0.998		Zone Average C/E		0.995
	Standard Deviation		0.008		Standard Deviation		0.009

TABLE 4.12 ZPPR-18B: Axial Reaction Rate Distributions in Matrix 249-75 (outer core)

		$^{235}U(n,f)$		$^{238}U(n,\gamma)$[a]		$^{238}U(n,f)$	
Zone	z(mm)	Exp.	C/E	Exp.	C/E	Exp.	C/E
AB	737.4	1.171	1.072	---	---	---	---
AB	686.6	1.310	1.066	---	---	0.0062	0.920
AB	635.8	1.509	1.036	---	---	0.0097	0.892
AB	585.0	1.752	1.012	---	---	0.0142	1.062
AB	534.2	1.999	1.005	---	---	0.0253	0.933
	Zone Average C/E		1.038				0.952
	Standard Deviation		0.030				0.075
OC D	483.4	2.185	1.016	0.2785	1.067	0.0520	0.887
OC D	432.6	2.499	1.018	0.3197	1.068	0.0648	0.956
OC D	381.8	2.899	0.998	0.3705	1.047	0.0791	0.958
OC D	331.0	3.225	1.001	0.4213	1.027	0.0931	0.939
OC D	280.2	3.552	1.001	0.4578	1.040	0.1037	0.939
OC D	229.4	3.914	0.991	0.5069	1.025	0.1119	0.959
OC D	178.6	4.141	0.996	0.5348	1.033	0.1196	0.957
OC D	127.8	4.402	0.987	0.5648	1.029	0.1274	0.947
OC D	77.0	4.576	0.997	0.5814	1.050	0.1309	0.969
OC D	50.3	4.675	0.986	0.5900	1.046	0.1326	0.967
OC D	26.2	4.702	0.987	0.5970	1.040	0.1344	0.960
	Zone Average C/E		0.998		1.043		0.949
	Standard Deviation		0.011		0.015		0.023

[a]Cell factor not measured for ^{238}U capture in the axial blanket.

TABLE 4.13 ZPPR-18B: Axial Reaction Rate Distributions in Matrix 149-75 (outer core)

		$^{235}U(n,f)$		$^{238}U(n,\gamma)$[a]		$^{238}U(n,f)$	
Zone	z(mm)	Exp.	C/E	Exp.	C/E	Exp.	C/E
OC D	26.2	4.735	0.993	0.6147	1.024	0.1379	0.949
OC D	50.3	4.728	1.001	0.6143	1.031	0.1371	0.960
OC D	77.0	4.795	0.990	0.6097	1.042	0.1392	0.949
OC D	127.8	4.686	0.987	0.6019	1.028	0.1367	0.940
OC D	178.6	4.565	0.986	0.5853	1.029	0.1303	0.958
OC D	229.4	4.395	0.986	0.5603	1.035	0.1250	0.958
OC D	280.2	4.107	0.984	0.5271	1.026	0.1187	0.931
OC D	331.0	3.770	0.994	0.4887	1.027	0.1070	0.947
OC D	381.8	3.463	0.989	0.4459	1.029	0.0957	0.933
OC D	432.6	3.075	0.996	0.3900	1.053	0.0806	0.917
OC D	483.4	2.704	1.008	0.3440	1.059	0.0638	0.875
Zone Average C/E			0.992		1.035		0.938
Standard Deviation			0.007		0.012		0.025
AB	534.2	2.534	0.994	--	--	0.0295	0.977
AB	585.0	2.279	0.989	--	--	0.0177	1.043
AB	635.8	2.006	1.007	--	--	0.0131	0.816
AB	686.6	1.735	1.055	--	--	0.0080	0.884
AB	737.4	1.584	1.056	--	--	--	--
Zone Average C/E			1.020				0.930
Standard Deviation			0.033				0.100

[a]Cell factor not measured for ^{238}U capture in the axial blanket.

TABLE 4.14 ZPPR-18B: Axial ^{235}U Fission Distributions in Matrix 246-57 and 146-57

	Matrix 246-57[a]			Matrix 146-57[b]		
Zone	z(mm)	Exp.	C/E	Zone	z(mm)	Exp.	C/E
AB	737.4	1.371	1.013	AB	737.4	3.655	1.040
AB	686.6	1.556	1.016	AB	686.6	3.990	1.041
AB	635.8	1.818	1.001	AB	635.8	4.420	1.027
AB	585.0	2.139	1.000	AB	585.0	4.942	1.007
AB	534.2	2.521	0.993	AB	534.2	5.400	1.009
	Zone Average C/E		1.005		Zone Average C/E		1.025
	Standard Deviation		0.010		Standard Deviation		0.016
IC SM	483.4	2.885	0.995	IC SM	483.4	5.551	1.026
IC SM	432.6	3.362	0.990	IC SM	432.6	6.106	1.018
IC SM	381.8	3.821	0.995	IC SM	381.8	6.674	1.014
IC SM	331.0	4.254	1.002	IC SM	331.0	7.227	1.003
IC SM	280.2	4.742	0.994	IC SM	280.2	7.676	1.001
IC SM	229.4	5.181	0.997	IC SM	229.4	8.036	1.010
IC SM	178.6	5.595	1.002	IC SM	178.6	8.253	0.996
IC SM	127.8	5.970	1.011	IC SM	127.8	8.303	0.990
IC SM	77.0	6.461	1.001	IC SM	77.0	8.160	1.007
IC SM	50.3	6.668	1.015	IC SM	50.3	7.984	0.997
IC SM	26.2	7.052	1.000	IC SM	26.2	7.695	0.997
	Zone Average C/E		1.000		Zone Average C/E		0.995
	Standard Deviation		0.007		Standard Deviation		0.011

[a] Adjacent to control rod.
[b] Adjacent to CRP.

TABLE 4.15 Summary of C/E Results for ^{235}U Fission in ZPPR-18B

Radial Distribution[a]	Zone	Number of Foils	Mean C/E	Standard Deviation
z = +28 cm	Inner Core	45	0.993	0.008
	Outer Core	7	0.981	0.006
z = +5 cm	Inner Core	46	1.002	0.007
	Outer Core	11	0.992	0.009
z = -5 cm	Inner Core	60	1.006	0.010
	Outer Core	11	0.998	0.013
z = -28 cm	Inner Core	61	1.005	0.011
	Outer Core	11	1.000	0.013

[a]Results at the x-axis, 15° and 30° combined. Results along the y-axis excluded.

TABLE 4.16 ZPPR-18B: Reaction Rate Ratios along the x-axis at z = -5.16 cm

		F5/F9		C8/F9		F8/F9	
Matrix	Zone	Exp.	C/E	Exp.	C/E	Exp.	C/E
249 49	IC SF	1.061	1.003	0.1403	1.042	0.02348	1.031
249 50	IC SF	1.059	1.006	0.1408	1.038	0.02370	1.026
249 51	IC SM	1.065	0.998	0.1347	1.029	0.02404	1.016
249 52	IC SF	1.057	1.002	0.1393	1.042	0.02427	1.010
249 53	IC SM	1.063	0.993	0.1336	1.031	0.02489	1.001
249 54	IC SF	1.058	0.997	0.1395	1.035	0.02583	0.996
249 55	IC SM	1.060	0.998	0.1344	1.027	0.02502	0.996
249 56	IC SF	1.069	0.993	0.1421	1.026	0.02462	0.989
249 57	IC SM	1.056	1.007	0.1337	1.039	0.02366	1.028
249 58	IC SF	1.055	1.007	0.1389	1.051	0.02437	1.020
249 59	IC SF	1.059	0.999	0.1392	1.044	0.02537	1.014
249 60	IC SM	1.057	1.002	0.1335	1.034	0.02492	1.000
249 61	IC SF	1.060	1.002	0.1385	1.051	0.02416	1.010
249 62	IC SF	1.061	1.005	0.1401	1.045	0.02439	0.995
249 63	IC SM	1.068	0.997	0.1338	1.039	0.02402	1.008
249 64	IC SF	1.058	1.007	0.1395	1.048	0.02427	1.005
249 65	IC SF	1.062	1.003	0.1383	1.056	0.02443	1.008
249 66	IC SM	1.060	1.003	0.1329	1.043	0.02441	1.001
249 67	IC SF	1.055	1.005	0.1374	1.057	0.02360	1.029
249 68	IC SM	1.063	0.995	0.1330	1.037	0.02384	1.019
249 69	IC SF	1.051	1.004	0.1381	1.047	0.02400	1.020
249 70	IC SM	1.060	0.993	0.1344	1.020	0.02387	1.038
249 71	IC SF	1.044	1.008	0.1370	1.049	0.02453	1.014
249 72	IC SM	1.049	1.002	0.1323	1.032	0.02518	1.003
	Zone Average C/E		1.001		1.040		1.012
	Standard Deviation		0.005		0.010		0.013
249 73	OC SF	1.056	0.993	0.1388	1.029	0.02570	1.027
249 74	OC SF	1.047	0.996	0.1357	1.044	0.02728	1.025
249 75	OC D	1.056	0.993	0.1333	1.053	0.02997	0.974
249 76	OC SF	1.068	0.992	0.1394	1.035	0.02736	1.005
249 77	OC SF	1.093	1.007	0.1414	1.070	0.02490	0.943
	Zone Average C/E		0.996		1.046		0.995
	Standard Deviation		0.006		0.016		0.036

TABLE 4.17 ZPPR-18B: Reaction Rate Ratios at 15° to the x-axis at z = -5.16 cm

		F5/F9		C8/F9		F8/F9	
Matrix	Zone	Exp.	C/E	Exp.	C/E	Exp.	C/E
248 50	IC SF	1.044	1.013	0.1403	1.039	0.02402	1.013
248 52	IC SM	1.055	1.002	0.1334	1.034	0.02431	1.011
248 53	IC SF	1.047	1.005	0.1375	1.053	0.02486	1.010
247 54	IC SF	1.054	0.990	0.1388	1.041	0.02503	0.995
247 56	IC SF	1.037	0.999	0.1397	1.042	0.02418	0.989
247 57	IC SF	1.027	1.008	0.1370	1.064	0.02396	0.996
246 57	IC SM	0.977	1.025	0.1323	1.042	0.02303	0.998
246 58	IC SF	1.035	0.999	0.1377	1.055	0.02388	0.988
246 59	IC SM	1.048	1.000	0.1335	1.033	0.02403	0.999
246 60	IC SF	1.053	1.000	0.1379	1.053	0.02381	1.013
245 61	IC SF	1.038	1.019	0.1354	1.074	0.02409	1.024
245 62	IC SM	1.057	1.001	0.1343	1.029	0.02441	0.992
244 63	IC SM	1.062	1.001	0.1333	1.039	0.02385	1.000
244 64	IC SF	1.063	0.999	0.1388	1.051	0.02391	0.995
244 65	IC SM	1.058	1.001	0.1324	1.043	0.02326	1.031
244 66	IC SF	1.055	1.001	0.1392	1.044	0.02397	1.015
243 67	IC SF	1.043	0.987	0.1398	1.038	0.02477	0.985
243 68	IC SF	1.042	1.005	0.1387	1.043	0.02429	1.019
243 69	IC SM	1.042	1.003	0.1330	1.033	0.02431	1.000
243 70	IC SF	1.017	1.011	0.1398	1.029	0.02433	0.977
242 70	IC SM	1.044	1.004	0.1359	1.017	0.02478	0.964
	CR						
	Zone Average C/E		1.003		1.043		1.001
	Standard Deviation		0.008		0.013		0.016
242 73	OC SF	1.024	1.014	0.1397	1.028	0.02632	0.977
241 73	OC SF	1.063	0.997	0.1409	1.025	0.02615	1.016
241 74	OC SF	1.050	0.996	0.1384	1.032	0.02750	0.998
241 75	OC D	1.042	1.006	0.1357	1.040	0.03035	0.941
241 76	OC SF	1.047	0.999	0.1371	1.047	0.02758	1.004
240 77	OC SF	1.086	0.988	0.1426	1.042	0.02609	0.946
	Zone Average C/E		1.000		1.036		0.980
	Standard Deviation		0.009		0.009		0.031

TABLE 4.18 ZPPR-18B: Reaction Rate Ratios in Matrix 249-49 and 149-49 (core center)

Matrix	Zone	z(mm)	F5/F9 Exp.	F5/F9 C/E	C8/F9 Exp.	C8/F9 C/E	F8/F9 Exp.	F8/F9 C/E
249 49	IC SF	483.4	1.102	1.037	0.1453	1.077	0.02028	0.947
249 49	IC SF	432.6	1.089	1.017	0.1438	1.057	0.02149	1.012
249 49	IC SF	380.5	1.077	1.009	0.1439	1.038	0.02300	1.006
249 49	IC SF	356.4	1.087	0.993	0.1440	1.031	0.02391	0.987
249 49	IC SF	280.2	1.072	1.000	0.1414	1.042	0.02352	1.017
249 49	IC SF	229.4	1.065	1.003	0.1410	1.041	0.02404	1.003
249 49	IC SF	178.6	1.061	1.005	0.1418	1.033	0.02353	1.027
249 49	IC SF	127.8	1.066	1.000	0.1412	1.037	0.02366	1.023
249 49	IC SF	77.0	1.073	0.993	0.1412	1.036	0.02429	0.997
249 49	IC SF	50.3	1.061	1.003	0.1403	1.042	0.02348	1.031
249 49	IC SF	26.2	1.052	1.013	0.1388	1.054	0.02398	1.011
149 49	IC SF	26.2	1.055	1.010	0.1385	1.056	0.02346	1.033
149 49	IC SF	50.3	1.073	0.992	0.1413	1.035	0.02408	1.006
149 49	IC SF	77.0	1.065	1.001	0.1413	1.036	0.02417	1.003
149 49	IC SF	127.8	1.062	1.004	0.1407	1.042	0.02383	1.017
149 49	IC SF	178.6	1.065	1.003	0.1408	1.041	0.02369	1.021
149 49	IC SF	229.4	1.059	1.010	0.1398	1.050	0.02398	1.006
149 49	IC SF	280.2	1.073	1.001	0.1429	1.033	0.02397	0.998
149 49	IC SF	356.4	1.079	1.003	0.1435	1.035	0.02334	1.008
149 49	IC SF	380.5	1.094	0.996	0.1441	1.039	0.02323	0.991
149 49	IC SF	432.6	1.093	1.018	0.1441	1.059	0.02259	0.955
149 49	IC SF	483.4	1.111	1.035	0.1453	1.082	0.02055	0.922
	Zone Average C/E			1.007		1.045		1.001
	Standard Deviation			0.012		0.014		0.028

TABLE 4.19 ZPPR-18B: Summary of Reaction Rate Ratio Analysis

		$^{235}U(n,f)/^{239}Pu(n,f)$			$^{238}U(n,\gamma)/^{239}Pu(n,f)$			$^{238}U(n,f)/^{239}Pu(n,f)$		
Distribution	Zone	No.	C/E	S.D.	No.	C/E	S.D.	No.	C/E	S.D.
x-Axis z = 5 cm	IC	24	1.001	0.005	24	1.040	0.010	24	1.012	0.013
	OC	5	0.996	0.006	5	1.046	0.016	5	0.995	0.036
15° z = 5 cm	IC	21	1.003	0.008	21	1.043	0.013	21	1.001	0.016
	OC	6	1.000	0.009	6	1.036	0.009	6	0.980	0.031
Axial 149-49	IC	22	1.007	0.012	22	1.045	0.014	22	1.001	0.028
All Data		77	1.003	0.009	77	1.042	0.012	77	1.002	0.024

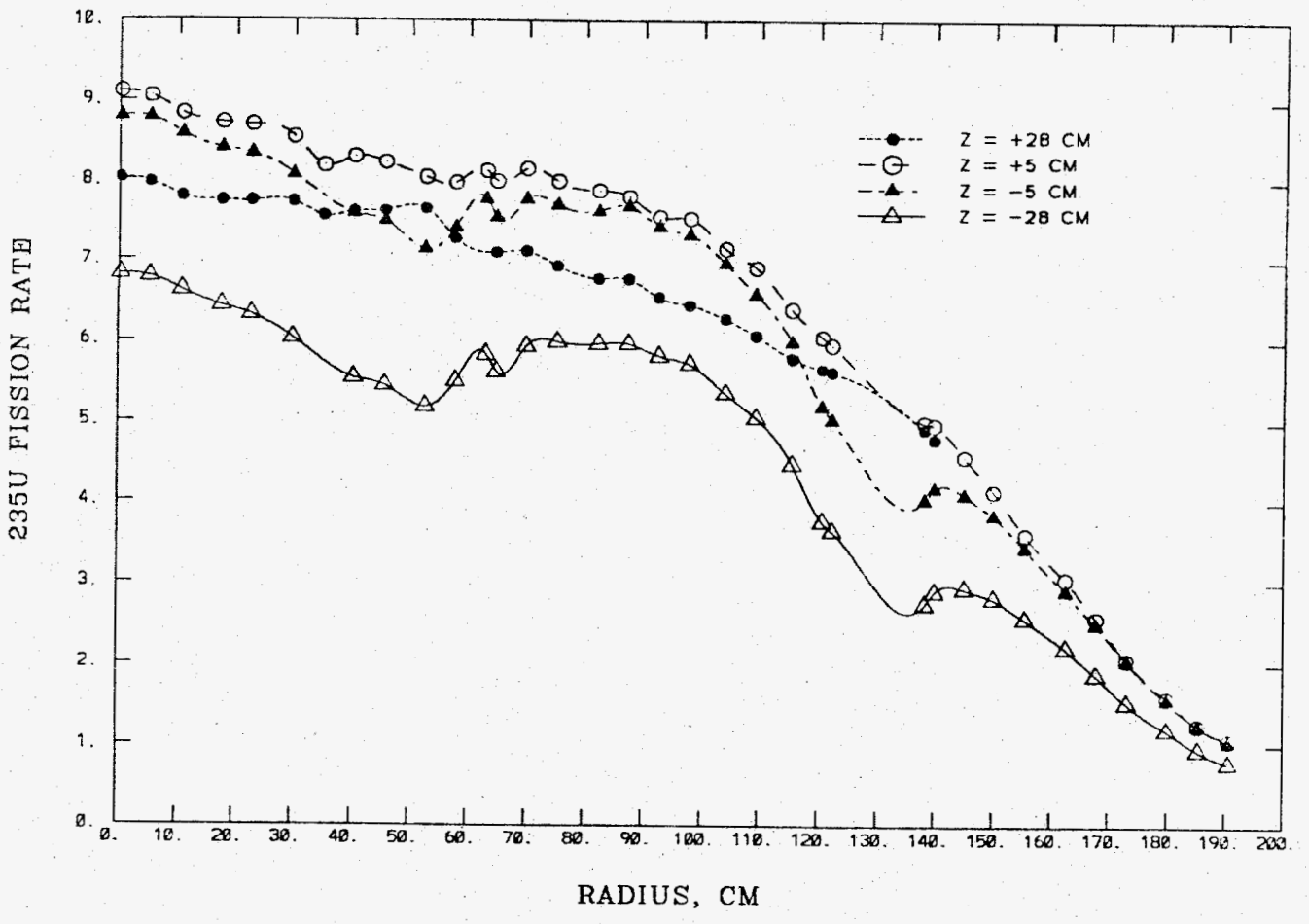

Fig. 4.1 Measured ^{235}U Radial Fission Distributions at Four Axial Heights at 15° to the X-axis of ZPPR-18B

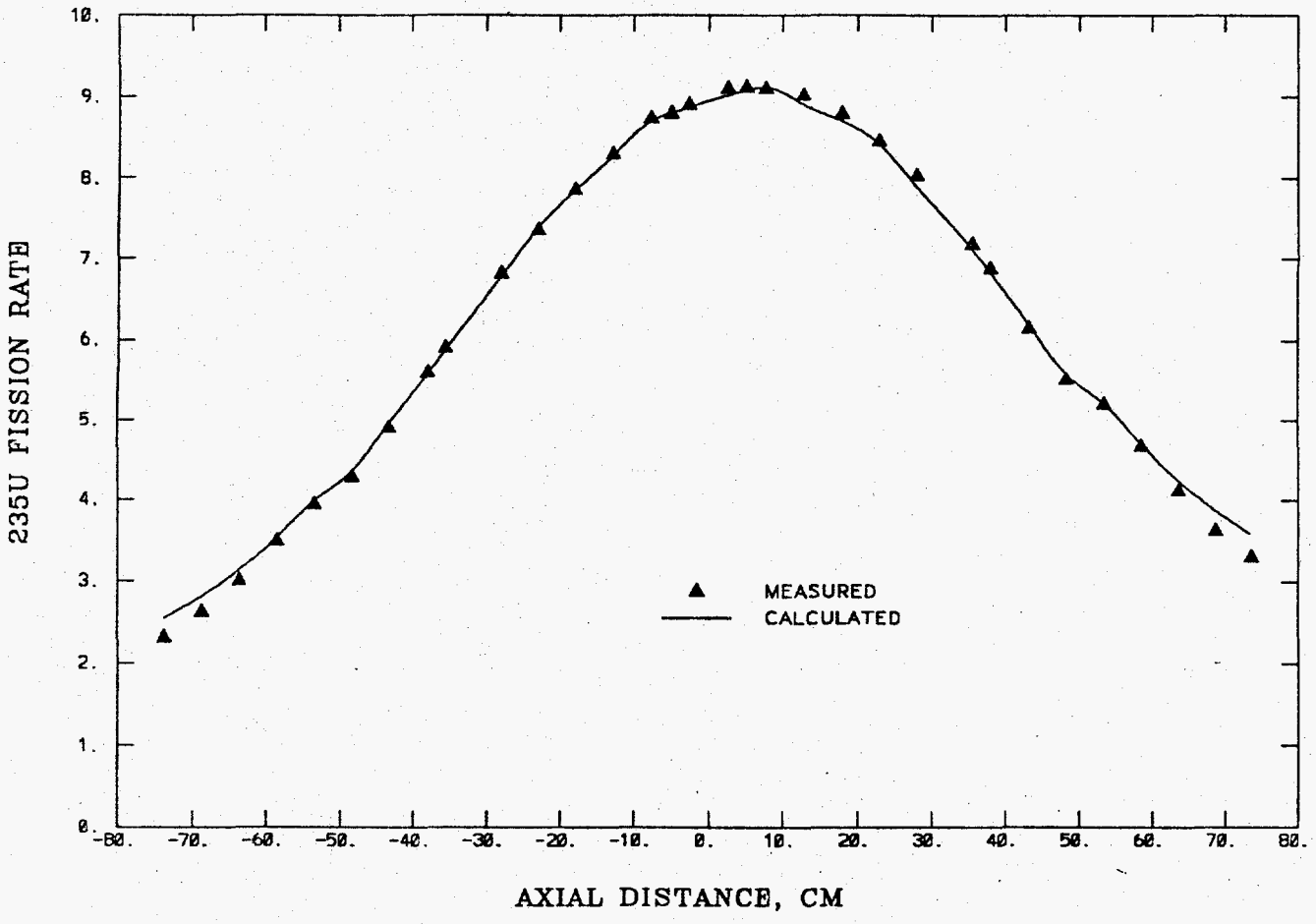

Fig. 4.2 Measured and Calculated Axial Distributions for ^{235}U Fission Near the Center of ZPPR-18B

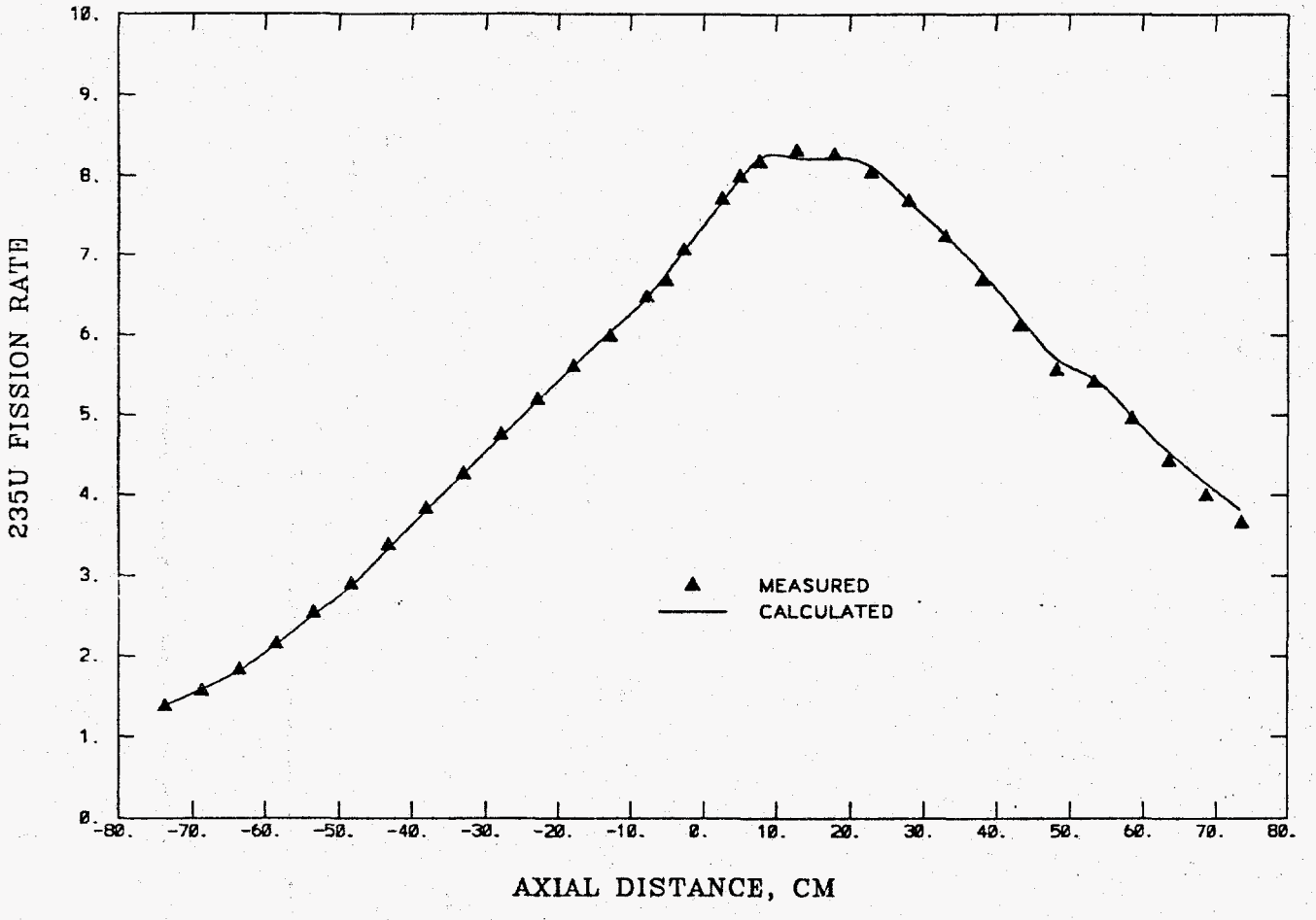

Fig. 4.3 Measured and Calculated Axial Distributions for ^{235}U Fission Next to an Inner Ring Control rod in ZPPR-18B

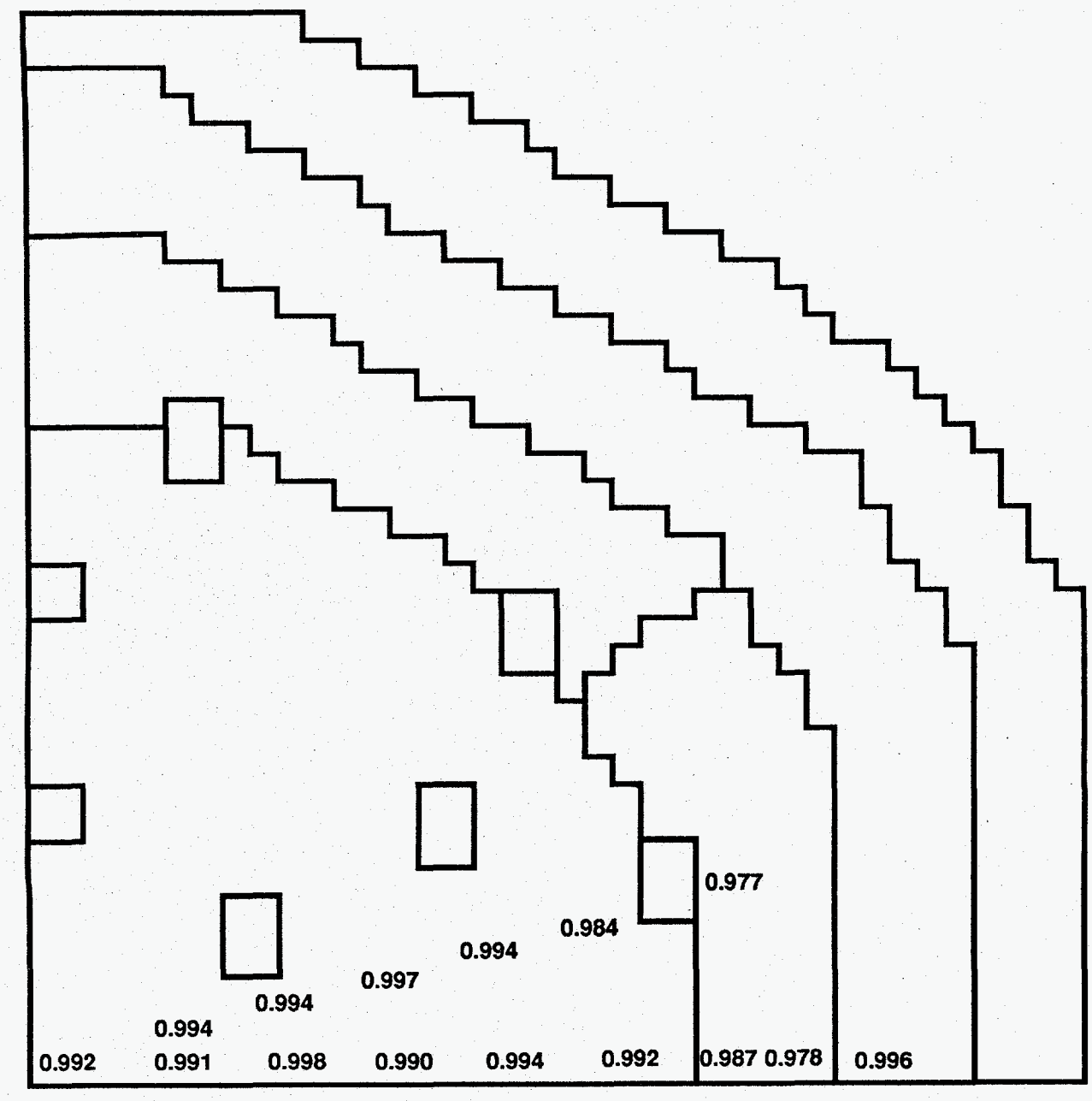

Fig. 4.4 Summary of C/E Results for ^{235}U Fission in ZPPR-18B at 28 cm Above the Midplane (CRP half)

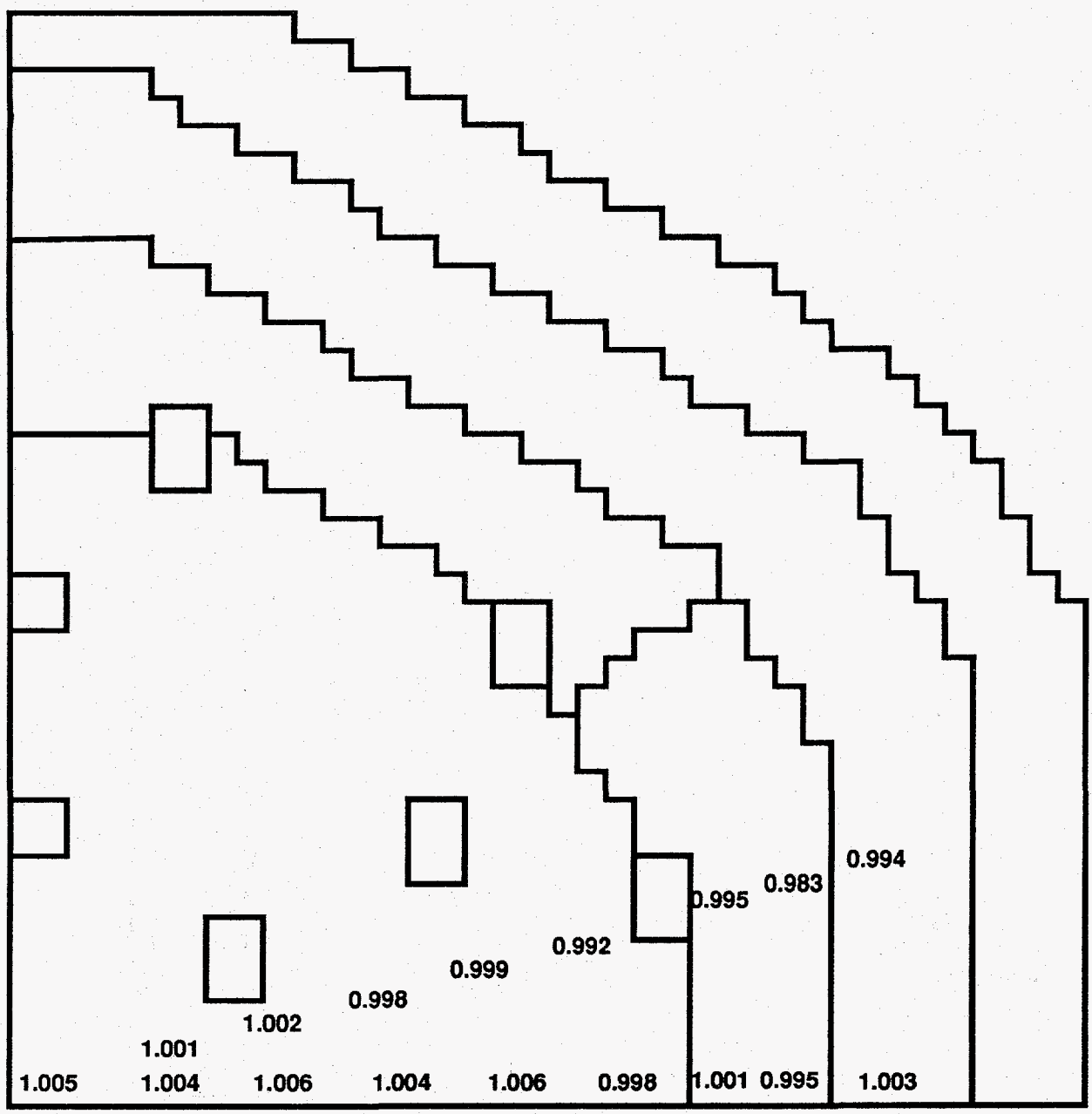

Fig. 4.5 Summary of C/E Results for ^{235}U Fission in ZPPR-18B at 5 cm Above the Midplane (CRP half)

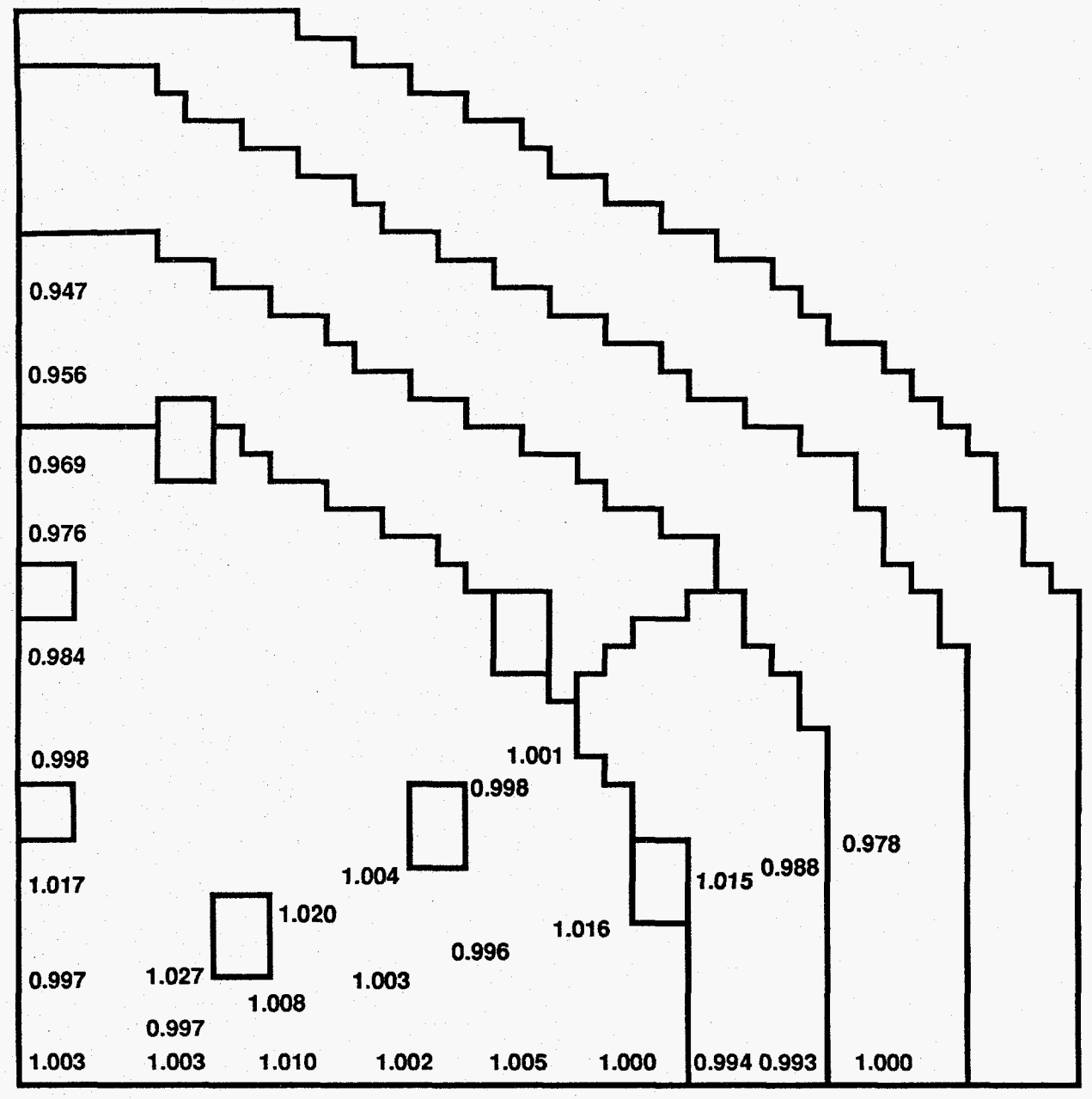

Fig. 4.6 Summary of C/E Results for ^{235}U Fission in ZPPR-18B at 5 cm Below the Midplane (CR half)

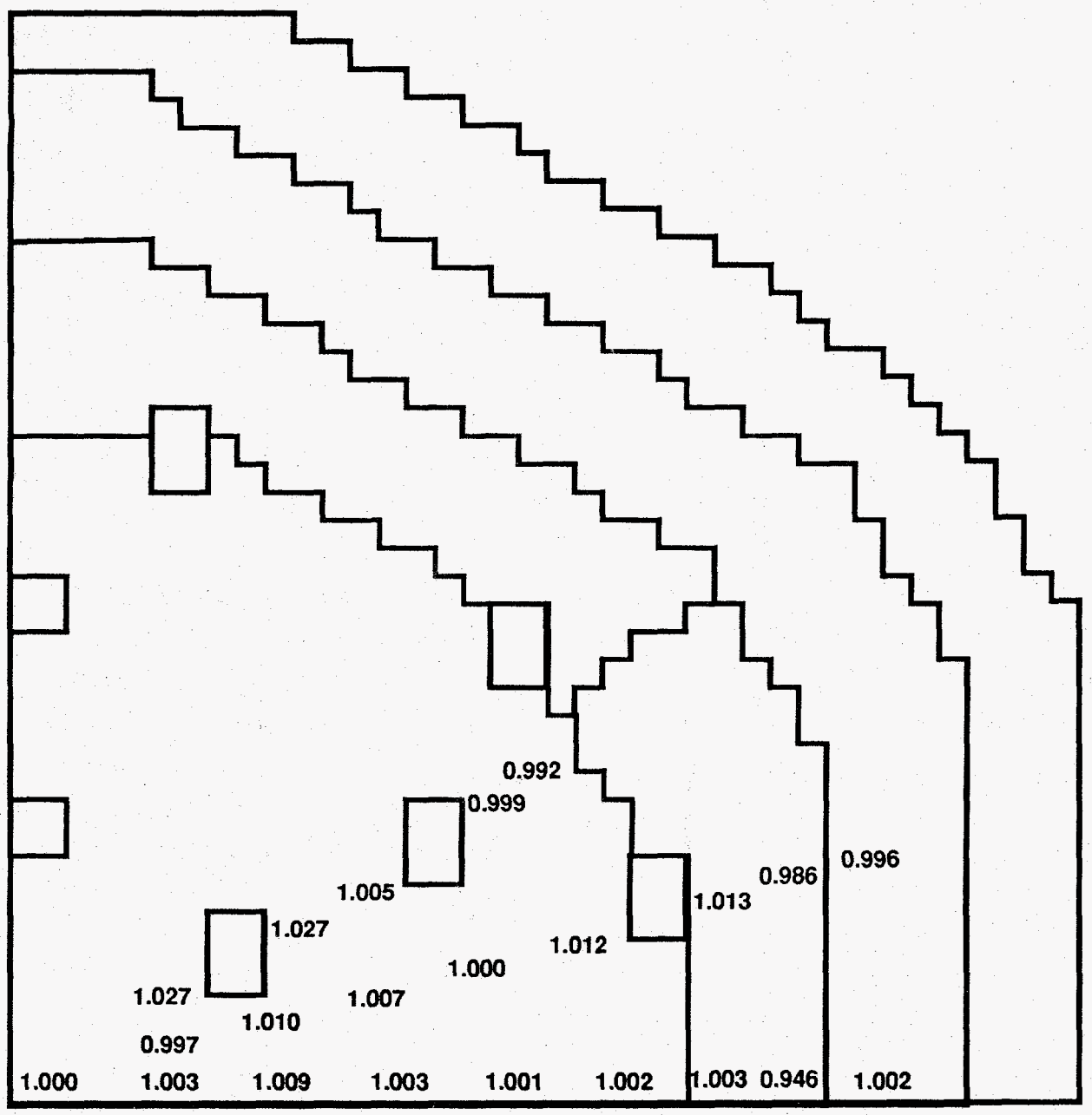

Fig. 4.7 Summary of C/E Results for ^{235}U Fission in ZPPR-18B at 28 cm Below the Midplane (CR half)

5. BASIC DATA FOR REACTION RATE DISTRIBUTIONS IN ZPPR-18A AND ZPPR-18B

(D. W. Maddison and J. M. Gasidlo)

5.1 Introduction

Reaction rate maps are measured by first choosing a location in a cell to place the irradiation foil. These "mapping" foils are always placed in the same location in a drawer for a specific type of cell. Then, a pattern of drawers is chosen to provide the reactor distribution desired, such as a radial map or an axial distribution.

5.2 Discussion of Foil Locations

The foils were first placed in stainless steel foil holders which were then loaded into the drawers between the vertical columns* of materials. For drawers with one fuel column the foil was placed adjacent to the fuel on the side closer to the core center. For drawers with two fuel columns, the foil was placed adjacent to the fuel plate closer to the core center on the side of the plate closer to the drawer center. The drawer column for the mapping foils in any matrix position in the reactor are given below.

	Matrix Columns ≤ 48		Matrix Column ≥ 49	
Reactor Half 1	SF,SM	D	SF,SM	D
Core	IJ	JK	GH	FG
AB	IJ	IJ	GH	GH
RB	IJ		GH	
RR/AR	TC		TC	

*ZPPR drawers are divided into sixteen 3.175 mm (1/8 in.) wide vertical columns designed by letters A through P. The letter A denotes the column at the left as one faces the drawer. The letters FG, for example, indicate the foil is between columns F and G, and is centered 19.050 mm (0.750 in.) from the left side of the drawer.

	Matrix Columns ≤ 48		Matrix Column ≥ 49	
Reactor Half 2	SF,SM	D	SF,SM	D
Core	GH	FG	IJ	JK
AB	GH	GH	IJ	IJ
RB	GH		IJ	
RR/AR	TC		TC	

Where SF is a drawer with one fuel column that has iron oxide plates on both sides of the fuel plate, SM is a drawer with one fuel column that has depleted uranium metal plates on both sides of the fuel plate, D is a drawer with two fuel columns, core is the fueled region, AB is the axial blanket in a fueled drawer, RB is the radial blanket and AR/RR is the axial or radial reflector. There are some ^{235}U foils in the axial and radial reflectors which are given a drawer location of "TC". For this location, the foil holder was placed horizontally across the top of the drawer. The foil was centered above drawer columns HI and the foil was centered 25.654 mm above the mid-height of the drawer.

The basic data for the radial maps and axial distributions in ZPPR-18A are given in Tables 5.1 - 5.3. The basic data for ZPPR-18B were measured in two irradiations. There were 10 common locations for ^{235}U foils in the two irradiations for comparing the power histories. The weighted average fission ratio of the common foils was 1.0008 with one standard deviation of 0.0020. Since this was close to unity, the two data sets were merged using the average of the two foils for the common locations. The basic data for the merged data sets are given in Tables 5.4 - 5.8.

In both 18A and 18B, all foils were centered on the listed axial positions as measured from the reactor midplane. The ^{235}U foils were centered 13.8 mm above, the ^{238}U foils were centered on, and the ^{239}Pu foils were centered 13.8 mm below the mid-height of the drawer.

The core configurations and operating rod parameters for 18A are given in ANL-ZPR-489, Section 8, and for 18B in Section 4 of this report.

5.3 Discussion of Foil Data and Uncertainties

In all of the tables, the data are given in units of 10^{-18} fissions or captures per sec per atom in the irradiated foil at an estimated reactor power of one watt. The second number associated with each reaction rate is a one standard deviation estimate of the random uncertainty. The uncertainties given in the tables are solely due to counting statistics and data reduction. They include the effects of peak integration, interference peak corrections, corrections for other reactions in the foils, irradiation history and foil positioning in the counter system. Other uncertainties due to cell-averaging factors are discussed in Section 6. Other uncertainties such as those due to detector calibrations are not included. The uncertainties are discussed in greater detail by Brumbach and Gasidlo.[1]

REFERENCE

1. "In-Cell Reaction Rate Distributions and Cell-Average Reaction Rates in Fast Critical Assemblies," ANL-85-44, August 1985.

TABLE 5.1 Basic Data for Radial Distributions of $^{239}Pu(n,f)$ in ZPPR-18A

Matrix	Loc[a]	$^{239}Pu(n,f)$[b]	Matrix	Loc[a]	$^{239}Pu(n,f)$[b]
x-axis data at z = 51.6 mm			15° data at z = 51.6 mm		
149 50	GH	8.790 0.043	148 50	GH	8.738 0.042
149 51	GH	8.474 0.044	148 52	GH	8.515 0.039
149 52	GH	8.651 0.040	148 53	GH	8.608 0.040
149 53	GH	8.473 0.042	147 54	GH	8.386 0.041
149 54	GH	8.472 0.040	147 55	GH	8.261 0.041
149 55	GH	8.297 0.042	147 56	GH	8.360 0.041
149 56	GH	8.369 0.043	147 57	GH	8.344 0.039
149 57	GH	8.232 0.040	146 57	GH*	8.253 0.039
149 58	GH	8.320 0.039	146 58	GH	8.269 0.040
149 59	GH	8.100 0.040	146 59	GH	7.938 0.037
149 60	GH	7.855 0.038	146 60	GH	7.927 0.039
149 61	GH	7.884 0.043	145 60	GH	7.857 0.038
149 62	GH	7.832 0.041	145 61	GH	7.836 0.038
149 63	GH	7.607 0.036	145 62	GH	7.512 0.038
149 64	GH	7.609 0.035	144 63	GH	7.302 0.035
149 65	GH	7.439 0.037	144 64	GH	7.332 0.035
149 66	GH	7.115 0.033	144 65	GH	7.068 0.033
149 67	GH	7.051 0.035	144 66	GH	7.047 0.036
149 68	GH	6.744 0.036	143 67	GH	6.832 0.039
149 69	GH	6.580 0.033	143 68	GH	6.626 0.037
149 70	GH	6.273 0.032	143 69	GH	6.311 0.034
149 71	GH	6.092 0.030	143 70	GH	6.234 0.032
149 72	GH	5.757 0.031	142 70	GH	6.064 0.032
149 73	GH	5.574 0.030	142 73	GH	5.516 0.028
149 74	GH	5.224 0.030	141 73	GH	5.433 0.030
149 75	FG*	4.703 0.026	141 74	GH	4.899 0.026
149 76	GH	4.128 0.024	141 75	GH	4.365 0.024
149 77	GH	3.519 0.022	141 76	GH	3.773 0.026
			140 77	GH	3.075 0.021

[a] In-drawer column which designates the foil location in the drawer. The ^{239}Pu foils were centered 13.8 mm below the mid-height of the drawer. All foils were centered 51.6 mm from the reactor midplane except "*" which were at 50.3 mm.

[b] Experimental results in units of 10^{-18} fissions per atom per second at a reactor power of approximately one watt. The second number is one standard deviation uncertainty. See text for details.

TABLE 5.2 Basic Data for Radial Distributions of ^{235}U and ^{238}U Reaction Rates in ZPPR-18A

Matrix	Loc[a]	$^{235}U(n,f)$[b]	$^{238}U(n,f)$[b]	$^{238}U(n,\gamma)$[b]
x-axis data at z = 51.6 mm				
149 50	GH	9.266 0.037	0.2253 0.0029	1.3195 0.0077
149 51	GH	9.026 0.038	0.2183 0.0025	1.1308 0.0061
149 52	GH	9.175 0.038	0.2203 0.0026	1.3016 0.0070
149 53	GH	8.910 0.038	0.2144 0.0026	1.1049 0.0066
149 54	GH	9.219 0.050	0.2153 0.0023	1.2692 0.0073
149 55	GH	8.771 0.040	0.2092 0.0026	1.0852 0.0060
149 56	GH	8.922 0.042	0.2145 0.0027	1.2637 0.0067
149 57	GH	8.674 0.040	0.2099 0.0025	1.0716 0.0064
149 58	GH	8.833 0.039	0.2081 0.0028	1.2588 0.0068
149 59	GH	8.664 0.041	0.2025 0.0027	1.2404 0.0071
149 60	GH	8.274 0.035	0.1979 0.0026	1.0373 0.0058
149 61	GH	8.417 0.037	0.1916 0.0027	1.2037 0.0063
149 62	GH	8.354 0.036	0.1954 0.0029	1.1954 0.0067
149 63	GH	8.112 0.037	0.1911 0.0033	1.0163 0.0057
149 64	GH	8.069 0.035	0.1912 0.0028	1.1578 0.0068
149 65	GH	7.907 0.036	0.1819 0.0032	1.1424 0.0068
149 66	GH	7.497 0.032	0.1802 0.0023	0.9349 0.0054
149 67	GH	7.444 0.032	0.1826 0.0024	1.0563 0.0059
149 68	GH	7.088 0.034	0.1641 0.0025	0.8841 0.0048
149 69	GH	6.987 0.031	0.1666 0.0025	0.9900 0.0057
149 70	GH	6.599 0.032		
149 71	GH	6.472 0.029	0.1585 0.0023	0.9060 0.0058
149 72	GH	6.066 0.028	0.1504 0.0024	0.7519 0.0044
149 73	GH	5.865 0.028	0.1487 0.0023	0.8260 0.0051
149 74	GH	5.470 0.026	0.1493 0.0022	0.7701 0.0044
149 76	GH	4.404 0.024	0.1122 0.0021	0.6156 0.0040
149 77	GH	3.797 0.019	0.0901 0.0023	0.5413 0.0046
149 78	GH	3.227 0.017	0.0401 0.0013	0.3939 0.0033
149 79	GH	2.655 0.015	0.0205 0.0012	0.3138 0.0024
149 80	GH	2.132 0.013	0.0121 0.0009	0.2492 0.0021
149 81	GH	1.738 0.011	0.0060 0.0008	0.1935 0.0018
149 82	GH	1.486 0.010	0.0049 0.0009	0.1530 0.0016
149 83	TC	1.550 0.012		
x-axis data at z = 280.2 mm				
149 50	GH	7.778 0.037	0.1739 0.0027	1.1210 0.0061
149 51	GH	7.488 0.035	0.1723 0.0027	0.9392 0.0053
149 52	GH	7.622 0.037	0.1769 0.0027	1.0880 0.0059
149 53	GH	7.359 0.034	0.1704 0.0031	0.9228 0.0052
149 54	GH	7.485 0.038	0.1688 0.0027	1.0659 0.0061
149 55	GH	7.356 0.036	0.1617 0.0025	0.9049 0.0051
149 56	GH	7.338 0.034	0.1695 0.0028	1.0648 0.0057
149 57	GH	7.226 0.034	0.1666 0.0025	0.9005 0.0051
149 58	GH	7.374 0.036	0.1633 0.0024	1.0496 0.0056

TABLE 5.2 (contd)

Matrix	Loc[a]	$^{235}U(n,f)$[b]	$^{238}U(n,f)$[b]	$^{238}U(n,\gamma)$[b]
149 59	GH	7.157 0.037	0.1650 0.0029	1.0268 0.0061
149 60	GH	6.901 0.033	0.1552 0.0031	0.8681 0.0050
149 61	GH	6.953 0.034	0.1635 0.0022	0.9828 0.0055
149 62	GH	6.953 0.033	0.1583 0.0030	0.9909 0.0054
149 63	GH	6.694 0.032	0.1539 0.0023	0.8320 0.0047
149 64	GH	6.687 0.031	0.1626 0.0025	0.9461 0.0054
149 65	GH	6.653 0.031	0.1500 0.0026	0.9495 0.0053
149 66	GH	6.272 0.031	0.1432 0.0020	0.7817 0.0049
149 67	GH	6.190 0.031	0.1464 0.0022	0.8788 0.0052
149 68	GH	5.858 0.030	0.1378 0.0021	0.7230 0.0044
149 69	GH	5.745 0.030	0.1429 0.0022	0.8122 0.0048
149 70	GH	5.421 0.027	0.1270 0.0024	0.6767 0.0040
149 71	GH	5.295 0.026	0.1241 0.0022	0.7594 0.0045
149 72	GH	4.941 0.027	0.1205 0.0024	0.6195 0.0038
149 73	GH	4.839 0.027	0.1237 0.0026	0.6810 0.0041
149 74	GH	4.481 0.024		
149 76	GH	3.578 0.020		
149 77	GH	3.096 0.017	0.0720 0.0020	0.4468 0.0031
149 78	GH	2.652 0.018		
149 79	GH	2.190 0.013		
149 80	GH	1.744 0.012		
149 81	GH	1.418 0.011		
149 82	GH	1.219 0.009		
15° data at z = 51.6 mm				
148 50	GH	9.211 0.040	0.2235 0.0024	1.3126 0.0069
148 52	GH	8.959 0.038	0.2126 0.0026	1.1106 0.0061
148 53	GH	9.109 0.038	0.2165 0.0026	1.2826 0.0075
147 54	GH	9.183 0.043	0.2107 0.0026	1.2673 0.0065
147 55	GH	8.807 0.040	0.2062 0.0026	1.0976 0.0065
147 56	GH	9.024 0.042	0.2115 0.0026	1.2906 0.0069
147 57	GH	9.019 0.041	0.2062 0.0025	1.2749 0.0068
146 57	GH*		0.1875 0.0026	1.1027 0.0058
146 58	GH	9.001 0.043	0.1982 0.0026	1.2704 0.0068
146 59	GH	8.447 0.038	0.1873 0.0027	1.0590 0.0058
146 60	GH	8.443 0.035	0.1929 0.0024	1.1985 0.0071
145 60	GH	8.227 0.036	0.1851 0.0027	1.0194 0.0060
145 61	GH	8.221 0.034	0.1930 0.0029	1.1830 0.0066
145 62	GH	7.947 0.035	0.1833 0.0029	0.9968 0.0056
144 63	GH	7.713 0.033	0.1826 0.0030	0.9708 0.0061
144 64	GH	7.781 0.037	0.1824 0.0026	1.0963 0.0060
144 65	GH	7.417 0.034	0.1801 0.0030	0.9201 0.0059
144 66	GH	7.461 0.033	0.1786 0.0025	1.0522 0.0059
143 67	GH	7.191 0.034	0.1650 0.0023	1.0302 0.0055
143 68	GH	7.038 0.032	0.1630 0.0023	1.0004 0.0057
143 69	GH	6.668 0.030	0.1552 0.0031	0.8322 0.0052
143 70	GH	6.688 0.030	0.1442 0.0026	0.9598 0.0055

TABLE 5.2 (contd)

Matrix	Loc[a]	$^{235}U(n,f)$[b]	$^{238}U(n,f)$[b]	$^{238}U(n,\gamma)$[b]
142 70	GH	6.442 0.028	0.1379 0.0022	0.7932 0.0045
142 73	GH	5.935 0.031	0.1342 0.0021	0.8533 0.0047
141 73	GH	5.703 0.025	0.1324 0.0024	0.8336 0.0048
141 74	GH	5.123 0.024	0.1346 0.0021	0.7343 0.0043
141 75	GH	4.525 0.022	0.1280 0.0022	0.6403 0.0044
141 76	GH	3.919 0.021	0.1053 0.0019	0.5530 0.0036
140 77	GH	3.215 0.017	0.0829 0.0017	0.4672 0.0033
140 78	GH	2.747 0.015	0.0367 0.0012	0.3340 0.0027
140 79	GH	2.225 0.013	0.0181 0.0010	0.2689 0.0022
139 80	GH	1.682 0.011	0.0114 0.0010	0.1988 0.0021
139 81	GH	1.349 0.009	0.0069 0.0008	0.1532 0.0016
139 82	GH	1.140 0.008	0.0050 0.0008	0.1172 0.0014
15° data at z = 280.2 mm				
148 50	GH	7.709 0.035	0.1760 0.0027	1.1015 0.0060
148 52	GH	7.434 0.034	0.1699 0.0028	0.9259 0.0057
148 53	GH	7.563 0.035	0.1738 0.0026	1.0788 0.0064
147 54	GH	7.478 0.035	0.1715 0.0025	1.0755 0.0058
147 55	GH	7.335 0.037		
147 56	GH	7.488 0.037	0.1661 0.0026	1.0744 0.0058
147 57	GH	7.450 0.035	0.1645 0.0026	1.0794 0.0058
146 57	GH		0.1512 0.0026	0.9147 0.0051
146 58	GH	7.428 0.033	0.1614 0.0023	1.0600 0.0059
146 59	GH	7.033 0.034	0.1514 0.0028	0.8789 0.0053
146 60	GH	7.019 0.033		
145 60	GH	6.872 0.033	0.1522 0.0028	0.8541 0.0051
145 61	GH	6.772 0.029		
145 62	GH	6.528 0.032	0.1521 0.0025	0.8204 0.0047
144 63	GH	6.402 0.031	0.1424 0.0024	0.7990 0.0046
144 64	GH	6.426 0.031		
144 65	GH	6.169 0.029	0.1417 0.0023	0.7633 0.0048
144 66	GH	6.141 0.028		
143 67	GH	5.935 0.030	0.1385 0.0021	0.8470 0.0049
143 68	GH	5.794 0.029		
143 69	GH	5.524 0.027	0.1248 0.0024	0.6826 0.0041
143 70	GH	5.517 0.028	0.1171 0.0021	0.7923 0.0045
142 70	GH	5.353 0.027	0.1138 0.0022	0.6614 0.0039
142 73	GH	4.915 0.024	0.1096 0.0022	0.7077 0.0047
141 73	GH	4.786 0.023	0.1078 0.0023	0.6957 0.0042
141 74	GH	4.220 0.021	0.1071 0.0022	0.6020 0.0038
141 75	GH	3.727 0.023		
141 76	GH	3.235 0.019	0.0861 0.0017	0.4552 0.0032
140 77	GH	2.682 0.018	0.0647 0.0017	0.3814 0.0028
140 78	GH	2.226 0.016		
140 79	GH	1.811 0.012		
139 80	GH	1.370 0.009		
139 81	GH	1.094 0.008		
139 82	GH	0.931 0.008		

TABLE 5.2 (contd)

Matrix	Loc[a]	$^{235}U(n,f)$[b]	$^{238}U(n,f)$[b]	$^{238}U(n,\gamma)$[b]
30° data at z = 51.6 mm				
146 54	GH	8.870 0.040	0.1996 0.0031	1.1026 0.0062
145 55	GH	8.940 0.041	0.1890 0.0026	1.1128 0.0063
144 58	GH	8.812 0.038	0.1782 0.0029	1.0948 0.0060
143 58	GH	8.831 0.042	0.1825 0.0025	1.2956 0.0066
143 59	GH	8.273 0.037	0.1813 0.0029	1.0347 0.0056
142 60	GH	7.925 0.035	0.1843 0.0026	0.9939 0.0057
142 61	GH	7.996 0.038	0.1807 0.0028	1.1524 0.0061
142 62	GH	8.021 0.036	0.1755 0.0024	1.1526 0.0064
141 62	GH	7.957 0.036	0.1716 0.0025	1.1479 0.0061
140 65	GH	7.375 0.034	0.1506 0.0023	0.9196 0.0051
139 65	GH	7.381 0.035	0.1512 0.0025	1.0919 0.0061
139 66	GH	6.806 0.035	0.1562 0.0024	0.8423 0.0054
138 67	GH	6.463 0.035	0.1551 0.0022	0.7991 0.0051
138 68	GH	6.386 0.031	0.1614 0.0023	0.9021 0.0052
137 68	GH	6.126 0.031	0.1567 0.0023	0.7637 0.0047
30° data at z = 280.2 mm				
146 54	GH	7.347 0.035		
145 55	GH	7.520 0.035		
144 58	GH	7.298 0.037		
143 58	GH	7.398 0.038		
143 59	GH	6.881 0.032		
142 60	GH	6.614 0.030		
142 61	GH	6.702 0.031		
142 62	GH	6.646 0.034		
141 62	GH	6.596 0.029		
140 65	GH	6.148 0.028		
139 65	GH	6.192 0.031		
139 66	GH	5.719 0.032		
138 67	GH	5.262 0.028		
138 68	GH	5.249 0.029		
137 68	GH	5.006 0.026		
y-axis data at z = 51.6 mm				
148 49	GH	9.127 0.041		
147 49	GH	9.167 0.039		
146 49	GH	8.919 0.037		
145 49	GH	9.183 0.042		
144 49	GH	9.001 0.038		
143 49	GH	8.764 0.039		
142 49	GH	8.881 0.038		
141 49	GH	8.795 0.041		
138 49	GH	8.338 0.038		
137 49	GH	7.844 0.036		
136 49	GH	7.810 0.035		

TABLE 5.2 (contd)

Matrix	Loc[a]	$^{235}U(n,f)$[b]	$^{238}U(n,f)$[b]	$^{238}U(n,\gamma)$[b]
135 49	GH	7.627 0.036		
134 49	GH	7.363 0.034		
133 49	GH	7.460 0.033		
130 49	GH	6.578 0.032		
129 49	GH	6.327 0.029		
128 49	GH	5.868 0.029		
127 49	GH	5.706 0.026		
126 49	GH	5.410 0.025		
125 49	CD	4.976 0.029	0.1476 0.0023	0.6730 0.0040
124 49	HI	4.548 0.026	0.1394 0.0021	0.6133 0.0040
123 49	CD	4.173 0.023	0.1287 0.0022	0.5670 0.0041
122 49	HI	3.707 0.023	0.1131 0.0019	0.5045 0.0035
121 49	HI	3.178 0.020	0.0989 0.0018	0.4354 0.0032
120 49	CD	2.668 0.015	0.0784 0.0018	0.3758 0.0029
119 49	HI	2.211 0.015	0.0580 0.0016	0.3067 0.0027

[a] In-drawer column which designates the foil location in the drawer. The ^{235}U foils were centered 13.8 mm above and the ^{238}U foils were centered on the mid-height of the drawer. All foils were centered 51.6 mm from the reactor midplane except "*" which were at 50.3.

[b] Experimental results in units of 10^{-18} fissions or captures per atom per second at a reactor power of approximately one watt. The second number is one standard deviation of uncertainty. See text for details.

TABLE 5.3 Basic Reaction Rate Data for Axial Distributions in ZPPR-18A

z,mm[a]	Loc[b]	^{239}Pu(n,f)[c]	^{235}U(n,f)[c]	^{238}U(n,f)[c]	^{238}U(n,γ)[c]
	data in matrix position 149 49				
26.2	GH	8.856 0.048	9.294 0.037	0.2193 0.0026	1.3440 0.0066
50.3	GH	8.834 0.042	9.273 0.037	0.2173 0.0025	1.3368 0.0065
77.0	GH	8.735 0.044	9.191 0.037	0.2293 0.0038	1.3241 0.0070
127.8	GH	8.519 0.042	9.005 0.037	0.2112 0.0027	1.3027 0.0067
178.6	GH	8.231 0.040	8.664 0.036	0.2017 0.0027	1.2523 0.0064
229.4	GH	7.799 0.039	8.217 0.035	0.1932 0.0025	1.1912 0.0061
280.2	GH	7.263 0.034	7.699 0.033	0.1751 0.0024	1.1094 0.0062
356.4	GH	6.390 0.033	6.803 0.030	0.1567 0.0023	0.9915 0.0054
380.5	GH	6.064 0.030	6.603 0.030	0.1444 0.0021	0.9360 0.0050
432.6	GH	5.320 0.028	5.781 0.026	0.1212 0.0021	0.8464 0.0046
483.4	GH	4.728 0.026	5.231 0.026	0.0966 0.0018	0.7704 0.0043
534.2	GH		4.840 0.022	0.0449 0.0017	0.7109 0.0042
585.0	GH		4.329 0.021	0.0253 0.0012	0.6348 0.0039
635.8	GH		3.785 0.019	0.0158 0.0011	0.5603 0.0035
686.6	GH		3.347 0.018	0.0110 0.0012	0.4994 0.0033
737.4	GH		2.987 0.016	0.0071 0.0010	0.4497 0.0032
839.0	TC		3.219 0.017		
889.8	TC		3.046 0.017		
	data in matrix position 149 75				
26.2	FG		4.938 0.023	0.1455 0.0021	0.7037 0.0040
50.3	FG		4.917 0.023	0.1438 0.0023	0.6969 0.0040
77.0	FG		4.890 0.022	0.1450 0.0028	0.6921 0.0046
127.8	FG		4.725 0.023	0.1377 0.0028	0.6745 0.0041
178.6	FG		4.593 0.023	0.1316 0.0023	0.6465 0.0040
229.4	FG		4.310 0.020	0.1248 0.0023	0.6141 0.0038
280.2	FG		4.038 0.019	0.1163 0.0024	0.5694 0.0038
331.0	FG		3.677 0.017	0.1040 0.0025	0.5233 0.0038
381.8	FG		3.312 0.018	0.0904 0.0022	0.4769 0.0032
432.6	FG		2.989 0.018	0.0790 0.0019	0.4283 0.0030
483.4	FG		2.594 0.016	0.0610 0.0017	0.3838 0.0029
534.2	FG		2.418 0.014	0.0284 0.0014	0.3309 0.0025
585.0	FG		2.147 0.012	0.0149 0.0011	0.2937 0.0027
635.8	FG		1.884 0.011	0.0100 0.0011	0.2546 0.0022
686.6	FG		1.654 0.011	0.0070 0.0009	0.2210 0.0020
737.4	FG		1.485 0.010		
839.0	TC		1.556 0.011		
889.8	TC		1.492 0.010		
	data in matrix position 146 57				
26.2	GH		8.974 0.036		
50.3	GH		8.919 0.036		
77.0	GH		8.905 0.036		
127.8	GH		8.684 0.036		

TABLE 5.3 (contd)

z, mm[a]	Loc[b]	$^{239}Pu(n,f)^{c}$	$^{235}U(n,f)^{c}$	$^{238}U(n,f)^{c}$	$^{238}U(n,\gamma)^{c}$
178.6	GH		8.290 0.036		
229.4	GH		7.916 0.034		
280.2	GH		7.436 0.031		
331.0	GH		6.848 0.031		
381.8	GH		6.310 0.028		
432.6	GH		5.690 0.027		
483.4	GH		5.183 0.024		
534.2	GH		5.026 0.024		
585.0	GH		4.580 0.021		
635.8	GH		4.088 0.021		
686.6	GH		3.708 0.019		
737.4	GH		3.379 0.019		

[a]Distance from the reactor interface to the center of the foil.
[b]In-drawer column which designates the foil location in the drawer. The ^{235}U foils were centered 13.8 mm above, the ^{238}U foils were centered on, and the ^{239}Pu foils were centered 13.8 mm below the mid-height of the drawer.
[c]Experimental results in units of 10^{-18} fissions or captures per atom per second at a reactor power of approximately one watt. The second number is one standard deviation uncertainty. See text for details.

TABLE 5.4 Basic Data for Radial Distributions of $^{239}Pu(n,f)$ in ZPPR-18B

Matrix	Loc[a]	$^{239}Pu(n,f)$[b]	Matrix	Loc[b]	$^{239}Pu(n,f)$
x-axis data at z = 51.6 mm[c]			15° data at z = 51.6 mm[c]		
249 50	IJ	8.333 0.040	248 50	IJ	8.316 0.040
249 51	IJ	8.075 0.040	248 52	IJ	7.973 0.038
249 52	IJ	8.139 0.038	248 53	IJ	8.002 0.038
249 53	IJ	7.855 0.036	247 54	IJ	7.688 0.037
249 54	IJ	7.864 0.040	247 56	IJ	7.350 0.034
249 55	IJ	7.579 0.038	247 57	IJ	7.330 0.037
249 56	IJ	7.508 0.037	246 57	IJ*	6.771 0.034
249 57	IJ	7.450 0.037	246 58	IJ	6.930 0.037
249 58	IJ	7.607 0.038	246 59	IJ	7.082 0.037
249 59	IJ	7.616 0.038	246 60	IJ	7.417 0.038
249 60	IJ	7.485 0.038	245 60	IJ	7.146 0.037
249 61	IJ	7.680 0.040	245 61	IJ	7.516 0.038
249 62	IJ	7.674 0.039	245 62	IJ	7.300 0.037
249 63	IJ	7.503 0.042	244 63	IJ	7.194 0.035
249 64	IJ*	7.643 0.040	244 64	IJ	7.260 0.037
249 65	IJ	7.468 0.038	244 65	IJ	7.032 0.035
249 66	IJ	7.144 0.036	244 66	IJ	6.978 0.036
249 67	IJ	7.049 0.036	243 67	IJ	6.565 0.034
249 68	IJ	6.651 0.035	243 68	IJ	6.336 0.034
249 69	IJ	6.543 0.034	243 69	IJ	5.757 0.032
249 70	IJ	6.115 0.033	243 70	IJ	5.204 0.029
249 71	IJ	5.927 0.032	242 70	IJ	4.899 0.028
249 72	IJ	5.529 0.031	242 73	IJ	3.907 0.024
249 73	IJ	5.285 0.031	241 73	IJ	3.898 0.024
249 74	JK	4.928 0.031	241 74	IJ	3.913 0.024
249 75	JK*	4.443 0.024	241 75	JK	3.699 0.024
249 76	IJ	3.825 0.025	241 76	IJ	3.298 0.021
249 77	IJ	3.290 0.021	240 77	IJ	2.715 0.019

[a] In-drawer column which designates the foil location in the drawer. The ^{239}Pu foils were centered 13.8 mm below the mid-height of the drawer. All foils were centered 51.6 mm from the reactor midplane except "*" which were at 50.3 mm.

[b] Experimental results in units of 10^{-18} fissions per atom per second at a reactor power of approximately one watt. The second number is one standard deviation uncertainty. See text for details.

TABLE 5.5 Basic Data for Radial Distributions of $^{235}U(n,f)$ in Half 2 of ZPPR-18B

Matrix	Loc[a]	$^{235}U(n,f)$[b]	$^{238}U(n,f)$[b]	$^{238}U(n,\gamma)$[b]
	data on the x-axis at z = 280.2 mm[c]			
249 50	IJ	6.777 0.022	0.1557 0.0026	0.9749 0.0053
249 51	IJ	6.564 0.032	0.1542 0.0024	0.8273 0.0050
249 52	IJ	6.539 0.033	0.1552 0.0024	0.9285 0.0055
249 53	IJ	6.281 0.031	0.1542 0.0025	0.7905 0.0045
249 54	IJ	6.281 0.032	0.1599 0.0025	0.8974 0.0052
249 55	IJ	5.971 0.032	0.1458 0.0026	0.7453 0.0046
249 56	IJ	5.970 0.030	0.1439 0.0027	0.8589 0.0048
249 57	IJ	5.848 0.029	0.1350 0.0025	0.7292 0.0042
249 58	IJ	6.062 0.029	0.1460 0.0028	0.8699 0.0053
249 59	IJ	6.119 0.032	0.1516 0.0026	0.8683 0.0056
249 60	IJ	6.005 0.029	0.1499 0.0026	0.7610 0.0044
249 61	IJ	6.261 0.030	0.1522 0.0029	0.9027 0.0050
249 62	IJ	6.359 0.030	0.1502 0.0029	0.9182 0.0051
249 63	IJ	6.150 0.030	0.1454 0.0025	0.7744 0.0049
249 64	IJ		0.1490 0.0029	0.9118 0.0054
249 65	IJ	6.194 0.021	0.1467 0.0025	0.8893 0.0049
249 66	IJ	5.984 0.031	0.1398 0.0026	0.7393 0.0046
249 67	IJ	5.837 0.031	0.1374 0.0025	0.8337 0.0047
249 68	IJ	5.497 0.030	0.1302 0.0023	0.6863 0.0040
249 69	IJ	5.349 0.028	0.1282 0.0025	0.7642 0.0044
249 70	IJ	4.987 0.028	0.1211 0.0027	0.6243 0.0041
249 71	IJ	4.773 0.026	0.1149 0.0024	0.6767 0.0045
249 72	IJ	4.439 0.025	0.1098 0.0023	0.5562 0.0035
249 73	IJ	4.236 0.023	0.1118 0.0023	0.6046 0.0037
249 74	JK	3.943 0.024	0.1109 0.0025	0.5515 0.0035
249 76	IJ	3.147 0.018	0.0851 0.0021	0.4464 0.0029
249 77	IJ	2.723 0.016	0.0618 0.0017	0.3902 0.0032
249 78	IJ	2.318 0.018		
249 79	IJ	1.934 0.014		
249 80	IJ	1.554 0.013		
249 81	IJ	1.277 0.012		
249 82	IJ	1.075 0.009		
	data on the 15° radial at z = 280.2 mm[c]			
248 50	IJ	6.682 0.033	0.1594 0.0025	0.9550 0.0052
248 52	IJ	6.375 0.032	0.1531 0.0024	0.7954 0.0047
248 53	IJ	6.314 0.031	0.1531 0.0023	0.9010 0.0049
247 54	IJ	6.022 0.031	0.1486 0.0025	0.8715 0.0048
247 56	IJ	5.536 0.032	0.1384 0.0025	0.8089 0.0046
247 57	IJ	5.440 0.027	0.1359 0.0026	0.8052 0.0047
246 58	IJ	5.175 0.027	0.1199 0.0024	0.6226 0.0038
246 59	IJ	5.451 0.028	0.1229 0.0026	0.7617 0.0044
246 60	IJ	5.829 0.029	0.1299 0.0024	0.7000 0.0042
245 60	IJ	5.575 0.028	0.1334 0.0023	0.7123 0.0041
245 61	IJ	5.922 0.029		

TABLE 5.5 (contd)

Matrix	Loc[a]	$^{235}U(n,f)$[b]	$^{238}U(n,f)$[b]	$^{238}U(n,\gamma)$[b]
245 62	IJ	5.941 0.031	0.1423 0.0024	0.7561 0.0044
244 63	IJ	5.918 0.029	0.1377 0.0024	0.7408 0.0043
244 64	IJ	5.956 0.031		
244 65	IJ	5.771 0.030	0.1358 0.0024	0.7176 0.0042
244 66	IJ	5.709 0.030		
243 67	IJ	5.344 0.029	0.1268 0.0022	0.7740 0.0044
243 68	IJ	5.042 0.027	0.1236 0.0024	0.7222 0.0045
243 69	IJ	4.433 0.026	0.1074 0.0024	0.5621 0.0036
243 70	IJ	3.846 0.024	0.0998 0.0023	0.5609 0.0036
242 70	IJ	3.678 0.024	0.0870 0.0021	0.4677 0.0034
242 73	IJ	2.717 0.017	0.0751 0.0020	0.3884 0.0030
241 73	IJ	2.870 0.018	0.0774 0.0021	0.3994 0.0031
241 74	IJ	2.927 0.019	0.0788 0.0020	0.4153 0.0029
241 75	JK	2.806 0.019	0.0819 0.0020	0.3988 0.0028
241 76	IJ	2.551 0.015	0.0694 0.0019	0.3630 0.0026
240 77	IJ	2.196 0.014	0.0528 0.0014	0.3185 0.0026
240 78	IJ	1.866 0.015		
240 79	IJ	1.532 0.013		
239 80	IJ	1.197 0.011		
239 81	IJ	0.950 0.010		
239 82	IJ	0.801 0.007		
data on the 30° radial at z = 280.2 mm[c]				
246 54	IJ	5.645 0.029		
245 55	IJ	4.763 0.026		
244 58	IJ	4.425 0.024		
243 58	IJ	4.788 0.026		
243 59	IJ	5.240 0.026		
242 60	IJ	5.659 0.029		
242 61	IJ	5.980 0.030		
242 62	IJ	6.096 0.030		
241 62	IJ	6.118 0.030		
240 65	IJ	5.802 0.030		
239 65	IJ	5.749 0.029		
239 66	IJ	5.156 0.026		
238 67	IJ	4.684 0.025		
238 68	IJ	4.604 0.025		
237 68	IJ	4.317 0.025		
data on the x-axis at z = 51.6 mm[c]				
249 50	IJ	8.771 0.027	0.2063 0.0030	1.2621 0.0065
249 51	IJ	8.511 0.037	0.2031 0.0030	1.0684 0.0058
249 52	IJ	8.557 0.036	0.2063 0.0029	1.2196 0.0063
249 53	IJ	8.272 0.036	0.2046 0.0031	1.0310 0.0055
249 54	IJ	8.271 0.035	0.2122 0.0030	1.1797 0.0066
249 55	IJ	7.955 0.038	0.1984 0.0030	1.0007 0.0060
249 56	IJ	7.978 0.025	0.1931 0.0028	1.1479 0.0066

TABLE 5.5 (contd)

Matrix	Loc[a]	$^{235}U(n,f)$[b]	$^{238}U(n,f)$[b]	$^{238}U(n,\gamma)$[b]
249 57	IJ	7.792 0.035	0.1844 0.0027	0.9784 0.0053
249 58	IJ	7.981 0.036	0.1936 0.0026	1.1367 0.0063
249 59	IJ	8.023 0.036	0.2017 0.0028	1.1395 0.0065
249 60	IJ	7.832 0.035	0.1951 0.0028	0.9816 0.0058
249 61	IJ	8.094 0.038	0.1938 0.0029	1.1446 0.0065
249 62	IJ	8.094 0.037	0.1955 0.0029	1.1559 0.0066
249 63	IJ	7.939 0.036	0.1886 0.0027	0.9856 0.0063
249 64	IJ*		0.1937 0.0027	1.1465 0.0059
249 65	IJ	7.883 0.031	0.1905 0.0029	1.1112 0.0063
249 66	IJ	7.496 0.033	0.1825 0.0026	0.9329 0.0055
249 67	IJ	7.393 0.033	0.1737 0.0025	1.0418 0.0059
249 68	IJ	7.002 0.032	0.1660 0.0026	0.8691 0.0052
249 69	IJ	6.836 0.031	0.1640 0.0026	0.9716 0.0052
249 70	IJ	6.417 0.029	0.1527 0.0026	0.8073 0.0048
249 71	IJ	6.151 0.028	0.1518 0.0023	0.8734 0.0048
249 72	IJ	5.741 0.026	0.1457 0.0024	0.7188 0.0042
249 73	IJ	5.548 0.026	0.1419 0.0024	0.7890 0.0045
249 74	JK	5.131 0.024	0.1404 0.0023	0.7191 0.0044
249 76	IJ	4.061 0.020	0.1093 0.0020	0.5735 0.0037
249 77	IJ	3.535 0.019	0.0825 0.0019	0.5080 0.0035
249 78	IJ	3.049 0.019	0.0366 0.0012	0.3704 0.0031
249 79	IJ	2.473 0.015	0.0201 0.0010	0.2940 0.0025
249 80	IJ	1.995 0.013	0.0118 0.0009	0.2273 0.0023
249 81	IJ	1.613 0.011	0.0069 0.0008	0.1763 0.0019
249 82	IJ	1.392 0.011	0.0043 0.0008	0.1423 0.0016
249 83	TC	1.431 0.011		
data on the 15° radial at z = 51.6 mm[c]				
248 50	IJ	8.635 0.041	0.2086 0.0031	1.2542 0.0068
248 52	IJ	8.332 0.036	0.2029 0.0029	1.0452 0.0060
248 53	IJ	8.329 0.036	0.2078 0.0028	1.1829 0.0066
247 54	IJ	8.060 0.038	0.2009 0.0029	1.1470 0.0070
247 56	IJ	7.582 0.033	0.1856 0.0025	1.1047 0.0058
247 57	IJ	7.484 0.033	0.1834 0.0027	1.0800 0.0061
246 57	IJ*		0.1642 0.0026	0.8722 0.0048
246 58	IJ	7.131 0.032	0.1729 0.0026	1.0265 0.0060
246 59	IJ	7.346 0.032	0.1781 0.0029	0.9288 0.0055
246 60	IJ	7.764 0.037	0.1844 0.0027	1.0998 0.0062
245 60	IJ	7.480 0.035	0.1790 0.0026	0.9384 0.0056
245 61	IJ	7.759 0.036	0.1891 0.0028	1.0939 0.0066
245 62	IJ	7.637 0.034	0.1865 0.0027	0.9628 0.0056
244 63	IJ	7.564 0.034	0.1796 0.0027	0.9417 0.0061
244 64	IJ	7.675 0.034	0.1813 0.0028	1.0837 0.0062
244 65	IJ	7.364 0.032	0.1711 0.0026	0.9150 0.0054
244 66	IJ	7.317 0.033	0.1747 0.0027	1.0449 0.0060
243 67	IJ	6.959 0.031	0.1698 0.0026	0.9874 0.0057
243 68	IJ	6.571 0.033	0.1607 0.0024	0.9452 0.0055
243 69	IJ	5.939 0.029	0.1465 0.0028	0.7521 0.0043

TABLE 5.5 (contd)

Matrix	Loc[a]	$^{235}U(n,f)$[b]	$^{238}U(n,f)$[b]	$^{238}U(n,\gamma)$[b]
243 70	IJ	5.317 0.025	0.1284 0.0023	0.7774 0.0044
242 70	IJ	5.074 0.027	0.1221 0.0022	0.6466 0.0041
242 73	IJ	3.998 0.021	0.1058 0.0022	0.5790 0.0039
241 73	IJ	4.140 0.022	0.1049 0.0022	0.5826 0.0036
241 74	IJ	4.087 0.021	0.1124 0.0023	0.5822 0.0036
241 75	JK	3.839 0.020	0.1139 0.0022	0.5498 0.0034
241 76	IJ	3.434 0.019	0.0950 0.0020	0.4862 0.0031
240 77	IJ	2.898 0.016	0.0714 0.0016	0.4228 0.0028
240 78	IJ	2.486 0.016	0.0316 0.0012	0.2985 0.0028
240 79	IJ	2.057 0.014	0.0181 0.0010	0.2458 0.0025
239 80	IJ	1.569 0.012	0.0095 0.0009	0.1782 0.0018
239 81	IJ	1.257 0.010	0.0060 0.0008	0.1363 0.0016
239 82	IJ	1.065 0.009	0.0032 0.0009	0.1107 0.0017
data on the 30° radial at z = 51.6 mm[c]				
246 54	IJ	7.658 0.035	0.1846 0.0026	0.9696 0.0052
245 55	IJ	6.755 0.034	0.1651 0.0027	0.8764 0.0049
244 58	IJ	6.286 0.031	0.1489 0.0028	0.8122 0.0047
243 58	IJ	6.736 0.031	0.1591 0.0028	0.9480 0.0052
243 59	IJ	7.140 0.032	0.1682 0.0029	0.9008 0.0050
242 60	IJ	7.430 0.035	0.1763 0.0029	0.9364 0.0052
242 61	IJ	7.727 0.034	0.1819 0.0029	1.1016 0.0058
242 62	IJ	7.766 0.034	0.1763 0.0029	1.1138 0.0059
241 62	IJ	7.827 0.036	0.1697 0.0028	1.1269 0.0059
240 65	IJ	7.361 0.035	0.1579 0.0026	0.9087 0.0050
239 65	IJ	7.324 0.036	0.1612 0.0026	1.0702 0.0057
239 66	IJ	6.710 0.035	0.1581 0.0030	0.8383 0.0048
238 67	IJ	6.144 0.031	0.1478 0.0026	0.7727 0.0048
238 68	IJ	6.039 0.036	0.1502 0.0027	0.8636 0.0048
237 68	IJ	5.690 0.031	0.1450 0.0028	0.7313 0.0047
data on the y-axis at z = 51.6 mm[c]				
247 49	IJ	8.619 0.041		
246 49	IJ	8.323 0.039		
245 49	IJ	8.372 0.039		
244 49	IJ	8.128 0.038		
243 49	IJ	7.498 0.036		
242 49	IJ	7.120 0.035		
241 49	IJ	6.131 0.029		
238 49	IJ	6.671 0.031		
237 49	IJ	7.098 0.033		
236 49	IJ	7.586 0.034		
235 49	IJ	7.732 0.036		
234 49	IJ	7.555 0.035		
233 49	IJ	7.933 0.037		
230 49	IJ	7.071 0.033		

TABLE 5.5 (contd)

Matrix	Loc[a]	$^{235}U(n,f)$[b]	$^{238}U(n,f)$[b]	$^{238}U(n,\gamma)$[b]
229 49	IJ	6.737 0.033		
228 49	IJ	6.331 0.030		
227 49	IJ	6.109 0.029		
226 49	IJ	5.778 0.030		
225 49	MN	5.273 0.025		
224 49	HI	4.890 0.025		
223 49	MN	4.528 0.024		
222 49	HI	4.000 0.023		
221 49	HI	3.469 0.019		
220 49	MN	2.948 0.018		
219 49	HI	2.439 0.017		

[a]In-drawer column which designates the foil location in the drawer. The ^{235}U foils were centered 13.8 mm above and the ^{238}U foils were centered on the mid-height of the drawer.

[b]Experimental results in units of 10^{-18} fissions per atom per second at a reactor power of approximately one watt. The second number is one standard deviation of uncertainty. See text for details.

[c]Distance from the reactor interface to the center of the foil except "*" which were at 50.3 mm.

TABLE 5.6 Basic Data for Radial Distributions of $^{235}U(n,f)$ in Half 1 of ZPPR-18B

Matrix	Loc[a]	$^{235}U(n,f)$[b]	$^{235}U(n,f)$[b]
x-axis data at		z = 51.6 mm,[c]	z = 280.2 mm[c]
149 50	GH	9.040 0.042	7.962 0.040
149 51	GH	8.761 0.042	7.730 0.039
149 52	GH	8.781 0.045	7.800 0.039
149 53	GH	8.593 0.041	7.631 0.038
149 54	GH	8.624 0.040	7.752 0.038
149 55	GH	8.312 0.039	7.491 0.039
149 56	GH	8.409 0.026	7.578 0.024
149 57	GH	8.202 0.036	7.399 0.033
149 58	GH	8.375 0.037	7.528 0.033
149 59	GH	8.375 0.038	7.412 0.034
149 60	GH	8.174 0.038	7.151 0.033
149 61	GH	8.320 0.039	7.278 0.035
149 62	GH	8.279 0.038	7.275 0.035
149 63	GH	8.097 0.039	7.051 0.035
149 65	GH	8.025 0.026	6.950 0.023
149 66	GH	7.618 0.035	6.558 0.031
149 67	GH	7.567 0.035	6.510 0.030
149 68	GH	7.147 0.033	6.183 0.030
149 69	GH	6.977 0.033	6.046 0.030
149 70	GH	6.568 0.030	5.655 0.028
149 71	GH	6.375 0.031	5.481 0.029
149 72	GH	5.931 0.030	5.087 0.027
149 73	FG	5.656 0.030	4.917 0.026
149 74	GH	5.256 0.029	4.555 0.026
149 76	GH	4.184 0.024	3.620 0.023
149 77	GH	3.622 0.022	3.145 0.020
149 78	GH	3.071 0.017	2.641 0.016
149 79	GH	2.538 0.016	2.204 0.015
149 80	GH	2.027 0.016	1.725 0.013
149 81	GH	1.662 0.011	1.424 0.012
149 82	GH	1.410 0.013	1.231 0.012
15° data at		z = 51.6 mm,[c]	z = 280.2 mm[c]
148 50	GH	8.978 0.043	
148 52	GH	8.651 0.043	7.678 0.038
148 53	GH	8.687 0.042	7.728 0.041
147 54	GH	8.535 0.042	7.721 0.040
147 55	GH	8.117 0.036	7.493 0.034
147 56	GH	8.292 0.038	7.602 0.034
147 57	GH	8.218 0.037	7.612 0.033
146 58	GH	8.036 0.035	7.642 0.035
146 59	GH	7.912 0.036	7.213 0.034
146 60	GH	8.120 0.038	

TABLE 5.6 (contd)

Matrix	Loc[a]	$^{235}U(n,f)$[b]		$^{235}U(n,f)$[b]	
145 60	GH	7.931	0.037	7.042	0.032
145 61	GH	8.146	0.040	7.105	0.035
145 62	GH	7.932	0.037	6.877	0.033
144 63	GH	7.816	0.038	6.720	0.034
144 64	GH	7.793	0.037	6.757	0.033
144 65	GH	7.488	0.034	6.483	0.033
144 66	GH	7.523	0.034	6.436	0.033
143 67	GH	7.143	0.033	6.273	0.030
143 68	GH	6.903	0.032	6.064	0.030
143 69	GH	6.345	0.031	5.748	0.028
143 70	GH	6.067	0.031	5.676	0.029
142 70	GH	5.840	0.030	5.520	0.028
142 73	GH	5.037	0.026	4.947	0.026
141 73	GH	5.008	0.025	4.826	0.024
141 74	GH	4.565	0.024	4.259	0.024
141 75	FG	4.141	0.026	3.757	0.023
141 76	GH	3.597	0.022	3.237	0.021
140 77	GH	3.049	0.020	2.665	0.017
140 78	GH	2.566	0.018		
140 79	GH	2.071	0.013		
139 80	GH	1.599	0.014		
139 81	GH	1.262	0.013		
139 82	GH	1.091	0.011		

[a] In-drawer column which designates the foil location in the drawer. The ^{235}U foils were centered 13.8 mm above the mid-height of the drawer.

[b] Experimental results in units of 10^{-18} fissions per atom per second at a reactor power of approximately one watt. The second number is one standard deviation uncertainty. See text for details.

[c] Distance from the reactor interface to the center of the foil.

TABLE 5.7 Basic Data for Axial Distributions of ^{239}Pu and ^{238}U Reaction Rates in ZPPR-18B

Matrix	z,mm[a]	Loc[b]	$^{239}Pu(n,f)$[c]	$^{238}U(n,f)$[c]	$^{238}U(n,\gamma)$[c]
249 49	737.4	IJ		0.0066 0.0011	0.3440 0.0027
249 49	686.6	IJ		0.0102 0.0013	0.3853 0.0027
249 49	635.8	IJ		0.0138 0.0011	0.4371 0.0029
249 49	585.0	IJ		0.0225 0.0013	0.5077 0.0033
249 49	534.2	IJ		0.0354 0.0015	0.5757 0.0036
249 49	483.4	IJ	3.928 0.023	0.0833 0.0020	0.6322 0.0037
249 49	432.6	IJ	4.532 0.025	0.1018 0.0021	0.7114 0.0040
249 49	380.5	IJ	5.212 0.028	0.1251 0.0022	0.8063 0.0049
249 49	356.4	IJ	5.450 0.029	0.1361 0.0025	0.8441 0.0050
249 49	280.2	IJ	6.380 0.033	0.1568 0.0031	0.9700 0.0056
249 49	229.4	IJ	6.935 0.034	0.1742 0.0026	1.0521 0.0058
249 49	178.6	IJ	7.438 0.037	0.1828 0.0028	1.1339 0.0059
249 49	127.8	IJ	7.822 0.039	0.1933 0.0031	1.1869 0.0062
249 49	77.0	IJ	8.175 0.038	0.2074 0.0029	1.2411 0.0075
249 49	50.3	IJ	8.321 0.042	0.2041 0.0028	1.2557 0.0064
249 49	26.2	IJ	8.500 0.042	0.2128 0.0029	1.2686 0.0064
149 49	26.2	GH	8.663 0.040	0.2123 0.0029	1.2899 0.0065
149 49	50.3	GH	8.527 0.041	0.2145 0.0029	1.2955 0.0066
149 49	77.0	GH	8.582 0.041	0.2167 0.0029	1.3037 0.0066
149 49	127.8	GH	8.525 0.044	0.2121 0.0028	1.2895 0.0065
149 49	178.6	GH	8.298 0.042	0.2053 0.0029	1.2568 0.0064
149 49	229.4	GH	8.019 0.040	0.2008 0.0029	1.2059 0.0062
149 49	280.2	GH	7.513 0.036	0.1881 0.0031	1.1546 0.0061
149 49	356.4	GH	6.688 0.033	0.1631 0.0026	1.0324 0.0054
149 49	380.5	GH	6.317 0.031	0.1533 0.0028	0.9787 0.0057
149 49	432.6	GH	5.667 0.030	0.1338 0.0025	0.8914 0.0049
149 49	483.4	GH	5.014 0.028	0.1077 0.0023	0.8066 0.0056
149 49	534.2	GH		0.0475 0.0017	0.7540 0.0043
149 49	585.0	GH		0.0284 0.0012	0.6846 0.0039
149 49	635.8	GH		0.0177 0.0011	0.6018 0.0036
149 49	686.6	GH		0.0114 0.0010	0.5335 0.0033
149 49	737.4	GH		0.0077 0.0010	0.4763 0.0033
249 75	686.6	JK		0.0058 0.0009	0.1774 0.0019
249 75	635.8	JK		0.0090 0.0012	0.2075 0.0018
249 75	585.0	JK		0.0132 0.0011	0.2423 0.0020
249 75	534.2	JK		0.0238 0.0013	0.2727 0.0022
249 75	483.4	JK		0.0526 0.0017	0.3203 0.0024
249 75	432.6	JK		0.0659 0.0020	0.3595 0.0026
249 75	381.8	JK		0.0807 0.0022	0.4075 0.0028
249 75	331.0	JK		0.0949 0.0022	0.4634 0.0034
249 75	280.2	JK		0.1057 0.0025	0.5036 0.0032
249 75	229.4	JK		0.1141 0.0025	0.5576 0.0035
249 75	178.6	JK		0.1219 0.0024	0.5884 0.0036
249 75	127.8	JK		0.1299 0.0026	0.6213 0.0038

TABLE 5.7 (contd)

Matrix	z,mm[a]	Loc[b]	$^{239}Pu(n,f)$[c]	$^{238}U(n,f)$[c]	$^{238}U(n,\gamma)$[c]
249 75	77.0	JK		0.1334 0.0023	0.6395 0.0040
249 75	50.3	JK		0.1352 0.0024	0.6490 0.0038
249 75	26.2	JK		0.1370 0.0022	0.6568 0.0041
149 75	26.2	FG		0.1405 0.0028	0.6762 0.0040
149 75	50.3	FG		0.1397 0.0027	0.6758 0.0040
149 75	77.0	FG		0.1419 0.0025	0.6707 0.0039
149 75	127.8	FG		0.1393 0.0027	0.6621 0.0039
149 75	178.6	FG		0.1328 0.0025	0.6439 0.0039
149 75	229.4	FG		0.1274 0.0023	0.6164 0.0041
149 75	280.2	FG		0.1210 0.0024	0.5798 0.0036
149 75	331.0	FG		0.1090 0.0022	0.5377 0.0034
149 75	381.8	FG		0.0976 0.0021	0.4905 0.0036
149 75	432.6	FG		0.0820 0.0020	0.4386 0.0029
149 75	483.4	FG		0.0646 0.0016	0.3957 0.0027
149 75	534.2	FG		0.0277 0.0012	0.3437 0.0027
149 75	585.0	FG		0.0164 0.0015	0.3082 0.0023
149 75	635.8	FG		0.0121 0.0010	0.2705 0.0022
149 75	686.6	FG		0.0074 0.0009	0.2382 0.0020

[a]Distance from the reactor interface to the center of the foil.
[b]In-drawer column which designates the foil location in the drawer. The ^{238}U foils were centered on and the ^{239}Pu foils were centered 13.8 mm below the mid-height of the drawer.
[c]Experimental results in units of 10^{-18} fissions or captures per atom per second at a reactor power of approximately one watt. The second number is one standard deviation uncertainty. See text for details.

TABLE 5.8 Basic Data for Axial Distributions of $^{235}U(n,f)$ in ZPPR-18B

Matrix	z,mm[a]	Loc[b]	$^{235}U(n,f)$[c]	Matrix	Loc[b]	$^{235}U(n,f)$[c]
249 49	737.4	IJ	2.306 0.014	249 64	IJ	2.231 0.016
249 49	686.6	IJ	2.609 0.016	249 64	IJ	2.497 0.017
249 49	635.8	IJ	2.999 0.017	249 64	IJ	2.907 0.017
249 49	585.0	IJ	3.483 0.019	249 64	IJ	3.348 0.020
249 49	534.2	IJ	3.937 0.022	249 64	IJ	3.763 0.021
249 49	483.4	IJ	4.327 0.022	249 64	IJ	4.108 0.023
249 49	432.6	IJ	4.919 0.023	249 64	IJ	4.645 0.025
249 49	380.5	IJ	5.584 0.026	249 64	IJ	5.257 0.027
249 49	356.4	IJ	5.891 0.027	249 64	IJ	5.796 0.029
249 49	280.2	IJ	6.804 0.031	249 64	IJ	6.333 0.032
249 49	229.4	IJ	7.348 0.032	249 64	IJ	6.785 0.031
249 49	178.6	IJ	7.846 0.036	249 64	IJ	7.273 0.035
249 49	127.8	IJ	8.286 0.036	249 64	IJ	7.664 0.036
249 49	77.0	IJ	8.721 0.037	249 64	IJ	7.914 0.040
249 49	50.3	IJ	8.782 0.036	249 64	IJ	8.038 0.035
249 49	26.2	IJ	8.887 0.037	249 64	IJ	8.097 0.037
149 49	26.2	GH	9.087 0.038	149 64	GH	8.185 0.039
149 49	50.3	GH	9.101 0.038	149 64	GH	8.213 0.041
149 49	77.0	GH	9.087 0.038	149 64	GH	8.127 0.034
149 49	127.8	GH	9.004 0.037	149 64	GH	8.080 0.039
149 49	178.6	GH	8.783 0.037	149 64	GH	7.823 0.035
149 49	229.4	GH	8.444 0.035	149 64	GH	7.531 0.038
149 49	280.2	GH	8.017 0.034	149 64	GH	7.085 0.033
149 49	356.4	GH	7.174 0.031	149 64	GH	6.598 0.036
149 49	380.5	GH	6.874 0.030	149 64	GH	5.989 0.030
149 49	432.6	GH	6.175 0.028	149 64	GH	5.472 0.029
149 49	483.4	GH	5.566 0.026	149 64	GH	4.866 0.025
149 49	534.2	GH	5.204 0.026	149 64	GH	4.543 0.024
149 49	585.0	GH	4.669 0.024	149 64	GH	4.073 0.023
149 49	635.8	GH	4.116 0.021	149 64	GH	3.636 0.021
149 49	686.6	GH	3.622 0.019	149 64	GH	3.183 0.020
149 49	737.4	GH	3.300 0.018	149 64	GH	2.860 0.018
249 75	737.4	JK	1.171 0.011	246 57	IJ	1.376 0.011
249 75	686.6	JK	1.309 0.011	246 57	IJ	1.562 0.011
249 75	635.8	JK	1.508 0.014	246 57	IJ	1.824 0.014
249 75	585.0	JK	1.751 0.014	246 57	IJ	2.146 0.014
249 75	534.2	JK	2.002 0.015	246 57	IJ	2.530 0.017
249 75	483.4	JK	2.198 0.016	246 57	IJ	2.813 0.016
249 75	432.6	JK	2.507 0.017	246 57	IJ	3.279 0.020
249 75	381.8	JK	2.898 0.020	246 57	IJ	3.726 0.021
249 75	331.0	JK	3.223 0.019	246 57	IJ	4.149 0.022
249 75	280.2	JK	3.551 0.020	246 57	IJ	4.624 0.024
249 75	229.4	JK	3.912 0.024	246 57	IJ	5.052 0.025
249 75	178.6	JK	4.140 0.024	246 57	IJ	5.456 0.027

TABLE 5.8 (contd)

Matrix	z,mm[a]	Loc[b]	$^{235}U(n,f)$[c]	Matrix	Loc[b]	$^{235}U(n,f)$[c]
249 75	127.8	JK	4.400 0.025	246 57	IJ	5.822 0.028
249 75	77.0	JK	4.574 0.024	246 57	IJ	6.300 0.030
249 75	50.3	JK	4.674 0.024	246 57	IJ	6.502 0.029
249 75	26.2	JK	4.700 0.023	246 57	IJ	6.877 0.030
149 75	26.2	FG	4.734 0.027	146 57	GH	7.691 0.036
149 75	50.3	FG	4.727 0.026	146 57	GH	7.979 0.038
149 75	77.0	FG	4.794 0.023	146 57	GH	8.155 0.037
149 75	127.8	FG	4.685 0.028	146 57	GH	8.298 0.037
149 75	178.6	FG	4.563 0.023	146 57	GH	8.248 0.037
149 75	229.4	FG	4.394 0.024	146 57	GH	8.031 0.037
149 75	280.2	FG	4.106 0.023	146 57	GH	7.671 0.035
149 75	331.0	FG	3.768 0.021	146 57	GH	7.223 0.032
149 75	381.8	FG	3.462 0.020	146 57	GH	6.670 0.032
149 75	432.6	FG	3.084 0.018	146 57	GH	6.102 0.030
149 75	483.4	FG	2.720 0.017	146 57	GH	5.548 0.028
149 75	534.2	FG	2.537 0.015	146 57	GH	5.429 0.028
149 75	585.0	FG	2.278 0.014	146 57	GH	4.968 0.026
149 75	635.8	FG	2.005 0.013	146 57	GH	4.443 0.023
149 75	686.6	FG	1.734 0.014	146 57	GH	4.011 0.023
149 75	737.4	FG	1.583 0.014	146 57	GH	3.675 0.023

[a]Distance from the reactor interface to the center of the foil.
[b]In-drawer column which designates the foil location in the drawer. The ^{235}U foils were centered 13.8 mm above the mid-height of the drawer.
[c]Experimental results in units of 10^{-18} fissions or captures per atom per second at a reactor power of approximately one watt. The second number is one standard deviation uncertainty. See text for details.

6. IN-CELL REACTION RATE MEASUREMENTS AND CELL FACTORS FOR ZPPR-18A AND ZPPR-18B (J. M. Gasidlo and D. W. Maddison)

6.1 Introduction

Reaction rate maps are measured by placing foils in matrix positions chosen to measure specific distributions as a radial map or an axial distribution. These "mapping" foils are always placed in the same location in a drawer for a specific type of cell. Then, cell factors are used to convert the reaction rates measured in the mapping foil to reaction rates averaged over the materials used to construct the cell.

6.2 Description of the In-Cell Measurements

Cell factors were measured in special experiments where the ordinary plates used to build the reactor were replaced with special plates. Ordinary ZPPR fuel plates were replaced with two half-thickness fuel plates for which the sum of the fuel alloy is equal to one ordinary fuel plate. Foils were placed between and on the outer surfaces of the two half-thickness fuel plates. The 6.35 mm U_3O_8 and 3.175 mm depleted uranium metal plates were replaced with special plates that have slots machined across the width of the plates in which special foils can be placed to measure the integral of the reaction rate across the width of the plate. Because the number of special plates is limited, the 6.35 mm U_3O_8 plates were sometimes replaced with two 3.175 mm U_3O_8 plates (the 3.175 mm depleted uranium metal plates with 1.588 mm plates) and the plate average was measured by a foil placed between the two plates.

The foils were first placed in stainless steel or aluminum holders, or in the slots of the special plates. The foil holders were then placed between the vertical columns* of materials in the drawers. The

*ZPPR drawers are divided into sixteen 3.175 mm (1/8 in.) wide vertical columns designated by letters A through P. The letter A denotes the column at the left as one faces the drawer. The letters FG, for example, indicate the foil is between columns F and G, and is centered 19.050 mm (0.750 in.) from the left side of the drawer.

special plates replaced the normal plates used in the drawers. (These plates are designated by a negative sign in front of the in-drawer column location.) Foils were placed in, between or on the surface of any plates containing the foil material: ^{239}Pu foils are used only at fuel plates whereas ^{235}U and ^{238}U foils are used at fuel plates, depleted uranium metal plates and depleted uranium oxide plates. In all cells at least one foil of each type was placed in the "mapping foil" location.

In ZPPR-18 the cell studies were directed towards measuring cell factors in cells different from those in ZPPR-17 and repeating the cell studies done adjacent to control rod positions (CRPs) and control rods (CRs). Cell studies were not done in the ^{235}U fueled drawers. Measurements of cell factors in ^{235}U fueled cores indicate that the cell factor for $^{235}U(n,f)$ can be set equal to unity ± 1% for the ^{235}U fueled drawers. Cell factors for ^{238}U in the ^{235}U fueled drawers will be measured in a subsequent assembly. For all other types of cells in ZPPR-18, the cell factors from ZPPR-17 were used without change.

For the cell studies adjacent to CRPs and CRs, half of the cell was measured on one side of the CRP (or CR) and half on the other side. Even then, there was not sufficient room in the cell to contain the necessary foils and foil holders. In that case, the column of 6.35 mm U_3O_8 plates on the side of the cell away from the cell studies was replaced with a 3.18 mm column of U_3O_8 plates and a 1.59 mm column of alternating depleted uranium metal and stainless steel plates. This substitution made room for the cell study foils and changed the uranium content in that column by 0.2%.

The basic data for cell studies in the two irradiations in ZPPR-18B were combined and are given in Tables 6.1 and 6.2. The data are given in units of 10^{-18} fission or captures per second per atom in the irradiated foil at an estimated reactor power of one watt. The second number associated with each reaction is one standard deviation estimate of the uncertainty. As described below in Section 6.4 the uncertainties given in the tables are solely due to counting statistics and data reduction. They include the effects of peak integration, interference peak corrections,

corrections for other reactions in the foils, irradiation history and foil positioning in the counter system.

6.3 Derivation of Cell-Averaging Factors

The results of special experiments were used to convert the data from the special plate measurements to in-plate or plate-averaged reaction rates. These plate-averaged reaction rates were divided by calculated values to remove the effects of the gross reactor flux distribution, atom-weighted plate-by-plate to determine the cell-averaged reaction rate, and divided by the mapping foil value to determine the cell factor. This process is described in greater detail in ANL-85-44.

6.4 Discussion of Cell Factors and Uncertainties

The cell factors for ZPPR-18A and 18B are given in Table 6.3. The second number associated with each cell factor is a one standard deviation estimate of the uncertainty. The uncertainties in the cell factors are solely due to propagation of the uncertainties in the basic data tables. They are systematic for the use of a single cell factor, but they are random when applied to the cell-averaged reaction rates for different cell factors. The listed uncertainties do not include systematic uncertainties such as deriving plate-averaged reaction rates from half-thickness plate data or other uncertainties such as those due to detector calibrations. See ANL-85-44 for a discussion of these additional uncertainties.

Under the heading "ENVIRONMENT" is listed the type of cell and cell environment for which the cell factor is applicable. The mapping foil is always located in the center drawer, the center drawer has the two indicated drawers on either side, and the mapping foil is located closer to the left-hand drawer. (See Section 5.2 on the method used for specifying the in-drawer location of mapping foils.) The key is: SF is a drawer with one fuel column that has iron oxide plates on both sides of the fuel plate, SM is a drawer with one fuel column that has depleted uranium metal plates on both sides of the fuel plate, D is a drawer with two fuel columns, F is any fueled drawer, AB is axial blanket, RB is radial blanket, and R is axial

or radial reflector. The code F/SF/RB means that the cell factor is used for a drawer with one fuel column that has iron oxide plates on both sides of the fuel plate with any fueled drawer on one side and a radial blanket drawer on the other with the mapping foil closer to the fueled drawer.

TABLE 6.1. Basic Data for ^{239}Pu(n,f) Cell Studies in ZPPR-18B

Matrix	z,mm[a]	Loc[b]	^{239}Pu(n,f)[c]	Matrix	z,mm[a]	Loc[b]	^{239}Pu(n,f)[c]
244 40	51.6	GH	6.054 0.033	244 43	77.0	GH	6.257 0.033
244 40	51.6	HI	6.121 0.033	244 43	77.0	HI	6.053 0.033
244 40	51.6	IJ	6.292 0.032	244 43	77.0	IJ	5.993 0.033
144 40	254.8	GH	7.078 0.035	144 43	254.8	GH	7.473 0.040
144 40	254.8	HI	7.004 0.033	144 43	254.8	HI	7.277 0.036
144 40	254.8	IJ	7.155 0.034	144 43	254.8	IJ	7.382 0.037
148 37	77.0	GH	7.704 0.038	148 35	77.0	GH	7.769 0.038
148 37	77.0	HI	7.683 0.039	148 35	77.0	HI	7.656 0.037
148 37	77.0	IJ	7.686 0.039	148 35	77.0	IJ	7.749 0.038
148 37	254.8	GH	6.943 0.035	148 35	127.8	GH	7.689 0.039
148 37	254.8	HI	6.923 0.034	148 35	127.8	HI	7.620 0.039
148 37	254.8	IJ	6.979 0.035	148 35	127.8	IJ	7.693 0.037
150 24	77.0	DE	4.727 0.026	148 35	483.4	GH	4.531 0.027
150 24	77.0	EF	4.818 0.026	148 35	483.4	HI	4.394 0.027
150 24	77.0	FG	4.894 0.027	148 35	483.4	IJ	4.610 0.026
148 24	77.0	JK	4.971 0.027				
148 24	77.0	KL	4.987 0.027				
148 24	77.0	LM	5.068 0.027				

[a]Distance from the reactor interface to the center of the foil

[b]In-drawer column which designates the foil location in the drawer. The ^{239}Pu foils were centered 13.8 mm below the mid-height of the drawer.

[c]Experimental results in units of 10^{-18} fissions per sec per atom at a reactor power of approximately one watt. The second number is one standard deviation uncertainty. See text for details.

TABLE 6.2 Basic Data for Cell Studies of ^{235}U and ^{238}U Reaction Rates in ZPPR-18B

Matrix	z,mm[a]	Loc[b]	$^{235}U(n,f)$[c]	$^{238}U(n,f)$[c]	$^{238}U(n,\gamma)$[c]
254 43	77.0	AB	6.767 0.030	0.1398 0.0026	0.9191 0.0055
244 43	77.0	~AB		0.1410 0.0029	0.9368 0.0056
244 43	77.0	GH	6.600 0.030	0.1516 0.0029	0.9547 0.0058
244 43	77.0	HI	6.296 0.026	0.1563 0.0025	0.8640 0.0048
244 43	77.0	IJ	6.298 0.029	0.1474 0.0028	0.9122 0.0051
244 43	77.0	~OP		0.1210 0.0024	0.8217 0.0055
254 43	77.0	OP	5.835 0.025	0.1196 0.0029	0.8131 0.0047
254 43	254.8	AB	5.251 0.024	0.1048 0.0024	0.7113 0.0052
244 43	254.8	~AB		0.1107 0.0026	0.7153 0.0045
244 43	254.8	GH	5.050 0.026	0.1173 0.0027	0.7308 0.0043
244 43	254.8	HI	4.844 0.022	0.1221 0.0024	0.6591 0.0039
244 43	254.8	IJ	4.783 0.021	0.1111 0.0024	0.6892 0.0041
244 43	254.8	~OP		0.0919 0.0022	0.6229 0.0041
254 43	254.8	OP	4.489 0.021	0.0953 0.0023	0.6202 0.0039
154 43	77.0	AB	8.344 0.034	0.1500 0.0030	1.1387 0.0060
144 43	77.0	~AB		0.1440 0.0028	1.1571 0.0064
144 43	77.0	GH	8.240 0.033	0.1750 0.0030	1.2043 0.0067
144 43	77.0	HI	8.102 0.033	0.1849 0.0029	1.0933 0.0057
144 43	77.0	IJ	8.272 0.034	0.1782 0.0028	1.1893 0.0066
144 43	77.0	~OP		0.1635 0.0029	1.1250 0.0064
154 43	77.0	OP	8.338 0.035	0.1618 0.0030	1.1081 0.0063
154 43	254.8	AB	8.231 0.035	0.1342 0.0030	1.1105 0.0059
144 43	254.8	~AB		0.1356 0.0028	1.1418 0.0064
144 43	254.8	GH	8.190 0.035	0.1618 0.0031	1.1860 0.0062
144 43	254.8	HI	7.917 0.034	0.1762 0.0028	1.0518 0.0056
144 43	254.8	IJ	8.034 0.035	0.1646 0.0029	1.1535 0.0060
144 43	254.8	~OP		0.1504 0.0029	1.0683 0.0067
154 43	254.8	OP	7.963 0.033	0.1485 0.0029	1.0446 0.0060
150 35	77.0	AB	8.166 0.036	0.1698 0.0024	1.0930 0.0060
148 35	77.0	~AB		0.1655 0.0031	1.1006 0.0063
148 35	77.0	GH	8.200 0.036	0.1928 0.0025	1.1626 0.0064
148 35	77.0	HI	8.106 0.036	0.2013 0.0029	1.0852 0.0057
148 35	77.0	IJ	8.203 0.037	0.1917 0.0026	1.1665 0.0065
148 35	77.0	~OP		0.1705 0.0032	1.1128 0.0063
150 35	77.0	OP	8.310 0.038	0.1712 0.0027	1.1059 0.0062
150 35	127.8	AB	8.026 0.036	0.1649 0.0024	1.0691 0.0056
148 35	127.8	~AB		0.1614 0.0032	1.0826 0.0062
148 35	127.8	GH	8.076 0.035	0.1896 0.0024	1.1595 0.0060
148 35	127.8	HI	7.979 0.036	0.2019 0.0028	1.0645 0.0056
148 35	127.8	IJ	8.024 0.035	0.1878 0.0026	1.1651 0.0061
148 35	127.8	~OP		0.1644 0.0028	1.0856 0.0062
150 35	127.8	OP	8.191 0.040	0.1650 0.0026	1.0814 0.0062

TABLE 6.2 (contd)

Matrix	z,mm[a]	Loc[b]	$^{235}U(n,f)$[c]	$^{238}U(n,f)$[c]	$^{238}U(n,\gamma)$[c]
150 35	483.4	AB	4.933 0.025	0.0742 0.0017	0.6499 0.0038
148 35	483.4	AB		0.0797 0.0021	0.6644 0.0044
148 35	483.4	GH	5.073 0.025	0.0907 0.0018	0.7393 0.0046
148 35	483.4	HI	5.039 0.025	0.0981 0.0019	0.6624 0.0038
148 35	483.4	IJ	5.247 0.026	0.0939 0.0020	0.8071 0.0046
148 35	483.4	OP		0.0772 0.0022	0.7054 0.0046
150 35	483.4	OP	5.051 0.026	0.0750 0.0017	0.6621 0.0039
254 40	51.6	AB	6.043 0.028	0.1243 0.0022	0.8215 0.0049
254 40	51.6	GG	6.329 0.029	0.1424 0.0023	0.7922 0.0045
244 40	51.6	GH	6.280 0.030	0.1417 0.0021	0.8103 0.0049
244 40	51.6	HI	6.412 0.030	0.1577 0.0025	0.8348 0.0046
244 40	51.6	IJ	6.561 0.032	0.1491 0.0022	0.8374 0.0046
254 40	51.6	JJ	6.616 0.031	0.1482 0.0025	0.8368 0.0047
254 40	51.6	OP	6.916 0.033	0.1423 0.0025	0.9225 0.0051
254 40	254.8	AB	4.390 0.022	0.0882 0.0018	0.6034 0.0036
254 40	254.8	GG	4.592 0.023	0.1059 0.0020	0.5925 0.0035
244 40	254.8	GH	4.579 0.024	0.1120 0.0018	0.6017 0.0035
244 40	254.8	HI	4.721 0.024	0.1223 0.0021	0.6165 0.0036
244 40	254.8	IJ	4.865 0.024	0.1128 0.0022	0.6285 0.0038
254 40	254.8	JJ	4.923 0.026	0.1120 0.0021	0.6244 0.0037
254 40	254.8	OP	5.201 0.025	0.1044 0.0019	0.6987 0.0044
154 40	51.6	AB	8.008 0.034	0.1523 0.0022	1.0427 0.0058
154 40	51.6	GG	7.809 0.033	0.1624 0.0025	0.9618 0.0056
144 40	51.6	GH	7.672 0.032	0.1731 0.0023	0.9694 0.0054
144 40	51.6	HI	7.722 0.032	0.1790 0.0025	0.9904 0.0056
144 40	51.6	IJ	7.816 0.033	0.1647 0.0023	0.9777 0.0055
154 40	51.6	JJ	7.793 0.033	0.1591 0.0022	0.9669 0.0054
154 40	51.6	OP	7.971 0.034	0.1383 0.0022	1.0756 0.0061
154 40	254.8	AB	7.773 0.033	0.1421 0.0023	1.0098 0.0060
154 40	254.8	GG	7.679 0.033	0.1529 0.0022	0.9254 0.0058
144 40	254.8	GH	7.540 0.031	0.1554 0.0023	0.9458 0.0058
144 40	254.8	HI	7.561 0.032	0.1666 0.0024	0.9579 0.0054
144 40	254.8	IJ	7.719 0.033	0.1543 0.0021	0.9520 0.0057
154 40	254.8	JJ	7.750 0.033	0.1472 0.0021	0.9436 0.0054
154 40	254.8	OP	5.792 0.025	0.1306 0.0021	1.0896 0.0060
150 37	77.0	AB	8.295 0.034	0.1693 0.0029	1.0978 0.0062
150 37	77.0	GG	8.095 0.033	0.1886 0.0038	1.0130 0.0055
148 37	77.0	GH	8.058 0.032	0.1943 0.0028	1.0183 0.0058
148 37	77.0	HI	8.021 0.034	0.2029 0.0030	1.0328 0.0055
148 37	77.0	IJ	8.030 0.034	0.1934 0.0027	1.0189 0.0053
150 37	77.0	JJ	8.113 0.034	0.1828 0.0028	1.0091 0.0054
150 37	77.0	OP	8.263 0.035	0.1742 0.0032	1.0907 0.0059

TABLE 6.2 (contd)

Matrix	z,mm[a]	Loc[b]	$^{235}U(n,f)$[c]	$^{238}U(n,f)$[c]	$^{238}U(n,\gamma)$[c]
150 37	254.8	AB	7.475 0.031	0.1462 0.0027	0.9803 0.0053
150 37	254.8	GG	7.301 0.030	0.1639 0.0029	0.9116 0.0051
148 37	254.8	GH	7.273 0.033	0.1705 0.0026	0.9145 0.0054
148 37	254.8	HI	7.266 0.031	0.1863 0.0027	0.9263 0.0050
148 37	254.8	IJ	7.274 0.031	0.1729 0.0027	0.9248 0.0054
150 37	254.8	JJ	7.301 0.031	0.1665 0.0031	0.9210 0.0051
150 37	254.8	OP	7.486 0.031	0.1485 0.0030	0.9892 0.0054
150 24	77.0	AB	4.975 0.024	0.1283 0.0021	0.6364 0.0044
150 24	77.0	DE	4.979 0.023	0.1427 0.0021	0.6618 0.0041
150 24	77.0	EF	4.974 0.023	0.1532 0.0022	0.6521 0.0042
150 24	77.0	FG	5.081 0.023	0.1513 0.0022	0.7188 0.0044
148 24	77.0	JK	5.124 0.022	0.1484 0.0024	0.7271 0.0044
148 24	77.0	KL	5.134 0.025	0.1557 0.0021	0.6787 0.0042
148 24	77.0	LM	5.179 0.024	0.1474 0.0021	0.7042 0.0048
148 24	77.0	OP	5.294 0.024	0.1321 0.0020	0.6987 0.0043
150 24	483.4	AB	2.866 0.015	0.0576 0.0014	0.3713 0.0031
150 24	483.4	DE	2.876 0.016	0.0655 0.0015	0.3919 0.0029
150 24	483.4	EF	2.854 0.015	0.0724 0.0014	0.3720 0.0035
150 24	483.4	FG	2.956 0.015	0.0676 0.0014	0.4318 0.0030
148 24	483.4	JK	3.015 0.016	0.0697 0.0016	0.4395 0.0030
148 24	483.4	KL	2.996 0.016	0.0716 0.0016	0.3902 0.0032
148 24	483.4	LM	3.062 0.017	0.0687 0.0014	0.4216 0.0030
148 24	483.4	OP	3.109 0.017	0.0614 0.0014	0.4061 0.0030

[a]Distance from the reactor interface to the center of the foil.
[b]In-drawer column which designates the foil location in the drawer. The ^{235}U foils were centered 13.8 mm above and the ^{238}U foils were centered on the mid-height of the drawer. A negative sign designates a plate-spanning averaging foil.
[c]Experimental results in units of 10^{-18} fissions or captures per atom per second at a reactor power of approximately one watt. The second number is one standard deviation uncertainty. See text for details.

TABLE 6.3 Cell-Averaging Factors for ZPPR-18A and ZPPR-18B

$^{239}Pu(n,f)$[a]	$^{235}U(n,f)$[a]	$^{238}U(n,f)$[a]	$^{238}U(n,\gamma)$[a]	Environment[b]	z,mm[c]
0.9954 .0058	1.0011 .0049	0.953 .011	0.9256 .0088	F-SF-F	0-381.8
0.9918 .0064	0.9950 .0052	0.949 .014	0.9089 .0079	F-SF-F	432.6
0.9881 .0069	0.9889 .0055	0.945 .016	0.8922 .0069	F-SF-F	483.4
0.9960 .0058	0.9983 .0047	0.961 .013	0.9293 .0059	F-SF-CRP	0-381.8
0.9839 .0060	0.9922 .0089	0.965 .014	0.9118 .0086	CRP-SF-F	0-381.8
0.9801 .0060	0.9760 .0051	0.966 .016	0.9170 .0063	F-SF-CR	0-381.8
1.0066 .0063	1.0072 .0058	0.978 .016	0.9490 .0065	CR-SF-F	0-381.8
0.9850 .0059	1.0020 .0057	0.978 .019	0.9020 .0051	F-SF-RB	0-381.8
0.9983 .0041	1.0082 .0046	0.954 .008	1.0161 .0045	F-SM-F	0-483.4
0.9967 .0058	1.0200 .0047	0.972 .016	1.0244 .0066	F-SM-CRP	0-483.4
0.9876 .0055	1.0006 .0047	0.969 .011	1.0181 .0065	CRP-SM-F	0-483.4
0.9826 .0060	0.9904 .0053	0.977 .018	1.0120 .0096	F-SM-CR	0-483.4
1.0077 .0064	1.0255 .0055	0.957 .018	1.0349 .0125	CR-SM-F	0-483.4
0.9958 .0060	1.0003 .0049	0.981 .016	0.9090 .0063	F-D-F	0-381.8
0.9917 .0073	0.9971 .0053	0.984 .017	0.8892 .0067	F-D-F	432.6
1.0 .01	0.9939 .0057	0.988 .017	0.8694 .0071	F-D-F	483.4
1.0 .01	1.0022 .0063	0.912 .026	1.0229 .0058	F-RB-RB	ALL
1.0 .01	0.9949 .0074	0.988 .071	1.0170 .0071	RB-RB-RB	ALL
1.0 .01	0.9791 .0085	0.838 .100	1.0508 .0090	RB-RB-RF	ALL
1.0 .01	1.0 .01	1.0 .01	1.0 .01	RR	ALL
1.0 .008	1.0005 .0059	1.081 .031	0.8815 .0061	AB-AB-AB (SC)	534.2
1.0 .008	1.0005 .0059	1.081 .053	0.8521 .0064	AB-AB-AB (SC)	585.0
1.0 .008	1.0005 .0070	1.081 .077	0.8340 .0060	AB-AB-AB (SC)	635.8
1.0 .008	1.0005 .0073	1.081 .16	0.8053 .0058	AB-AB-AB (SC)	686.6
1.0 .008	1.0005 .0074	1.081 .14	0.7817 .0064	AB-AB-AB (SC)	734.4
1.0 .008	0.9986 .0059	1.064 .052	0.8627 .0057	AB-AB-AB (DC)	534.2
1.0 .008	1.0005 .0059	1.081 .053	0.8361 .0064	AB-AB-AB (DC)	585.0
1.0 .008	1.0005 .0070	1.081 .077	0.8340 .0060	AB-AB-AB (DC)	635.8
1.0 .008	1.0005 .0073	1.081 .16	0.8053 .0058	AB-AB-AB (DC)	686.6
1.0 .008	1.0005 .0074	1.081 .14	0.7817 .0064	AB-AB-AB (DC)	734.4
1.0 .008	0.9947 .0055	1.012 .019	0.8410 .0045	AB-AB-CRP (SC)	534.2
1.0 .008	0.9947 .0055	1.047 .038	0.8145 .0040	AB-AB-CRP (SC)	585.0
1.0 .008	0.9947 .0055	1.047 .042	0.7839 .0061	AB-AB-CRP (SC)	635.8
1.0 .008	0.9947 .0055	1.047 .063	0.7551 .0052	AB-AB-CRP (SC)	686.6
1.0 .008	0.9947 .0055	1.047 .101	0.7262 .0042	AB-AB-CRP (SC)	737.4

TABLE 6.3 (contd)

$^{239}Pu(n,f)$[a]		$^{235}U(n,f)$[a]		$^{238}U(n,f)$[a]		$^{238}U(n,\gamma)$[a]		Environment[b]	z,mm[c]
1.0	.008	0.9964	.0085	0.967	.034	0.9241	.0212	AB-AB-CR (SC)	534.2
1.0	.008	0.9964	.0085	0.967	.052	0.8945	.0278	AB-AB-CR (SC)	585.0
1.0	.008	0.9964	.0085	0.967	.067	0.8868	.0280	AB-AB-CR (SC)	635.8
1.0	.008	0.9964	.0085	0.967	.097	0.8539	.0230	AB-AB-CR (SC)	686.6
1.0	.008	0.9964	.0085	0.967	.100	0.8377	.0253	AB-AB-CR (SC)	737.4

[a]The second number for each cell factor is one standard deviation uncertainty. See text for details.
[b]Type of cell and local environment. See text for key and discussion.
[c]Axial position to which this cell factor applies.

7. GAMMA RAY DOSE MEASUREMENTS IN ZPPR-18A AND ZPPR-18B (D. N. Olsen)

Gamma ray doses were measured in ZPPR-18A and ZPPR-18B as a function of axial and radial location using stainless-steel-encapsulated thermoluminescent dosimeters (TLDs). The LiF TLDs were 1 x 1 x 6 mm and were placed in holes in stainless steel cylinders. The TLDs are somewhat sensitive to neutron interactions in the LiF. No calculations were made for gamma dose in ZPPR-18.

The in-cell location of the TLDs varied among the drawer types. The TLDs spanned two drawer columns.* For all single-fuel-column drawers and all blanket drawers, the TLDs were in columns E and F. In double-fuel-column drawers, the location was columns C and D. In the CR and CRP drawers, the location was columns G and H. For the axial distributions in ZPPR-18B, the TLDs were in columns E and F in half 2 and in columns K and L in half 1.

Two radial distributions were measured in ZPPR-18A. The first was along the x-axis 76 mm above the axial midplane and the results are given in Table 7.1. The second was approximately 45° to the x-axis with detours to go through inner, middle and outer bank control positions. Results from the second radial distribution are given in Table 7.2.

A single axial dose distribution was measured in an inner-core location (145-63) in ZPPR-18A. This location is four drawers removed from the nearest control position. The drawer is a single-fuel-column drawer with iron oxide. Results are given in Table 7.3.

Many of the gamma dose distribution measurements were repeated in ZPPR-18B which had half-inserted control rods in the inner and outer banks. In core 18B, all radial distributions were measured 76 mm from the

---

*ZPPR drawers are divided into sixteen 3.175 mm (1/8 in.) wide vertical columns designated by letters A through P. The letter A denotes the column at the left as one faces the drawer.

interface in half two, which contained the inserted rods. Results from an x-axis distribution are given in Table 7.4. Results from a second radial distribution going through an inner-ring control rod, a middle-ring CRP and an outer-ring control rod are given in Table 7.5.

Axial distributions in ZPPR-18B were measured in both assembly halves. One location was 145-35 and 245-35, symmetrically equivalent to measurement location 145-63 in core 18A. A second location measured in ZPPR-18B was 1,247-42 which was one drawer removed from an inner-ring CR/CRP channel. Axial results from ZPPR-18B are given in Table 7.6.

Intra-cell variations in dose were also measured in ZPPR-18A. Results are given in Fig. 7.1. These results indicate the extent of in-cell variations and may be used to test calculations of "cell-average factors".

TABLE 7.1 Measured Dose Rates along the x-axis in ZPPR-18A

Matrix Location	Drawer Type[a]	Dose Rate,[b] mrd/s	Zone
149-49	SF	0.3716	Inner Core
149-50	SF	0.3768	Inner Core
149-51	SM	0.3360	Inner Core
149-52	SF	0.3685	Inner Core
149-53	SM	0.3271	Inner Core
149-54	SF	0.3489	Inner Core
149-55	SM	0.3286	Inner Core
149-56	SF	0.3484	Inner Core
149-57	SM	0.3172	Inner Core
149-58	SF	0.3512	Inner Core
149-59	SF	0.3551	Inner Core
149-60	SM	0.3134	Inner Core
149-61	SF	0.3417	Inner Core
149-62	SF	0.3478	Inner Core
149-63	SM	0.3000	Inner Core
149-64	SF	0.3376	Inner Core
149-65	SF	0.3315	Inner Core
149-66	SM	0.2892	Inner Core
149-67	SF	0.3219	Inner core
149-68	SM	0.2750	Inner Core
149-69	SF	0.2810	Inner Core
149-70	SM	0.2468	Inner Core
149-71	SF	0.2570	Inner Core
149-72	SM	0.2254	Inner Core
149-73	SF	0.2482	Outer Core
149-74	SF	0.2508	Outer Core
149-75	DF	0.2611	Outer Core
149-76	SF	0.2000	Outer Core
149-77	SF	0.1542	Outer Core
149-78	B	0.0782	Blanket
148-80	B	0.0202	Blanket
149-82	B	0.0199	Blanket

[a]SF is single-fuel column with iron oxide, SM is single-fuel column with depleted-uranium metal, DF is double fuel column and B is blanket.

[b]Total dose rate (not corrected for neutron contribution) at an estimated reactor power of 1 watt.

TABLE 7.2 Measured Dose Rates 45° to the x-axis and through Control Positions in ZPPR-18A

Matrix Location	Drawer Type[a]	Dose Rate,[b] mrd/s	Zone
148-50	SF	0.3621	Inner Core
147-51	SF	0.3721	Inner Core
146-52	SF	0.3637	Inner Core
145-53	SF	0.3578	Inner Core
144-54	SF	0.3470	Inner Core
144-55	SF	0.3420	Inner Core
144-56	CRP	0.2456	CRP
144-57	CRP	0.2481	CRP
144-58	SM	0.2855	Inner Core
144-59	SF	0.3368	Inner Core
143-60	SF	0.3310	Inner Core
142-61	SF	0.3262	Inner Core
141-62	SF	0.3025	Inner Core
140-63	CRP	0.2096	CRP
140-64	CRP	0.1980	CRP
140-65	SM	0.2375	Inner Core
141-66	SM	0.2525	Inner Core
142-67	SM	0.2472	Inner Core
142-68	SF	0.2714	Inner Core
142-69	SF	0.2671	Inner Core
142-70	SM	0.2238	Inner Core
142-71	CRP	0.1692	CRP
142-72	CRP	0.1666	CRP
142-73	SF	0.2107	Outer Core
142-76	DF	0.3808	Outer Core
142-77	SF	0.1396	Outer Core

[a]SF is single-fuel column with iron oxide, SM is single-fuel column with depleted-uranium metal, DF is double fuel column and CRP is control position.

[b]Total dose rate (not corrected for neutron contribution) at an estimated reactor power of 1 watt.

TABLE 7.3 Measured Axial Dose Distribution in Location 145-63 in ZPPR-18A

Axial Location, mm[a]	Dose Rate[b] mrd/s
72.2	0.3266
177.8	0.3022
279.4	0.2653
381.0	0.2180
584.2	0.0589
762.0	0.0294

[a]Distance from the reactor interface.

[b]Total dose rate (not corrected for neutron contribution) at an estimated reactor power of 1 watt.

TABLE 7.4 Measured Dose Rates along the x-axis in ZPPR-18B

Matrix Location	Drawer Type[a]	Dose Rate,[b] mrd/s	Zone
249-49	SF	0.3940	Inner Core
249-45	SM	0.3623	Inner Core
249-41	SM	0.3338	Inner Core
249-31	SF	0.3739	Inner Core
249-33	SF	0.3702	Inner Core
249-29	SF	0.3078	Inner Core
249-26	SM	0.2438	Inner Core
249-25	SF	0.2634	Outer Core
249-23	DF	0.2743	Outer Core
249-21	SF	0.1573	Outer Core
249-20	B	0.0893	Blanket
249-17	B	0.0292	Blanket
249-16	B	0.0212	Blanket
249-15	R	0.0134	Reflector

[a]SF is single-fuel column with iron oxide, SM is single-fuel column with depleted-uranium metal, DF is double fuel column and B is blanket and R is reflector.

[b]Total dose rate (not corrected for neutron contribution) at an estimated reactor power of 1 watt.

TABLE 7.5 Measured Dose Rates through Control Rods and Control Rod Positions in ZPPR-18B

Matrix Location	Drawer Type[a]	Dose Rate,[b] mrd/s	Zone
247-47	SF	0.4008	Inner Core
245-43	SM	0.2808	Inner Core
244-43	SF	0.2847	Inner Core
244-42	CR	0.2462	CR
244-41	CR	0.2433	CR
244-40	SM	0.2474	Inner Core
243-39	SM	0.3006	Inner Core
243-38	SF	0.3461	Inner Core
242-37	SF	0.3636	Inner Core
241-36	SF	0.3308	Inner Core
240-35	CRP	0.2425	CRP
240-34	CRP	0.2441	CRP
240-33	SM	0.2688	Inner Core
243-30	SF	0.3146	Inner Core
243-29	SM	0.2680	Inner Core
242-28	SM	0.2202	Inner Core
242-27	CR	0.1823	CR
242-26	CR	0.1740	CR
242-25	SF	0.1834	Outer Core
241-25	SF	0.1954	Outer Core
241-24	SF	0.1980	Outer Core
241-22	SF	0.1783	Outer Core

[a]SF is single-fuel column with iron oxide, SM is single-fuel column with depleted-uranium metal, CR is control rod and CRP is control position.

[b]Total dose rate (not corrected for neutron contribution) at an estimated reactor power of 1 watt.

TABLE 7.6 Measured Axial Dose Distributions in ZPPR-18B

Axial Location, mm[a]	Dose Rate[b] mr d/s	
	1,247-42	1,245-35
-762.0	0.0245	0.0285
-584.2	0.0552	0.0651
-482.6	0.1427	0.1578
-381.0	0.2050	0.2220
-279.4	0.2607	0.2802
-177.8	0.2942	0.3242
-76.2	0.3458	0.3506
76.2	0.3862	0.3737
177.8	0.3618	0.3556
279.4	0.3476	0.3122
381.0	0.2924	0.2534
482.6	0.2075	0.1881
584.2	0.0877	0.0758
762.0	0.0401	0.0387

[a]With respect to zero at the reactor interface, negative values in half two.

[b]Total dose rate (not corrected for neutron contribution) at an estimated power of 1 watt.

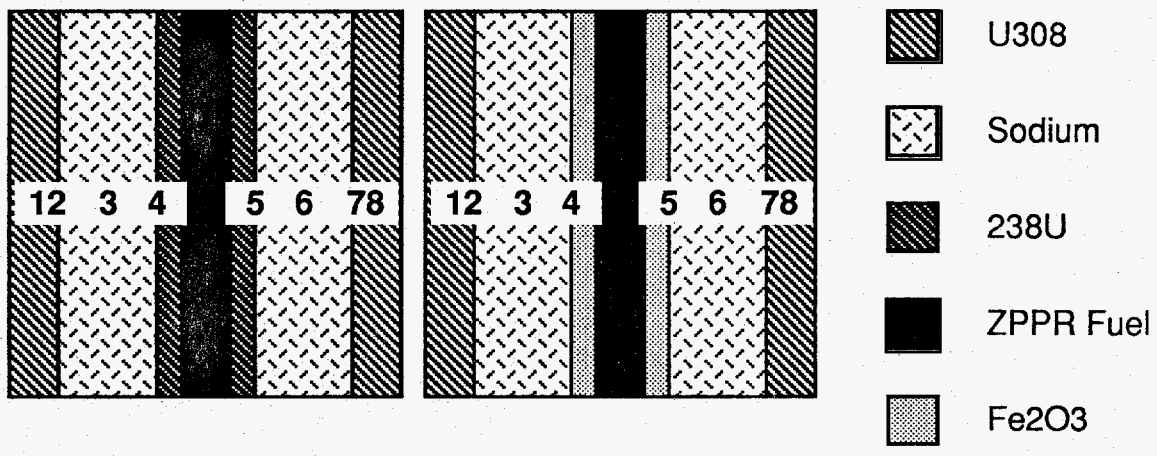

INTRA-CELL LOCATION	249-53	249-52
	DOSE RATE, mrd/s	
1	0.392	0.398
2	0.396	0.422
3	0.380	0.428
4	0.384	0.434
5	0.397	0.446
6	0.378	0.416
7	0.394	0.411
8	0.391	0.408

Fig. 7.1 Measured In-cell Gamma Dose Distributions in ZPPR-18A

8. CALCULATION MODELS FOR ZPPR-19A (G. L. Grasseschi and P. J. Collins)

ZPPR-19A was a variant of the ZPPR-18 series of cores designed to reduce the fundamental to first harmonic eigenvalue separation from about 4% Δk to about 2% Δk. The zone boundaries remained the same as in ZPPR-18, with distinct sectors in the outer core with uranium fuel and with plutonium fuel. The core was made near critical with the inner bank of six control rods fully inserted. The core required less fuel than did ZPPR-18C which had 18 control rods half-inserted. A detailed description of ZPPR-19A is given in ANL-ZPR-489, p. 2. No new drawer masters were required for ZPPR-19.

Calculations for ZPPR-19A used the cross section library generated for ZPPR-18 (ANL-ZPR-489, p. 12). The reactor model used xyz geometry with detailed compositions of each drawer master. The xy plan is given in Fig. 8.1. The different drawer types are described in ANL-ZPR-489, Tables 4.1 and 5.1.

Average compositions of each zone in ZPPR-19A are given in Table 8.1.

Table 8.1 Atom Densities by Zone and Drawer Type in ZPPR-19A

Isotope	Inner Core Average 0-20	Axial Blanket (IC) 20-31	Reflector Iron Block (IC) 31-36	Inner Core (ICSF) 0-20	Inner Core (ICSM) 0-20	Inner Core Single Pu 0-20
C	0.0001439	0.0000532	0.0005894	0.0000332	0.0000333	0.0000332
O	0.0120392	0.0088207	0.0	0.0137453	0.0088143	0.0118548
Na	0.0092004	0.0091883	0.0	0.0092715	0.0091481	0.0092241
Si	0.0001588	0.0001924	0.0001264	0.0001570	0.0001587	0.0001577
Al	0.0000041	0.0000029	0.0	0.0000040	0.0000040	0.0000040
Mn	0.0002305	0.0003420	0.0006847	0.0002287	0.0002289	0.0002288
Cr	0.0026943	0.0041649	0.0021198	0.0026684	0.0026773	0.0026718
Fe	0.0115495	0.0147985	0.0759668	0.0128536	0.0095173	0.0115745
Ni	0.0011851	0.0017648	0.0008612	0.0011678	0.0011814	0.0011730
Cu	0.0000304	0.0000440	0.0000271	0.0000293	0.0000313	0.0000301
Mo	0.0002503	0.0000346	0.0000136	0.0002397	0.0002383	0.0002392
U4	0.0	0.0	0.0	0.0	0.0	0.0
U5	0.0000169	0.0000179	0.0	0.0000127	0.0000234	0.0000168
U6	0.0	0.0	0.0	0.0	0.0	0.0
U8	0.0077009	0.0081559	0.0	0.0058158	0.0106485	0.0076686
P8	0.0000005	0.0	0.0	0.0000004	0.0000005	0.0000004
P9	0.0009274	0.0	0.0	0.0008878	0.0008791	0.0008844
P0	0.0001227	0.0	0.0	0.0001176	0.0001161	0.0001170
P1	0.0000071	0.0	0.0	0.0000065	0.0000069	0.0000067
P2	0.0000019	0.0	0.0	0.0000017	0.0000019	0.0000018
A1	0.0000113	0.0	0.0	0.0000108	0.0000107	0.0000108
P	0.0000052	0.0000102	0.0000238	0.0000053	0.0000051	0.0000052
S	0.0000011	0.0000081	0.0000314	0.0000010	0.0000011	0.0000010
Cl	0.0000006	0.0000003	0.0	0.0000003	0.0000003	0.0000003
Ca	0.0000020	0.0000021	0.0	0.0000021	0.0000021	0.0000021
Co	0.0000016	0.0000016	0.0000009	0.0000008	0.0000024	0.0000014

TABLE 8.1 (contd)

Isotope	Inner Core Double Pu 0-20.	Outer Core Average 0-20.	Outer Core Average 20-20.44	Axial Blanket (OC) 20.44-31	Reflector Iron Block (OC) 31-36.	Outer Core Pu Fuel 0-20.
C	0.0023102	0.0016072	0.0000430	0.0000550	0.0005923	0.0008296
O	0.0156589	0.0157892	0.0088279	0.0088211	0.0	0.0144145
Na	0.0087410	0.0087498	0.0093061	0.0092564	0.0	0.0091166
Si	0.0001814	0.0001676	0.0001702	0.0002039	0.0001167	0.0001656
Al	0.0000061	0.0000044	0.0000028	0.0000029	0.0	0.0000048
Mn	0.0002646	0.0002394	0.0002669	0.0003458	0.0006737	0.0002411
Cr	0.0031355	0.0028416	0.0031949	0.0040979	0.0019566	0.0028304
Fe	0.0110721	0.0143516	0.0113707	0.0145844	0.0760551	0.0122272
Ni	0.0014220	0.0012562	0.0013686	0.0017587	0.0007933	0.0012551
Cu	0.0000364	0.0000318	0.0000362	0.0000405	0.0000279	0.0000316
Mo	0.0004677	0.0001438	0.0000233	0.0000289	0.0000140	0.0003193
U4	0.0	0.0000093	0.0000077	0.0	0.0	0.0
U5	0.0000183	0.0009624	0.0008004	0.0000179	0.0	0.0000146
U6	0.0	0.0000044	0.0000037	0.0	0.0	0.0
U8	0.0083377	0.0068596	0.0082019	0.0081562	0.0	0.0066889
P8	0.0000010	0.0000003	0.0	0.0	0.0	0.0000007
P9	0.0017696	0.0005021	0.0	0.0	0.0	0.0011920
P0	0.0002341	0.0000752	0.0	0.0	0.0	0.0001786
P1	0.0000141	0.0000048	0.0	0.0	0.0	0.0000113
P2	0.0000039	0.0000017	0.0	0.0	0.0	0.0000041
A1	0.0000217	0.0000076	0.0	0.0	0.0	0.0000180
P	0.0000046	0.0000052	0.0000073	0.0000102	0.0000233	0.0000051
S	0.0000016	0.0000015	0.0000039	0.0000063	0.0000314	0.0000012
Cl	0.0000062	0.0000043	0.0000003	0.0000003	0.0	0.0000024
Ca	0.0000010	0.0000013	0.0000021	0.0000021	0.0	0.0000017
Co	0.0000045	0.0000025	0.0000025	0.0000023	0.0000017	0.0000019

TABLE 8.1 (contd)

Isotope	Axial Blanket (OC) Pu Fuel 20-31	Reflector Iron Block (OC) Pu Fuel 31-36	Outer Core (OC) Pu Fuel 0-20	Outer Core Single Pu 0-20	Outer Core U Fuel 0-20	Outer Core U Fuel 20-20.44
C	0.0000531	0.0005928	0.0023796	0.0000332	0.0012578	0.0000199
O	0.0088210	0.0	0.0161289	0.0137451	0.0097183	0.0051099
Na	0.0092557	0.0	0.0090421	0.0092985	0.0049102	0.0053839
Si	0.0001926	0.0001165	0.0001869	0.0001570	0.0000979	0.0000890
Al	0.0000029	0.0	0.0000061	0.0000041	0.0000024	0.0000017
Mn	0.0003418	0.0006744	0.0002729	0.0002283	0.0001378	0.0001228
Cr	0.0041641	0.0019578	0.0032323	0.0026649	0.0016495	0.0014400
Fe	0.0147923	0.0761458	0.0114182	0.0128413	0.0092018	0.0051367
Ni	0.0017667	0.0007914	0.0014630	0.0011662	0.0007276	0.0006244
Cu	0.0000444	0.0000274	0.0000369	0.0000293	0.0000185	0.0000175
Mo	0.0000348	0.0000138	0.0004825	0.0002391	0.0000093	0.0000086
U4	0.0	0.0	0.0	0.0	0.0000093	0.0000077
U5	0.0000179	0.0	0.0000187	0.0000127	0.0009563	0.0007928
U6	0.0	0.0	0.0	0.0	0.0000044	0.0000037
U8	0.0081561	0.0	0.0085400	0.0058281	0.0040424	0.0047667
P8	0.0	0.0	0.0000012	0.0000005	0.0	0.0
P9	0.0	0.0	0.0018152	0.0008855	0.0	0.0
P0	0.0	0.0	0.0002998	0.0001172	0.0	0.0
P1	0.0	0.0	0.0000195	0.0000071	0.0	0.0
P2	0.0	0.0	0.0000084	0.0000019	0.0	0.0
A1	0.0	0.0	0.0000317	0.0000110	0.0	0.0
P	0.0000101	0.0000234	0.0000049	0.0000053	0.0000030	0.0000031
S	0.0000081	0.0000314	0.0000016	0.0000010	0.0000010	0.0000007
Cl	0.0000003	0.0	0.0000064	0.0000003	0.0000034	0.0000002
Ca	0.0000021	0.0	0.0000010	0.0000021	0.0000006	0.0000012
Co	0.0000019	0.0000013	0.0000041	0.0000008	0.0000017	0.0000017

TABLE 8.1 (contd)

Isotope	Axial Blanket (OC) U Fuel 20.44-31	Reflector Iron Block (OC) U Fuel 31-36	Outer Core Single U (OCUS) 0-20	Outer Core Single U (OCUS) 20-20.44	Outer Core Double U (OCUD) 0-20	Outer Core Double U (OCUD) 20-20.44
C	0.0000326	0.0003426	0.0021064	0.0000340	0.0022470	0.0000349
O	0.0051059	0.0	0.0171001	0.0088278	0.0164429	0.0088278
Na	0.0053581	0.0	0.0083649	0.0092908	0.0086142	0.0093129
Si	0.0001228	0.0000676	0.0001684	0.0001481	0.0001700	0.0001602
Al	0.0000017	0.0	0.0000043	0.0000029	0.0000038	0.0000028
Mn	0.0002018	0.0003896	0.0002412	0.0002105	0.0002346	0.0002141
Cr	0.0023441	0.0011320	0.0028881	0.0024576	0.0028069	0.0025214
Fe	0.0083543	0.0439848	0.0177817	0.0087813	0.0137983	0.0089775
Ni	0.0010146	0.0004600	0.0012690	0.0010563	0.0012435	0.0011037
Cu	0.0000218	0.0000164	0.0000302	0.0000281	0.0000340	0.0000324
Mo	0.0000142	0.0000082	0.0000147	0.0000133	0.0000175	0.0000167
U4	0.0	0.0	0.0000109	0.0000082	0.0000217	0.0000189
U5	0.0000104	0.0	0.0011314	0.0008546	0.0022319	0.0019431
U6	0.0	0.0	0.0000052	0.0000039	0.0000105	0.0000090
U8	0.0047211	0.0	0.0073446	0.0082050	0.0065815	0.0082681
P8	0.0	0.0	0.0	0.0	0.0	0.0
P9	0.0	0.0	0.0	0.0	0.0	0.0
P0	0.0	0.0	0.0	0.0	0.0	0.0
P1	0.0	0.0	0.0	0.0	0.0	0.0
P2	0.0	0.0	0.0	0.0	0.0	0.0
A1	0.0	0.0	0.0	0.0	0.0	0.0
P	0.0000059	0.0000135	0.0000054	0.0000054	0.0000051	0.0000052
S	0.0000029	0.0000182	0.0000015	0.0000011	0.0000018	0.0000015
Cl	0.0000002	0.0	0.0000056	0.0000003	0.0000060	0.0000003
Ca	0.0000012	0.0	0.0000010	0.0000021	0.0000010	0.0000021
Co	0.0000015	0.0000012	0.0000010	0.0000010	0.0000050	0.0000049

TABLE 8.1 (contd)

Isotope	Radial Blanket 0-20	Radial Blanket 20-31	Radial Blanket 31-36	Radial Reflector 0-36	Axial Reflector 36-42	Empty Matrix 0-42
C	0.0000318	0.0000319	0.0005928	0.0002493	0.0002143	0.0000188
O	0.0193179	0.0193406	0.0	0.0	0.0	0.0
Na	0.0036444	0.0036359	0.0	0.0	0.0	0.0
Si	0.0001352	0.0001355	0.0001163	0.0008675	0.0008629	0.0000683
Al	0.0000021	0.0000021	0.0	0.0	0.0	0.0
Mn	0.0001937	0.0001941	0.0006746	0.0014119	0.0015241	0.0001059
Cr	0.0022430	0.0022455	0.0019586	0.0153499	0.0150441	0.0011891
Fe	0.0080226	0.0080330	0.0761527	0.0563344	0.0531084	0.0042791
Ni	0.0009584	0.0009588	0.0007902	0.0066625	0.0066621	0.0004802
Cu	0.0000279	0.0000280	0.0000271	0.0000386	0.0000172	0.0000172
Mo	0.0000132	0.0000131	0.0000136	0.0000322	0.0000083	0.0000083
U4	0.0	0.0	0.0	0.0	0.0	0.0
U5	0.0000369	0.0000370	0.0	0.0	0.0	0.0
U6	0.0	0.0	0.0	0.0	0.0	0.0
U8	0.0168314	0.0168695	0.0	0.0	0.0	0.0
P8	0.0	0.0	0.0	0.0	0.0	0.0
P9	0.0	0.0	0.0	0.0	0.0	0.0
P0	0.0	0.0	0.0	0.0	0.0	0.0
P1	0.0	0.0	0.0	0.0	0.0	0.0
P2	0.0	0.0	0.0	0.0	0.0	0.0
A1	0.0	0.0	0.0	0.0	0.0	0.0
P	0.0000050	0.0000050	0.0000235	0.0000465	0.0	0.0000028
S	0.0000010	0.0000010	0.0000314	0.0000335	0.0	0.0000007
Cl	0.0000001	0.0000001	0.0	0.0	0.0	0.0
Ca	0.0000009	0.0000009	0.0	0.0	0.0	0.0
Co	0.0000015	0.0000015	0.0000010	0.0	0.0	0.0

TABLE 8.1 (contd)

Isotope	Inner Ring Control Position 0-20	Inner Ring Control Position 20-36	Middle Ring Control Position 0-20	Middle Ring Control Position 20-36	Outer Ring Control Position 0-20	Outer Ring Control Position 20-36
C	0.0000312	0.0000309	0.0000312	0.0000309	0.0000311	0.0000309
O	0.0000013	0.0000013	0.0000013	0.0000013	0.0000013	0.0000013
Na	0.0182904	0.0184405	0.0182904	0.0184405	0.0182904	0.0184405
Si	0.0001661	0.0001649	0.0001661	0.0001649	0.0001657	0.0001649
Al	0.0000047	0.0000049	0.0000047	0.0000049	0.0000047	0.0000049
Mn	0.0002451	0.0002443	0.0002451	0.0002443	0.0002448	0.0002443
Cr	0.0029778	0.0029657	0.0029778	0.0029657	0.0029723	0.0029657
Fe	0.0105129	0.0104697	0.0105129	0.0104697	0.0104937	0.0104697
Ni	0.0013332	0.0013281	0.0013332	0.0013281	0.0013307	0.0013281
Cu	0.0000357	0.0000353	0.0000357	0.0000353	0.0000357	0.0000353
Mo	0.0000176	0.0000174	0.0000176	0.0000174	0.0000175	0.0000174
U4	0.0	0.0	0.0	0.0	0.0	0.0
U5	0.0	0.0	0.0	0.0	0.0	0.0
U6	0.0	0.0	0.0	0.0	0.0	0.0
U8	0.0	0.0	0.0	0.0	0.0	0.0
P8	0.0	0.0	0.0	0.0	0.0	0.0
P9	0.0	0.0	0.0	0.0	0.0	0.0
P0	0.0	0.0	0.0	0.0	0.0	0.0
P1	0.0	0.0	0.0	0.0	0.0	0.0
P2	0.0	0.0	0.0	0.0	0.0	0.0
A1	0.0	0.0	0.0	0.0	0.0	0.0
P	0.0000040	0.0000040	0.0000040	0.0000040	0.0000040	0.0000040
S	0.0000012	0.0000012	0.0000012	0.0000012	0.0000012	0.0000012
Cl	0.0000006	0.0000006	0.0000006	0.0000006	0.0000006	0.0000006
Ca	0.0000042	0.0000042	0.0000042	0.0000042	0.0000042	0.0000042
Co	0.0000038	0.0000037	0.0000038	0.0000037	0.0000038	0.0000037

TABLE 8.1 (contd)

Isotope	Radial Blanket Master 501 0-31	Radial Blanket Master 502 0-31	Radial Blanket Master 503 0-31
C	0.0000294	0.0000325	0.0000324
O	0.0	0.0226351	0.0220579
Na	0.0	0.0042352	0.0042350
Si	0.0001099	0.0001398	0.0001417
Al	0.0	0.0000024	0.0000024
Mn	0.0001648	0.0002005	0.0001984
Cr	0.0018487	0.0023279	0.0023140
Fe	0.0066628	0.0083268	0.0082484
Ni	0.0007495	0.0009950	0.0010098
Cu	0.0000249	0.0000275	0.0000317
Mo	0.0000124	0.0000127	0.0000150
U4	0.0	0.0	0.0
U5	0.0000865	0.0000290	0.0000285
U6	0.0	0.0	0.0
U8	0.0387435	0.0133322	0.0131212
P8	0.0	0.0	0.0
P9	0.0	0.0	0.0
P0	0.0	0.0	0.0
P1	0.0	0.0	0.0
P2	0.0	0.0	0.0
A1	0.0	0.0	0.0
P	0.0000046	0.0000052	0.0000047
S	0.0000010	0.0000010	0.0000012
Cl	0.0	0.0000001	0.0000001
Ca	0.0	0.0000010	0.0000010
Co	0.0	0.0000007	0.0000045

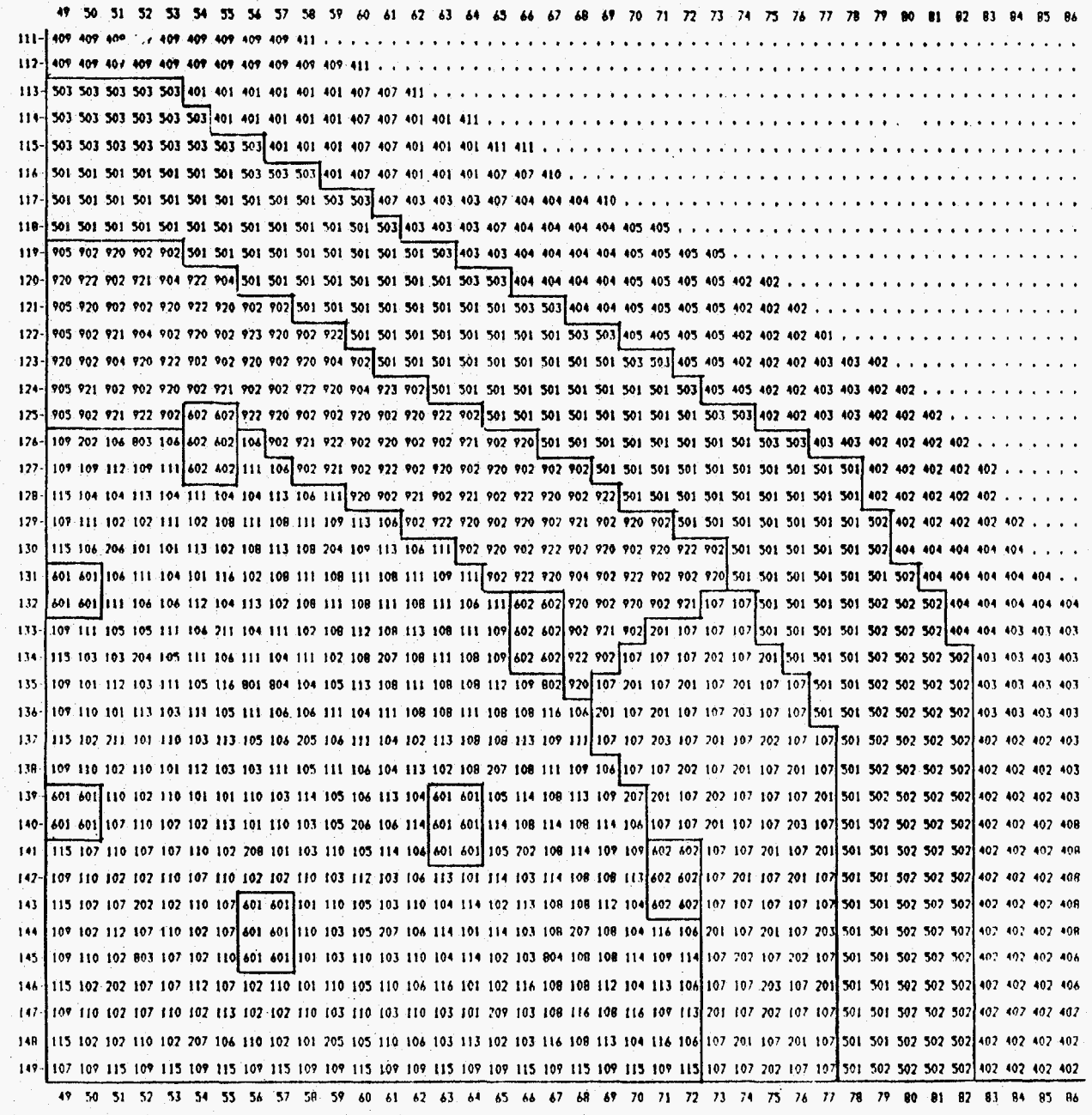

Fig. 8.1 The xyz Calculation Model for ZPPR-19A

9. CALCULATION MODELS FOR ZPPR-19B (G. L. Grasseschi and P. J. Collins)

ZPPR-19B was built to provide further data on the effects of the uranium fuel in the outer core. The uranium and plutonium fuel drawers were rearranged to give an approximately uniform distribution throughout the outer core. Measurements of reaction rates and control rod worths in ZPPR-19B were made to compare with those in ZPPR-18A which had uranium and plutonium sectors in the outer core. ZPPR-19B had substantially more uranium fuel than did ZPPR-18A since fuel was added in ZPPR-18B to improve the power distributions. Measurements in 18A and 19B cannot be compared directly, but it is believed that the change in the amount of fuel will have little effect on the analytical comparisons. A detailed description of ZPPR-19B is given in ANL-ZPR-489, p. 8.

Calculations for ZPPR-19B used the ZPPR-18 cross section library (ANL-ZPR-489, p. 12) in which cross sections processing was made using group dependent buckling for cells in the sector model. Calculations were made in xyz geometry with detailed compositions by drawer master as was done for ZPPR-18. The xy plan is given in Figure 9.1. The drawer masters shown in the figure are described in ANL-ZPR-489 Tables 4.1 and 5.1. Average composition for each zone in ZPPR-19B are given in Table 9.1.

TABLE 9.1 Atom Densities by Zone and Drawer Type in ZPPR-19B

Isotope	Inner Core Average 0-20	Axial Blanket (IC) 20-31	Reflector Iron Block (IC) 31-36	Inner Core (ICSF) 0-20	Inner Core (ICSM) 0-20	Inner Core Single Pu 0-20
C	0.0000332	0.0000532	0.0005873	0.0000332	0.0000332	0.0000332
O	0.0117067	0.0088210	0.0	0.0137453	0.0088141	0.0117067
Na	0.0092276	0.0091887	0.0	0.0092715	0.0091653	0.0092276
Si	0.0001577	0.0001923	0.0001258	0.0001570	0.0001586	0.0001577
Al	0.0000040	0.0000029	0.0	0.0000040	0.0000040	0.0000040
Mn	0.0002288	0.0003421	0.0006824	0.0002287	0.0002289	0.0002288
Cr	0.0026718	0.0041655	0.0021133	0.0026684	0.0026767	0.0026718
Fe	0.0114739	0.0148016	0.0756998	0.0128536	0.0095163	0.0114739
Ni	0.0011730	0.0017641	0.0008575	0.0011678	0.0011803	0.0011730
Cu	0.0000300	0.0000439	0.0000268	0.0000293	0.0000311	0.0000300
Mo	0.0002391	0.0000345	0.0000134	0.0002397	0.0002383	0.0002391
U4	0.0	0.0	0.0	0.0	0.0	0.0
U5	0.0000171	0.0000179	0.0	0.0000127	0.0000234	0.0000171
U6	0.0	0.0	0.0	0.0	0.0	0.0
U8	0.0078140	0.0081561	0.0	0.0058158	0.0106494	0.0078140
P8	0.0000004	0.0	0.0	0.0000004	0.0000005	0.0000004
P9	0.0008843	0.0	0.0	0.0008878	0.0008794	0.0008843
P0	0.0001170	0.0	0.0	0.0001176	0.0001162	0.0001170
P1	0.0000067	0.0	0.0	0.0000065	0.0000069	0.0000067
P2	0.0000018	0.0	0.0	0.0000017	0.0000019	0.0000018
A1	0.0000108	0.0	0.0	0.0000108	0.0000107	0.0000108
P	0.0000052	0.0000102	0.0000237	0.0000053	0.0000051	0.0000052
S	0.0000010	0.0000081	0.0000312	0.0000010	0.0000011	0.0000010
Cl	0.0000003	0.0000003	0.0	0.0000003	0.0000003	0.0000003
Ca	0.0000021	0.0000021	0.0	0.0000021	0.0000021	0.0000021
Co	0.0000014	0.0000014	0.0000007	0.0000008	0.0000023	0.0000014

TABLE 9.1 (contd)

Isotope	Outer Core Average 0-20	Outer Core Average 20-20.44	Axial Blanket (OC) 20.44-31	Reflector Iron Block (OC) 31-36	Outer Core Pu Fuel 0-20
C	0.0015216	0.0000430	0.0000547	0.0005929	0.0006277
O	0.0157793	0.0088366	0.0088298	0.0	0.0142449
Na	0.0087748	0.0093153	0.0092655	0.0	0.0091654
Si	0.0001667	0.0001699	0.0002019	0.0001167	0.0001635
Al	0.0000043	0.0000029	0.0000029	0.0	0.0000046
Mn	0.0002382	0.0002670	0.0003450	0.0006745	0.0002379
Cr	0.0028267	0.0031948	0.0041058	0.0019593	0.0027889
Fe	0.0146052	0.0113725	0.0146096	0.0761394	0.0123834
Ni	0.0012475	0.0013673	0.0017579	0.0007929	0.0012336
Cu	0.0000315	0.0000360	0.0000410	0.0000276	0.0000312
Mo	0.0001351	0.0000232	0.0000297	0.0000139	0.0002990
U4	0.0000088	0.0000073	0.0	0.0	0.0
U5	0.0009128	0.0007587	0.0000179	0.0	0.0000142
U6	0.0000042	0.0000035	0.0	0.0	0.0
U8	0.0068164	0.0082076	0.0081643	0.0	0.0064867
P8	0.0000003	0.0	0.0	0.0	0.0000006
P9	0.0004706	0.0	0.0	0.0	0.0011175
P0	0.0000623	0.0	0.0	0.0	0.0001479
P1	0.0000038	0.0	0.0	0.0	0.0000089
P2	0.0000010	0.0	0.0	0.0	0.0000024
A1	0.0000058	0.0	0.0	0.0	0.0000138
P	0.0000052	0.0000074	0.0000102	0.0000234	0.0000051
S	0.0000014	0.0000039	0.0000065	0.0000314	0.0000012
Cl	0.0000041	0.0000003	0.0000003	0.0	0.0000018
Ca	0.0000013	0.0000021	0.0000021	0.0	0.0000018
Co	0.0000022	0.0000022	0.0000021	0.0000015	0.0000018

TABLE 9.1 (contd)

Isotope	Axial Blanket (OC) Pu Fuel 20-31	Reflector Iron Block (OC) Pu Fuel 31-36	Outer Core (OC) Pu Fuel 0-20	Outer Core Single Pu 0-20	Outer Core U Fuel 0-20	Outer Core U Fuel 20-20.44
C	0.0000531	0.0005928	0.0023103	0.0000332	0.0021684	0.0000343
O	0.0088211	0.0	0.0156589	0.0137451	0.0168662	0.0088277
Na	0.0092557	0.0	0.0087864	0.0092992	0.0084761	0.0093001
Si	0.0001926	0.0001164	0.0001819	0.0001570	0.0001688	0.0001532
Al	0.0000029	0.0	0.0000060	0.0000041	0.0000041	0.0000029
Mn	0.0003419	0.0006746	0.0002649	0.0002283	0.0002381	0.0002119
Cr	0.0041646	0.0019583	0.0031388	0.0026652	0.0028492	0.0024835
Fe	0.0147953	0.0761507	0.0110838	0.0128424	0.0161911	0.0088611
Ni	0.0017661	0.0007907	0.0014237	0.0011664	0.0012555	0.0010753
Cu	0.0000443	0.0000273	0.0000364	0.0000293	0.0000317	0.0000298
Mo	0.0000347	0.0000137	0.0004688	0.0002390	0.0000158	0.0000147
U4	0.0	0.0	0.0	0.0	0.0000152	0.0000125
U5	0.0000179	0.0	0.0000183	0.0000127	0.0015647	0.0012962
U6	0.0	0.0	0.0	0.0	0.0000073	0.0000060
U8	0.0081562	0.0	0.0083531	0.0058272	0.0070436	0.0082305
P8	0.0	0.0	0.0000010	0.0000005	0.0	0.0
P9	0.0	0.0	0.0017747	0.0008852	0.0	0.0
P0	0.0	0.0	0.0002348	0.0001171	0.0	0.0
P1	0.0	0.0	0.0000141	0.0000071	0.0	0.0
P2	0.0	0.0	0.0000039	0.0000019	0.0	0.0
A1	0.0	0.0	0.0000218	0.0000110	0.0	0.0
P	0.0000102	0.0000234	0.0000047	0.0000053	0.0000053	0.0000053
S	0.0000081	0.0000314	0.0000016	0.0000010	0.0000016	0.0000013
Cl	0.0000003	0.0	0.0000062	0.0000003	0.0000058	0.0000003
Ca	0.0000021	0.0	0.0000010	0.0000021	0.0000010	0.0000021
Co	0.0000018	0.0000011	0.0000045	0.0000008	0.0000026	0.0000026

TABLE 9.1 (contd)

Isotope	Axial Blanket (OC) Pu Fuel 20.44-31	Reflector Iron Block (OC) U Fuel 31-36	Outer Core Single U (OCUS) 0-20	Outer Core Single U (OCUS) 20-20.44	Outer Core Double U (OCUD) 0-20	Outer Core Double U (OCUD) 20-20.44
C	0.0000557	0.0005919	0.0021064	0.0000340	0.0022637	0.0000349
O	0.0088209	0.0	0.0171001	0.0088278	0.0165071	0.0088277
Na	0.0092567	0.0	0.0083664	0.0092904	0.0086446	0.0093153
Si	0.0002084	0.0001167	0.0001684	0.0001481	0.0001694	0.0001610
Al	0.0000029	0.0	0.0000043	0.0000029	0.0000038	0.0000028
Mn	0.0003466	0.0006733	0.0002412	0.0002105	0.0002333	0.0002142
Cr	0.0040559	0.0019566	0.0028882	0.0024577	0.0027894	0.0025231
Fe	0.0144494	0.0759994	0.0177817	0.0087816	0.0137475	0.0089833
Ni	0.0017489	0.0007932	0.0012690	0.0010564	0.0012347	0.0011044
Cu	0.0000385	0.0000279	0.0000302	0.0000281	0.0000340	0.0000325
Mo	0.0000260	0.0000140	0.0000147	0.0000133	0.0000175	0.0000167
U4	0.0	0.0	0.0000109	0.0000082	0.0000217	0.0000192
U5	0.0000179	0.0	0.0011314	0.0008546	0.0022303	0.0019746
U6	0.0	0.0	0.0000052	0.0000039	0.0000104	0.0000092
U8	0.0081560	0.0	0.0073446	0.0082050	0.0065814	0.0082698
P8	0.0	0.0	0.0	0.0	0.0	0.0
P9	0.0	0.0	0.0	0.0	0.0	0.0
P0	0.0	0.0	0.0	0.0	0.0	0.0
P1	0.0	0.0	0.0	0.0	0.0	0.0
P2	0.0	0.0	0.0	0.0	0.0	0.0
A1	0.0	0.0	0.0	0.0	0.0	0.0
P	0.0000102	0.0000233	0.0000054	0.0000054	0.0000051	0.0000052
S	0.0000054	0.0000314	0.0000015	0.0000011	0.0000019	0.0000015
Cl	0.0000003	0.0	0.0000056	0.0000003	0.0000061	0.0000003
Ca	0.0000021	0.0	0.0000010	0.0000021	0.0000010	0.0000021
Co	0.0000023	0.0000017	0.0000010	0.0000010	0.0000050	0.0000050

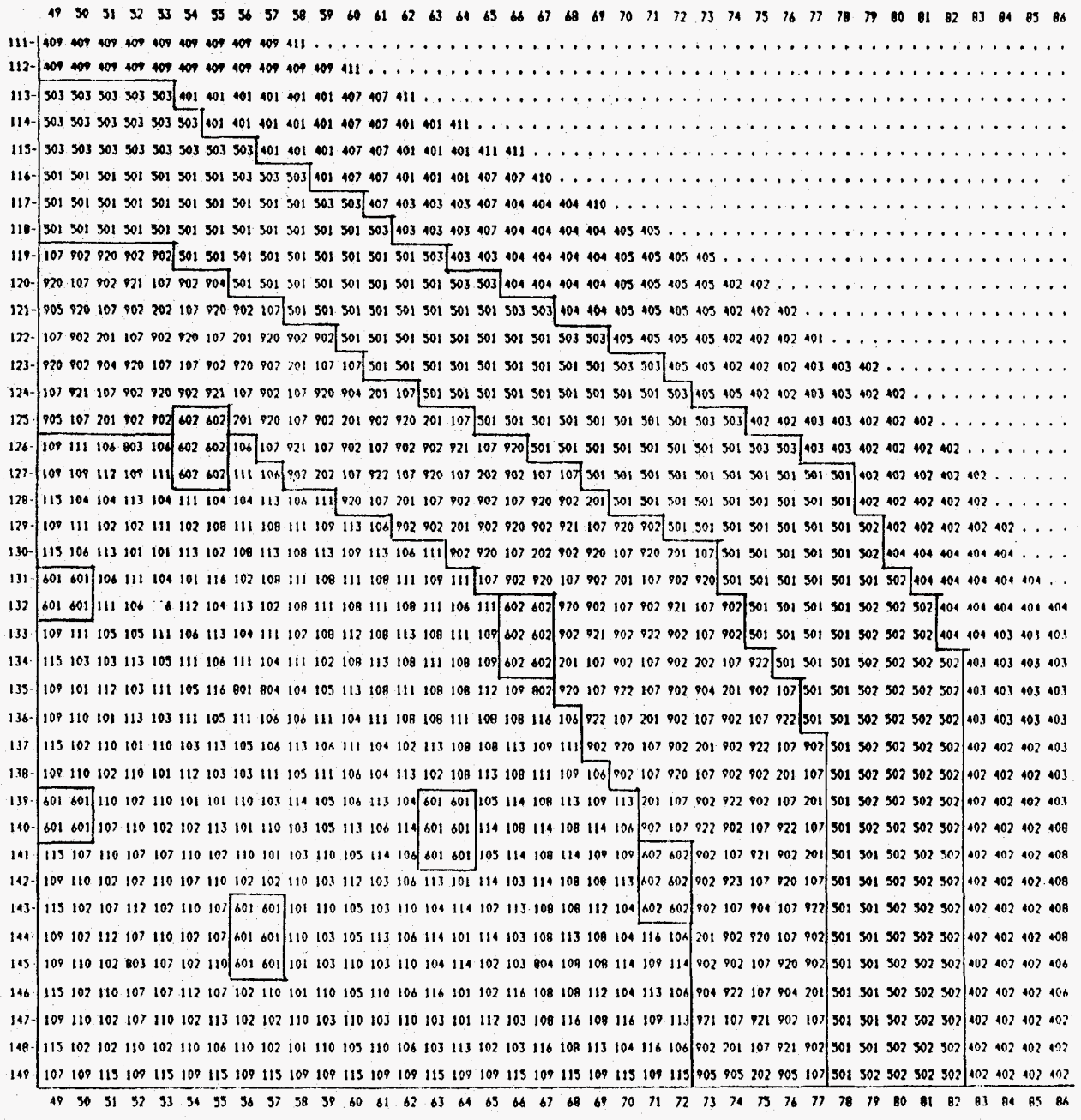

Fig. 9.1 The xyz Calculation Model for ZPPR-19B

10. CALCULATED K-EFFECTIVES, DELAYED NEUTRON PARAMETERS AND ^{241}PU DECAY COEFFICIENT FOR ZPPR-19A AND ZPPR-19B (G. L. Grasseschi and P. J. Collins)

10.1 k-effectives

Calculations for ZPPR-19A and ZPPR-19B were made with xyz models using finite-difference diffusion (FDDT), nodal diffusion (NDT) and nodal transport (NTT). The calculation models are given in Sections 8 and 9 of this report. Mesh sizes, node spacings and treatment of mismatch in uranium and plutonium fuel column lengths were consistent with those used for ZPPR-18.

Six group data were used for calculations of control rods in ZPPR-19B. Data were collapsed for each generic cell type using fluxes from a 21 group xyz diffusion calculation. Pseudo-absorption (buckling) terms for use in xy calculations were calculated from core/axial blanket leakages from a 6 group xyz diffusion calculation.

The calculated k-effectives (not C/E results) for the different models of ZPPR-19 are given in Table 10.1. A number of different calculations were made for ZPPR-19B because of requirements of calculating control rod worths (subcritical reference with shim rods withdrawn), reaction rates (critical reference with shim rods inserted) and for performing group collapse and buckling generation (generic master compositions). These provide a collection of the effects of different modeling approximations which are given in Table 10.2.

The errors due to modeling approximations are quite similar to those found for ZPPR-18 (ANL-ZPR-489, p. 45). Transport and diffusion mesh effects are larger in ZPPR-19A than in 19B due to the inserted control rods. The error due to six group condensation (0.0012) is less in 19B than in 18A (0.0021). The results in Table 10.2 also show the separability of corrections. For example, transport and mesh-size corrections are the same to 0.0001 Δk whether calculated with 6 groups or with 21 groups.

Experimental excess reactivities and operational data for ZPPR-19 are given in Tables 10.3 and 10.4. To derive an experimental value for k-effective, the data have been adjusted to a temperature of 293K (used in generating the cross section libraries). For comparison, the subcritical references have been adjusted to the interface gap and ^{241}Pu decay of the critical references. The calculated β-effective values are used to convert measured values in cents to Δk units. Note that the uncertainties shown are due to the operational measurements alone. The total uncertainty is typically 0.05% Δk but strongly correlated between the ZPPR-18 and ZPPR-19 cores since the majority of the fuel is common to the assemblies.

The criticality predictions for ZPPR-19, shown in Table 10.5, are similar to those for ZPPR-18. In particular, the nodal transport value for ZPPR-19B (0.9926) is close to that for 18A (0.9925) while cores 19A and 18B, with inserted control rods, have a higher k-effective by about 0.001.

10.2 Delayed Neutron Parameters

Delayed neutron parameters for ZPPR-19A and 19B were calculated with the xyz finite-difference diffusion models and 21 group data. The parameters are given in Tables 10.6 and 10.7. The increased β-effective for ZPPR-19B compared with ZPPR-18A (0.3786) is attributed to the additional ^{235}U which was added. The higher β-effective in 19A compared to that for 19B is attributed to the effect of the inner control rod bank which moves fluxes towards the outer core.

10.3 Plutonium Decay Coefficient for ZPPR-19

The ^{241}Pu decay coefficient for ZPPR-19 was estimated from the worths of ^{241}Pu and ^{241}Am which were calculated for ZPPR-18A (ANL-ZPR-489, p. 43). The worths were adjusted by the interval between the references for 18A and 19B (0.288 years). The decay coefficient for ZPPR-19B was calculated to be -0.02143 ¢ day^{-1}. This estimate is adequate within the 10% (1σ) uncertainty.

TABLE 10.1. Calculated k-effectives for ZPPR-19

	Core	Reactor Loading[a]	Number of Groups	Geometry	Mesh	Calculation Method[b]	Streaming	Shim Rods[c]	k-effective[d]
1	ZPPR-19A	C	21	xyz	38x39x9	NDT	Y	N	0.991024
2		C	21	xyz	38x39x9	NTT	Y	N	0.993869
3		C	21	xyz	38x39x20	FDDT	Y	N	0.993295
4		S	21	xyz	38x39x20	FDDT	Y	N	0.992258
5	ZPPR-19B	C	21	xyz	38x39x9	NDT	Y	N	0.991393
6		C	21	xyz	38x39x9	NTT	Y	N	0.993437
7		C	21	xyz	38x39x20	FDDT	Y	N	0.992258
8		S	21	xyz	38x39x9	NDT	Y	N	0.990089
9		S	21	xyz	38x39x9	NTT	Y	N	0.992118
10		S	21	xyz	38x39x20	FDDT	Y	N	0.990953
11		C	21	xyz	38x39x9	NDT	Y	Y	0.990977
12		C	21	xyz	38x39x9	NTT	Y	Y	0.993028
13		C	21	xyz	38x39x20	FDDT	N	N	0.995732
14		C	21	xyz	38x39x20	FDDT[e]	Y	N	0.991954
15		C	6	xyz	38x39x9	NDT	Y	N	0.990157
16		C	6	xyz	38x39x9	NTT	Y	N	0.992066
17		C	6	xyz	38x39x20	FDDT[e]	Y	N	0.990741
18		C	6	xyz	38x39x20	FDDT	Y	N	0.991028
19		C	6	xy	38x39	FDDT	Y	N	0.990589

[a] C = critical reference, S = subcritical reference.
[b] NDT = nodal diffusion, NTT = nodal transport, FDDT = finite-difference diffusion.
[c] Shim rods if inserted (Y) are close to position during foil irradiations.
[d] Not C/E values.
[e] Model with generic drawer master compositions averaged, for group collapse and buckling generation.

TABLE 10.2 Calculation Modelling Effects for ZPPR-19

Correction	Core	Cases[a]	Δk
Transport	19A	1-2	+0.002845
	19B	5-6	+0.002044
	19B	15-16 (6 groups)	+0.001909
	19B	8-9 (subcritical)	+0.002029
FDDT Mesh	19A	1-3	-0.002271
	19B	5-7	-0.000865
	19B	15-18 (6 groups)	-0.000871
	19B	8-10 (subcritical)	-0.000864
Streaming	19B	7-13	-0.003474
Energy Groups	19B	5-15 (NDT)	-0.001236
	19B	6-16 (NTT)	+0.001371
	19B	7-18 (FDDT)	+0.001230
Bucklings	19B	18-19 (6 groups)	+0.000439
All Master Models	19B	7-14	+0.000304
	19B	17-18 (6 groups)	+0.000287

[a]Refer to Table 10.1.

TABLE 10.3. Experimental k-effective Values for ZPPR-19A

	Almost Critical Reference	Subcritical Reference
Date	1/8/88	1/8/88
Loading	6	4
Reactor Run Number	8	6
Temperature, K	301.4	300.8
Interface Gap, mil[a]	53.8	54.7
Measured Excess Reactivity, ¢	-0.43 ± 0.02	-24.0 ± 0.1
Adjustment to 293K, ¢[b]	+10.50 ± 0.92	+9.75 ± 0.86
Adjustment to 53.8 mil, ¢[c]	---	+0.08 ± 0.01
Adjustment to 1/8/88, ¢[d]	---	---
Adjusted Reactivity, ¢	+10.1 ± 0.9	-14.7 ± 0.9
Experimental K-effective[e]	1.000410 ± 0.000037	0.999403 ± 0.000037

[a]On a scale with arbitrary zero.
[b]Using measured temperature coefficient $-1.25 \pm 0.11¢\ K^{-1}$.
[c]Using measured gap coefficient $-0.09 \pm 0.01¢\ mil^{-1}$.
[d]Using calculated ^{241}Pu decay coefficient $-0.02143¢\ day^{-1}$.
[e]Using calculated β-effective 0.004062.

TABLE 10.4. Experimental k-effective Values for ZPPR-19B

	Almost Critical Reference	Subcritical Reference
Date	1/29/88	2/8/88
Loading	21	28
Reactor Run Number	18	25
Temperature, K	299.2	300.5
Interface Gap, mil[a]	54.5	54.9
Measured Excess Reactivity, ¢	13.0 ± 0.1	-27.4 ± 0.2
Adjustment to 293K, ¢	+7.75 ± 0.68	+9.38 ± 0.83
Adjustment to 54.5 mil, ¢[c]	---	+0.04 ± 0.004
Adjustment to 1/29/88, ¢[d]	---	+0.21 ± 0.02
Adjusted Reactivity, ¢	+20.8 ± 0.7	-17.8 ± 0.8
Experimental K-effective[e]	1.000804 ± 0.000027	0.999312 ± 0.000031

[a]On a scale with arbitrary zero.
[b]Using measured temperature coefficient -1.25 ± 0.11¢ K^{-1}. (ZPPR-18A)
[c]Using measured gap coefficient -0.09 ± 0.01¢ mil^{-1}. (ZPPR-18A)
[d]Using calculated ^{241}Pu decay coefficient -0.02143¢ day^{-1}.
[e]Using calculated β-effective 0.003866.

TABLE 10.5 Comparison of Criticality Predictions for ZPPR-19A

	Ratio Calculation/Experiment[a]			
	ZPPR-19A		ZPPR-19B	
Calculation Model[a]	Critical	Subcritcal	Critical	Subcritical
Finite-difference Diffusion	0.9929	0.9929	0.9915	0.9916
Nodal Diffusion	0.9906	----	0.9906	0.9907
Nodal Transport	0.9935	----	0.9926	0.9928

[a]Calculations using xyz models with 21 energy groups.

TABLE 10.6 Delayed Neutron Parameters for ZPPR-19A

Family	a_i	λ_i, s^{-1}	$\beta_i, \%$
1	0.02592	0.01291	0.01053
2	0.20180	0.03157	0.08196
3	0.18331	0.13080	0.07445
4	0.37430	0.33809	0.15203
5	0.16426	1.3798	0.06671
6	0.05041	3.8157	0.02048

β-effective 0.4062%
Prompt neutron lifetime 4.798 x 10^{-7}s

TABLE 10.7 Delayed Neutron Parameters for ZPPR-19B

Family	a_i	λ_i, s^{-1}	$\beta_i, \%$
1	0.02501	0.01293	0.00967
2	0.20238	0.03154	0.07823
3	0.18339	0.13239	0.07089
4	0.37061	0.34088	0.14326
5	0.16635	1.3771	0.06431
6	0.05226	3.8050	0.02020

β-effective 0.3866%
Prompt neutron lifetime 5.144 x 10^{-7}s

11. SODIUM REACTIVITY WORTH IN ZPPR-19B (R. W. Goin)

In ZPPR Assembly 19B, the reactivity effect of adding (or deleting) sodium was measured using the plate-column oscillator technique. In this measurement, a 66 cm long column of 1.27 cm wide sodium cans was oscillated from fully inserted to 63.5 cm withdrawn. The reactivity effect of the oscillation was determined using inverse kinetics and correlated with the sodium column position. A least-squares spline-fitting technique was used to obtain the reactivity effect at each cm of travel, after correcting for reactor drift.

The measurement was then repeated using void cans in place of the sodium column. The result of the void can inverse kinetics output was subtracted from the sodium can oscillation to leave only the reactivity effect of sodium.

This measurement was done in matrix locations 149-40, 149-49, 155-49 and 149-58. In 149-58, a 101.6 cm long column was oscillated, and its stroke was limited to 30.5 cm from the interface.

Details of the experiment are given in Table 11.1. The material weights for each location are given in Table 11.2.

The integral worths, and differential sodium void worths, were obtained at 1 cm intervals from the reactor interface. The results are given in Tables 11.3 and 11.4 and in Figs. 11.1 and 11.2.

The integral worths of the 66 cm colums were arbitrarily normalized to 0.0 cents at the outermost position of travel. This normalization does not affect the differential worths, but does bias the integral worths. The 101.6 cm column measurement was normalized to the measurement in 149-40 at 30 cm.

Note that the measured differential void worth is in reality the sum of the sodium removal worth at the interface end of the sodium column, and the sodium addition worth at the reflector end. Because sodium has a positive

worth above 40 cm, the differential void worths for the 66 cm long column are too high in the first ~ 10 cm from the interface.

Because matrix positions 149-40 and 149-58 are in symmetrically equivalent locations, the comparison of the 101.6 cm long column oscillation in 149-58 with the 66 cm column in 149-40 provides a measure of the worth of adding sodium at the reflector end of the 66 cm column as it is withdrawn. The result of subtracting the 101.6 cm column measurement (in location 149-58) is shown in Figure 11.3.

This measurement provides two corrections to the 66 cm sodium column measurements. First, by plotting the worth above 66 cm and the uncorrected sodium worth on the same curve, the non-zero offset correction is obtained which gives the best overlap. This correction is 0.0085 ¢ ± 0.0015 ¢, and accounts for sodium still having a non-zero positive worth (as shown in Figure 11.3) when it is withdrawn 650 mm.

The second correction is to the point-by-point integral worth. When the 66 cm column is moved from the interface to 1 mm back, sodium displaces void in the space 660 mm to 661 mm, etc. The integral sodium worths including both corrections are shown in Figure 11.3.

An attempt was made to extract a similar correction to the differential worth. The differential void worth shown in Figure 11.2 contains a number of irregularities, particularly in location 149-49. The source of the dips and peaks in the differential worth is not presently known.

The result of correcting for the end effect is shown for the location 149-40 data in Figure 11.4. While the magnitude of the correction may be uncertain, it is clear that the void reactivity coefficient has a smaller positive value near the interface than the measurements using 66 cm long sodium columns would indicate.

These corrections were only done for location 149-40 because it is symmetric with the long column measurement. But it does indicate that the

measured sodium voiding reactivity effect per unit mass of sodium has a substantial correction of about 29% at the interface.

The uncertainties presented for the integral column worths only represent statistical uncertainties; those presented for the differential worths were estimated by $\sqrt{2}$ times the statistical uncertainty of the integral worth.

TABLE 11.1 Details of Sodium Void Worth Measurements in ZPPR-19B

Location	Description	Drawer Master	Reactor Run No.	Loading No.	Date
149-40	Sodium	19-0-835	22	25	2/3/88
149-40	Void	19-0-836	23	26	2/4/88
149-49	Sodium	19-0-835	22	25	2/3/88
149-49	Void	19-0-836	23	26	2/4/88
155-49	Sodium	19-0-839	24	27	2/5/88
155-49	Void	19-0-840	23	26	2/4/88
149-58	Sodium	19-0-837	22	25	2/3/88
149-58	Void	19-0-838	23	26	2/4/88

TABLE 11.2. Details of Sodium Cans and Void Cans

		Sodium Cans				Void Cans
Axial Sequence	Length in.	Serial No.	Total Mass g	Can Mass g	Na Mass g	Can Mass g
			149-40			
1	6	106581	143.65	61.22	82.43	61.55
2	7	33672	167.51	70.84	96.67	70.94
3	7	12426	166.58	70.15	96.43	71.30
4	6	106151	144.24	61.70	82.54	61.90
			149-49			
1	6	106605	145.19	62.88	82.31	62.26
2	7	34022	168.25	70.74	97.51	70.76
3	7	12330	167.68	70.75	96.93	70.91
4	6	110779	143.04	60.13	82.91	61.32
			155-49			
1	6	105965	144.63	61.63	83.00	61.89
2	7	107991	167.99	70.57	97.42	70.50
3	7	33671	166.70	69.99	96.71	69.61
4	6	11059	146.05	62.89	83.16	62.29
			149-58			
1	8	23732	189.55	79.21	110.34	79.34
2	8	23726	191.95	80.39	111.56	80.28
3	4	04030	98.23	43.39	54.84	43.04
4	8	24213	190.05	79.21	110.84	79.25
5	8	24926	189.06	80.74	108.32	80.79
6	4	04771	98.15	43.64	54.51	43.66

TABLE 11.3 Integral Reactivity Worth, in Cents, of Axial Sodium Column, ZPPR 19B

Distance from Interface (mm)	149-40	149-49	149-58, 305 mm Stroke	155-49
2.31	-0.05594±0.00055	-0.06531±0.00053	-0.04718±0.00050	-0.06551±0.00042
10.00	-0.05159±0.00051	-0.06150±0.00049	-0.04477±0.00046	-0.06088±0.00039
20.00	-0.04682±0.00057	-0.05691±0.00055	-0.04177±0.00051	-0.05650±0.00044
30.00	-0.04300±0.00050	-0.05270±0.00048	-0.03891±0.00046	-0.05390±0.00038
40.00	-0.03934±0.00055	-0.04816±0.00053	-0.03583±0.00049	-0.05091±0.00042
50.00	-0.03547±0.00050	-0.04300±0.00049	-0.03241±0.00046	-0.04655±0.00039
60.00	-0.03152±0.00052	-0.03766±0.00051	-0.02872±0.00048	-0.04141±0.00040
70.00	-0.02785±0.00053	-0.03348±0.00052	-0.02502±0.00048	-0.03728±0.00041
80.00	-0.02449±0.00049	-0.03052±0.00047	-0.02134±0.00046	-0.03428±0.00038
90.00	-0.02124±0.00054	-0.02707±0.00052	-0.01795±0.00049	-0.03107±0.00042
100.00	-0.01796±0.00050	-0.02216±0.00049	-0.01501±0.00046	-0.02695±0.00039
110.00	-0.01466±0.00052	-0.01632±0.00050	-0.01240±0.00047	-0.02224±0.00040
120.00	-0.01125±0.00054	-0.01175±0.00052	-0.00967±0.00049	-0.01831±0.00041
130.00	-0.00772±0.00049	-0.00868±0.00047	-0.00675±0.00045	-0.01529±0.00037
140.00	-0.00409±0.00054	-0.00596±0.00051	-0.00396±0.00049	-0.01242±0.00041
150.00	-0.00041±0.00051	-0.00274±0.00048	-0.00151±0.00046	-0.00908±0.00039
160.00	0.00320±0.00051	0.00090±0.00048	0.00072±0.00047	-0.00546±0.00039
170.00	0.00602±0.00054	0.00446±0.00051	0.00332±0.00049	-0.00238±0.00041
180.00	0.00793±0.00049	0.00786±0.00046	0.00637±0.00045	0.00003±0.00037
190.00	0.00959±0.00053	0.01103±0.00051	0.00953±0.00049	0.00224±0.00041
200.00	0.01168±0.00051	0.01386±0.00049	0.01239±0.00047	0.00477±0.00039
210.00	0.01411±0.00050	0.01637±0.00048	0.01494±0.00046	0.00758±0.00039
220.00	0.01640±0.00053	0.01889±0.00051	0.01713±0.00049	0.01053±0.00041
230.00	0.01845±0.00048	0.02144±0.00046	0.01896±0.00045	0.01358±0.00037
240.00	0.02033±0.00053	0.02371±0.00051	0.02052±0.00049	0.01635±0.00041
250.00	0.02213±0.00051	0.02516±0.00049	0.02195±0.00047	0.01827±0.00040
260.00	0.02384±0.00050	0.02595±0.00047	0.02329±0.00047	0.01941±0.00038
270.00	0.02516±0.00053	0.02736±0.00051	0.02463±0.00049	0.02056±0.00042
280.00	0.02602±0.00049	0.02976±0.00046	0.02603±0.00046	0.02191±0.00038
290.00	0.02675±0.00052	0.03247±0.00050	0.02725±0.00052	0.02341±0.00041
300.00	0.02794±0.00052	0.03417±0.00050	0.02794±0.00052	0.02494±0.00040
310.00	0.02956±0.00049	0.03489±0.00047	---	0.02644±0.00038
320.00	0.03077±0.00053	0.03520±0.00051	---	0.02735±0.00042
330.00	0.03126±0.00049	0.03534±0.00047	---	0.02747±0.00038
340.00	0.03121±0.00052	0.03535±0.00050	---	0.02712±0.00040
350.00	0.03098±0.00052	0.03537±0.00050	---	0.02716±0.00040
360.00	0.03062±0.00049	0.03539±0.00047	---	0.02762±0.00038
370.00	0.03044±0.00053	0.03533±0.00051	---	0.02786±0.00041
380.00	0.03059±0.00049	0.03516±0.00047	---	---

TABLE 11.3 (Contd)

Distance from Interface (mm)	149-40	149-49	149-58, 305 mm Stroke	155-49
390.00	0.03083±0.00051	0.03490±0.00049	---	0.02694±0.00040
400.00	0.03043±0.00053	0.03462±0.00050	---	0.02648±0.00041
410.00	0.02935±0.00048	0.03433±0.00046	---	0.02623±0.00037
420.00	0.02835±0.00053	0.03343±0.00051	---	0.02591±0.00041
430.00	0.02793±0.00050	0.03153±0.00048	---	0.02535±0.00039
440.00	0.02786±0.00051	0.02909±0.00049	---	0.02454±0.00040
450.00	0.02727±0.00053	0.02788±0.00051	---	0.02351±0.00041
460.01	0.02606±0.00048	0.02812±0.00046	---	0.02227±0.00037
470.01	0.02443±0.00053	0.02828±0.00051	---	0.02104±0.00041
480.01	0.02252±0.00050	0.02710±0.00048	---	0.02005±0.00039
490.01	0.02043±0.00050	0.02470±0.00048	---	0.01914±0.00039
500.01	0.01872±0.00053	0.02175±0.00051	---	0.01752±0.00041
510.01	0.01749±0.00048	0.01837±0.00046	---	0.01506±0.00037
520.01	0.01629±0.00053	0.01518±0.00051	---	0.01251±0.00041
530.01	0.01464±0.00051	0.01288±0.00049	---	0.01072±0.00039
540.01	0.01261±0.00050	0.01137±0.00048	---	0.00963±0.00039
550.01	0.01071±0.00053	0.00969±0.00051	---	0.00874±0.00041
560.01	0.00904±0.00048	0.00762±0.00046	---	0.00791±0.00037
570.01	0.00757±0.00053	0.00555±0.00051	---	0.00706±0.00041
580.01	0.00622±0.00051	0.00400±0.00049	---	0.00607±0.00040
590.01	0.00496±0.00050	0.00297±0.00048	---	0.00493±0.00039
600.01	0.00390±0.00054	0.00212±0.00052	---	0.00375±0.00042
610.01	0.00305±0.00049	0.00134±0.00047	---	0.00257±0.00038
620.01	0.00230±0.00054	0.00070±0.00052	---	0.00156±0.00042
630.01	0.00143±0.00052	0.00025±0.00050	---	0.00099±0.00040
640.01	0.00046±0.00057	0.00000±0.00055	---	0.00082±0.00044
650.01	0.00000±0.00053	0.00000±0.00051	---	0.00000±0.00041

TABLE 11.4 Differential Reactivity Worth, in Cents per Kilogram of Axial Sodium Column, ZPPR 19B

Distance from Interface (mm)	149-40	149-49	149-58, 305 m	155-49
2.31	1.1123±0.0381	0.9415±0.0373	0.5883±0.0310	1.2412±0.0293
10.00	0.9719±0.0395	0.8841±0.0388	0.5669±0.0320	0.9776±0.0300
20.00	0.7892±0.0387	0.8093±0.0381	0.5391±0.0315	0.6347±0.0293
30.00	0.6568±0.0371	0.7781±0.0365	0.5327±0.0301	0.4279±0.0281
40.00	0.6944±0.0374	0.8934±0.0368	0.5984±0.0303	0.6789±0.0283
50.00	0.7318±0.0355	1.0087±0.0350	0.6641±0.0289	0.9298±0.0269
60.00	0.7043±0.0377	0.8858±0.0371	0.6828±0.0306	0.8642±0.0285
70.00	0.6473±0.0354	0.6554±0.0348	0.6804±0.0286	0.6556±0.0267
80.00	0.5990±0.0360	0.4997±0.0354	0.6659±0.0291	0.5035±0.0272
90.00	0.6013±0.0369	0.7707±0.0363	0.5834±0.0299	0.6745±0.0279
100.00	0.6036±0.0350	1.0418±0.0345	0.5010±0.0284	0.8455±0.0265
110.00	0.6181±0.0374	0.9798±0.0368	0.4883±0.0303	0.8094±0.0283
120.00	0.6404±0.0353	0.7039±0.0345	0.5206±0.0286	0.6403±0.0267
130.00	0.6620±0.0357	0.4535±0.0341	0.5463±0.0289	0.4887±0.0269
140.00	0.6733±0.0371	0.5469±0.0352	0.4835±0.0301	0.5721±0.0281
150.00	0.6847±0.0350	0.6404±0.0332	0.4208±0.0284	0.6555±0.0264
160.00	0.6022±0.0372	0.6698±0.0352	0.4363±0.0302	0.6295±0.0281
170.00	0.4363±0.0354	0.6423±0.0336	0.5215±0.0288	0.5058±0.0269
180.00	0.2705±0.0350	0.6147±0.0335	0.6068±0.0288	0.3821±0.0268
190.00	0.3449±0.0368	0.5517±0.0352	0.5537±0.0302	0.4369±0.0282
200.00	0.4220±0.0346	0.4883±0.0330	0.4992±0.0284	0.4936±0.0265
210.00	0.4444±0.0365	0.4578±0.0349	0.4386±0.0301	0.5337±0.0279
220.00	0.3998±0.0353	0.4677±0.0337	0.3705±0.0291	0.5534±0.0269
230.00	0.3552±0.0348	0.4775±0.0333	0.3024±0.0288	0.5731±0.0267
240.00	0.3393±0.0369	0.3435±0.0354	0.2762±0.0305	0.4323±0.0283
250.00	0.3263±0.0345	0.1949±0.0330	0.2543±0.0291	0.2756±0.0264
260.00	0.2867±0.0363	0.1688±0.0347	0.2436±0.0308	0.1911±0.0278
270.00	0.2017±0.0356	0.3517±0.0340	0.2521±0.0306	0.2302±0.0272
280.00	0.1167±0.0346	0.5346±0.0332	0.2608±0.0331	0.2692±0.0266
290.00	0.1752±0.0369	0.4090±0.0354	0.1766±0.0372	0.2790±0.0283
300.00	0.2634±0.0345	0.2199±0.0330	0.0734±0.0372	0.2828±0.0264
310.00	0.2881±0.0360	0.0757±0.0344	---	0.2425±0.0276
320.00	0.1567±0.0358	0.0420±0.0343	---	0.0943±0.0274
330.00	0.0254±0.0345	0.0084±0.0331	---	-0.0540±0.0264
340.00	-0.0276±0.0369	0.0015±0.0354	---	-0.0314±0.0283
350.00	-0.0544±0.0346	0.0036±0.0332	---	0.0481±0.0264
360.00	-0.0631±0.0356	0.0007±0.0342	---	0.0911±0.0272
370.00	-0.0032±0.0361	-0.0211±0.0346	---	-0.0042±0.0276

TABLE 11.4 (Contd)

Distance from Interface (mm)	149-40	149-49	149-58, 305 m	155-49
380.00	0.0565±0.0345	-0.0428±0.0331	---	-0.0996±0.0264
390.00	-0.0094±0.0369	-0.0505±0.0354	---	-0.1046±0.0282
400.00	-0.1373±0.0346	-0.0513±0.0333	---	-0.0652±0.0265
410.00	-0.2352±0.0353	-0.0754±0.0339	---	-0.0366±0.0270
420.00	-0.1313±0.0363	-0.2571±0.0349	---	-0.0814±0.0278
430.00	-0.0275±0.0345	-0.4388±0.0330	---	-0.1261±0.0264
440.00	-0.0516±0.0368	-0.3560±0.0353	---	-0.1687±0.0281
450.00	-0.1650±0.0348	-0.0889±0.0334	---	-0.2095±0.0266
460.01	-0.2753±0.0351	0.1529±0.0336	---	-0.2463±0.0269
470.01	-0.3267±0.0366	-0.0942±0.0351	---	-0.2046±0.0280
480.01	-0.3782±0.0345	-0.3413±0.0330	---	-0.1629±0.0264
490.01	-0.3587±0.0366	-0.5032±0.0352	---	-0.2212±0.0281
500.01	-0.2708±0.0350	-0.5832±0.0336	---	-0.3760±0.0269
510.01	-0.1831±0.0348	-0.6631±0.0335	---	-0.5308±0.0267
520.01	-0.2616±0.0368	-0.5053±0.0353	---	-0.3995±0.0281
530.01	-0.3453±0.0345	-0.3401±0.0330	---	-0.2591±0.0264
540.01	-0.3737±0.0364	-0.2756±0.0349	---	-0.1732±0.0279
550.01	-0.3285±0.0353	-0.3450±0.0339	---	-0.1595±0.0270
560.01	-0.2833±0.0348	-0.4146±0.0333	---	-0.1459±0.0267
570.01	-0.2607±0.0369	-0.3342±0.0354	---	-0.1696±0.0283
580.01	-0.2409±0.0346	-0.2352±0.0333	---	-0.1980±0.0266
590.01	-0.2146±0.0365	-0.1653±0.0349	---	-0.2164±0.0280
600.01	-0.1762±0.0358	-0.1494±0.0344	---	-0.2163±0.0276
610.01	-0.1379±0.0361	-0.1336±0.0347	---	-0.2162±0.0277
620.01	-0.1493±0.0382	-0.1013±0.0366	---	-0.1474±0.0294
630.01	-0.1724±0.0405	-0.0650±0.0388	---	-0.0622±0.0311
640.01	-0.1525±0.0415	-0.0247±0.0398	---	-0.0533±0.0319
650.01	-0.0160±0.0415	0.0264±0.0398	---	-0.2509±0.0319

TABLE 11.5 Integral Reactivity Worth, in Cents, of Sodium Column in 149-40

Distance from Interface (mm)	Corrected, Adjusted	Worth Above 660 mm	Uncorrected
2.31	-0.03868±0.00183	0.00876±0.00072	-0.05594±0.00055
10.00	-0.03627±0.00180	0.00682±0.00067	-0.05159±0.00051
20.00	-0.03327±0.00185	0.00505±0.00075	-0.04682±0.00057
30.00	-0.03041±0.00179	0.00409±0.00066	-0.04300±0.00050
40.00	-0.02733±0.00183	0.00351±0.00072	-0.03934±0.00055
50.00	-0.02391±0.00179	0.00306±0.00066	-0.03547±0.00050
60.00	-0.02022±0.00181	0.00280±0.00068	-0.03152±0.00052
70.00	-0.01652±0.00182	0.00283±0.00070	-0.02785±0.00053
80.00	-0.01284±0.00179	0.00315±0.00065	-0.02449±0.00049
90.00	-0.00945±0.00182	0.00329±0.00071	-0.02124±0.00054
100.00	-0.00651±0.00179	0.00295±0.00066	-0.01796±0.00050
110.00	-0.00390±0.00181	0.00226±0.00068	-0.01466±0.00052
120.00	-0.00117±0.00182	0.00158±0.00071	-0.01125±0.00054
130.00	0.00175±0.00179	0.00097±0.00065	-0.00772±0.00049
140.00	0.00454±0.00182	0.00013±0.00071	-0.00409±0.00054
150.00	0.00699±0.00180	-0.00110±0.00067	-0.00041±0.00051
160.00	0.00922±0.00180	-0.00248±0.00067	0.00320±0.00051
170.00	0.01182±0.00182	-0.00270±0.00071	0.00602±0.00054
180.00	0.01487±0.00179	-0.00156±0.00065	0.00793±0.00049
190.00	0.01803±0.00182	-0.00006±0.00070	0.00959±0.00053
200.00	0.02089±0.00180	0.00071±0.00067	0.01168±0.00051
210.00	0.02344±0.00179	0.00083±0.00066	0.01411±0.00050
220.00	0.02563±0.00182	0.00073±0.00070	0.01640±0.00053
230.00	0.02746±0.00178	0.00051±0.00064	0.01845±0.00048
240.00	0.02902±0.00182	0.00019±0.00070	0.02033±0.00053
250.00	0.03045±0.00180	-0.00018±0.00068	0.02213±0.00051
260.00	0.03179±0.00180	-0.00055±0.00067	0.02384±0.00050
270.00	0.03313±0.00182	-0.00053±0.00071	0.02516±0.00053
280.00	0.03453±0.00179	0.00001±0.00065	0.02602±0.00049
290.00	0.03575±0.00182	0.00050±0.00072	0.02675±0.00052
300.00	0.03644±0.00182	0.00000±0.00072	0.02794±0.00052
310.00	0.03806±0.00166	---	0.02956±0.00049
320.00	0.03927±0.00168	---	0.03077±0.00053
330.00	0.03976±0.00166	---	0.03126±0.00049
340.00	0.03971±0.00167	---	0.03121±0.00052
350.00	0.03948±0.00167	---	0.03098±0.00052
360.00	0.03912±0.00166	---	0.03062±0.00049
370.00	0.03894±0.00168	---	0.03044±0.00053
380.00	0.03909±0.00166	---	0.03059±0.00049
390.00	0.03933±0.00167	---	0.03083±0.00051
400.00	0.03893±0.00168	---	0.03043±0.00053
410.00	0.03785±0.00166	---	0.02935±0.00048
420.00	0.03685±0.00168	---	0.02835±0.00053
430.00	0.03642±0.00167	---	0.02792±0.00050
440.00	0.03636±0.00167	---	0.02786±0.00051
450.00	0.03577±0.00168	---	0.02727±0.00053
460.01	0.03456±0.00166	---	0.02606±0.00048
470.01	0.03293±0.00168	---	0.02443±0.00053
480.01	0.03102±0.00167	---	0.02252±0.00050
490.01	0.02893±0.00167	---	0.02043±0.00050

TABLE 11.5 (Contd)

Distance from Interface (mm)	Corrected, Adjusted	Worth Above 660 mm.	Uncorrected
500.01	0.02722±0.00168	---	0.01872±0.00053
510.01	0.02599±0.00166	---	0.01749±0.00048
520.01	0.02480±0.00168	---	0.01630±0.00053
530.01	0.02314±0.00167	---	0.01464±0.00051
540.01	0.02111±0.00167	---	0.01261±0.00050
550.01	0.01921±0.00168	---	0.01071±0.00053
560.01	0.01754±0.00166	---	0.00904±0.00048
570.01	0.01607±0.00168	---	0.00757±0.00053
580.01	0.01472±0.00167	---	0.00622±0.00051
590.01	0.01346±0.00167	---	0.00496±0.00050
600.01	0.01240±0.00168	---	0.00390±0.00054
610.01	0.01155±0.00166	---	0.00305±0.00049
620.01	0.01080±0.00168	---	0.00230±0.00054
630.01	0.00993±0.00167	---	0.00143±0.00052
640.01	0.00896±0.00169	---	0.00046±0.00057
650.01	0.00850±0.00168	---	0.00000±0.00053

TABLE 11.6 Differential Reactivity Worth, in Cents per Kilogram, of Sodium Column in 149-40

Distance from Interface (mm)	Corrected, Adjusted	Worth Above 660 mm	Uncorrected
2.31	-0.5883±0.0621	-0.5241±0.0491	-1.1124±0.0381
10.00	-0.5669±0.0643	-0.4050±0.0508	-0.9719±0.0395
20.00	-0.5391±0.0631	-0.2500±0.0499	-0.7891±0.0387
30.00	-0.5327±0.0604	-0.1241±0.0477	-0.6568±0.0371
40.00	-0.5984±0.0610	-0.0960±0.0482	-0.6944±0.0374
50.00	-0.6641±0.0579	-0.0678±0.0458	-0.7319±0.0355
60.00	-0.6828±0.0614	-0.0215±0.0485	-0.7043±0.0377
70.00	-0.6804±0.0576	0.0331±0.0455	-0.6473±0.0354
80.00	-0.6659±0.0586	0.0668±0.0463	-0.5991±0.0360
90.00	-0.5834±0.0601	-0.0179±0.0475	-0.6013±0.0369
100.00	-0.5010±0.0571	-0.1025±0.0451	-0.6035±0.0350
110.00	-0.4883±0.0610	-0.1298±0.0482	-0.6181±0.0374
120.00	-0.5206±0.0576	-0.1198±0.0455	-0.6404±0.0353
130.00	-0.5463±0.0582	-0.1158±0.0460	-0.6621±0.0357
140.00	-0.4835±0.0604	-0.1898±0.0477	-0.6733±0.0371
150.00	-0.4208±0.0571	-0.2638±0.0451	-0.6846±0.0350
160.00	-0.4363±0.0606	-0.1659±0.0479	-0.6022±0.0372
170.00	-0.5215±0.0577	0.0852±0.0456	-0.4363±0.0354
180.00	-0.6068±0.0573	0.3363±0.0454	-0.2705±0.0350
190.00	-0.5537±0.0602	0.2088±0.0476	-0.3449±0.0368
200.00	-0.4992±0.0565	0.0772±0.0447	-0.4220±0.0346
210.00	-0.4386±0.0597	-0.0058±0.0473	-0.4444±0.0365
220.00	-0.3705±0.0577	-0.0293±0.0457	-0.3998±0.0353
230.00	-0.3024±0.0570	-0.0528±0.0451	-0.3552±0.0348
240.00	-0.2762±0.0605	-0.0631±0.0479	-0.3393±0.0369
250.00	-0.2543±0.0568	-0.0720±0.0451	-0.3263±0.0345
260.00	-0.2436±0.0599	-0.0431±0.0476	-0.2867±0.0363
270.00	-0.2521±0.0589	0.0504±0.0469	-0.2017±0.0356
280.00	-0.2608±0.0591	0.1441±0.0479	-0.1167±0.0346
290.00	-0.1766±0.0641	0.0013±0.0524	-0.1753±0.0369
300.00	-0.0734±0.0613	-0.1900±0.0507	-0.2634±0.0345
310.00	-0.2881±0.0360	---	-0.2881±0.0360
320.00	-0.1567±0.0358	---	-0.1567±0.0358
330.00	-0.0253±0.0345	---	-0.0253±0.0345
340.00	0.0277±0.0369	---	0.0277±0.0369
350.00	0.0544±0.0346	---	0.0544±0.0346
360.00	0.0630±0.0356	---	0.0630±0.0356
370.00	0.0032±0.0361	---	0.0032±0.0361
380.00	-0.0565±0.0345	---	-0.0565±0.0345
390.00	0.0093±0.0369	---	0.0093±0.0369
400.00	0.1373±0.0346	---	0.1373±0.0346
410.00	0.2352±0.0353	---	0.2352±0.0353
420.00	0.1314±0.0363	---	0.1314±0.0363
430.00	0.0275±0.0345	---	0.0275±0.0345
440.00	0.0517±0.0368	---	0.0517±0.0368
450.00	0.1650±0.0348	---	0.1650±0.0348
460.01	0.2754±0.0351	---	0.2754±0.0351
470.01	0.3267±0.0366	---	0.3267±0.0366
480.01	0.3780±0.0345	---	0.3780±0.0345
490.01	0.3586±0.0366	---	0.3586±0.0366

TABLE 11.6 (Contd)

Distance from Interface (mm)	Corrected, Adjusted	Worth Above 660 mm	Uncorrected
500.01	0.2709±0.0350	---	0.2709±0.0350
510.01	0.1831±0.0348	---	0.1831±0.0348
520.01	0.2617±0.0368	---	0.2617±0.0368
530.01	0.3454±0.0345	---	0.3454±0.0345
540.01	0.3737±0.0364	---	0.3737±0.0364
550.01	0.3285±0.0353	---	0.3285±0.0353
560.01	0.2833±0.0348	---	0.2833±0.0348
570.01	0.2607±0.0369	---	0.2607±0.0369
580.01	0.2408±0.0346	---	0.2408±0.0346
590.01	0.2146±0.0365	---	0.2146±0.0365
600.01	0.1763±0.0358	---	0.1763±0.0358
610.01	0.1379±0.0361	---	0.1379±0.0361
620.01	0.1493±0.0382	---	0.1493±0.0382
630.01	0.1724±0.0405	---	0.1724±0.0405
640.01	0.1526±0.0415	---	0.1526±0.0415
650.01	0.0160±0.0415	---	0.0160±0.0415

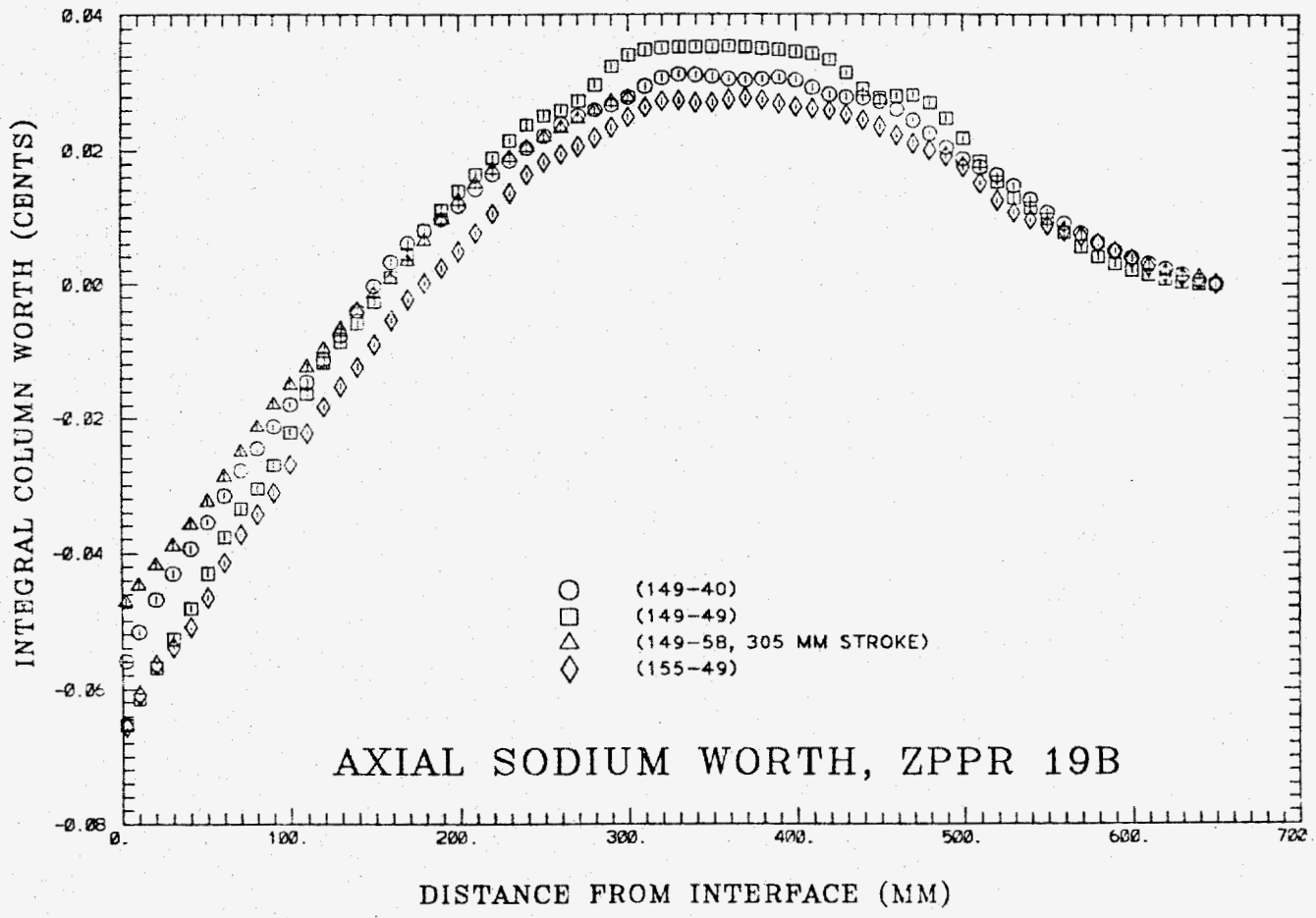

Fig. 11.1 Integral Sodium Worth Axial Profiles in ZPPR-19B

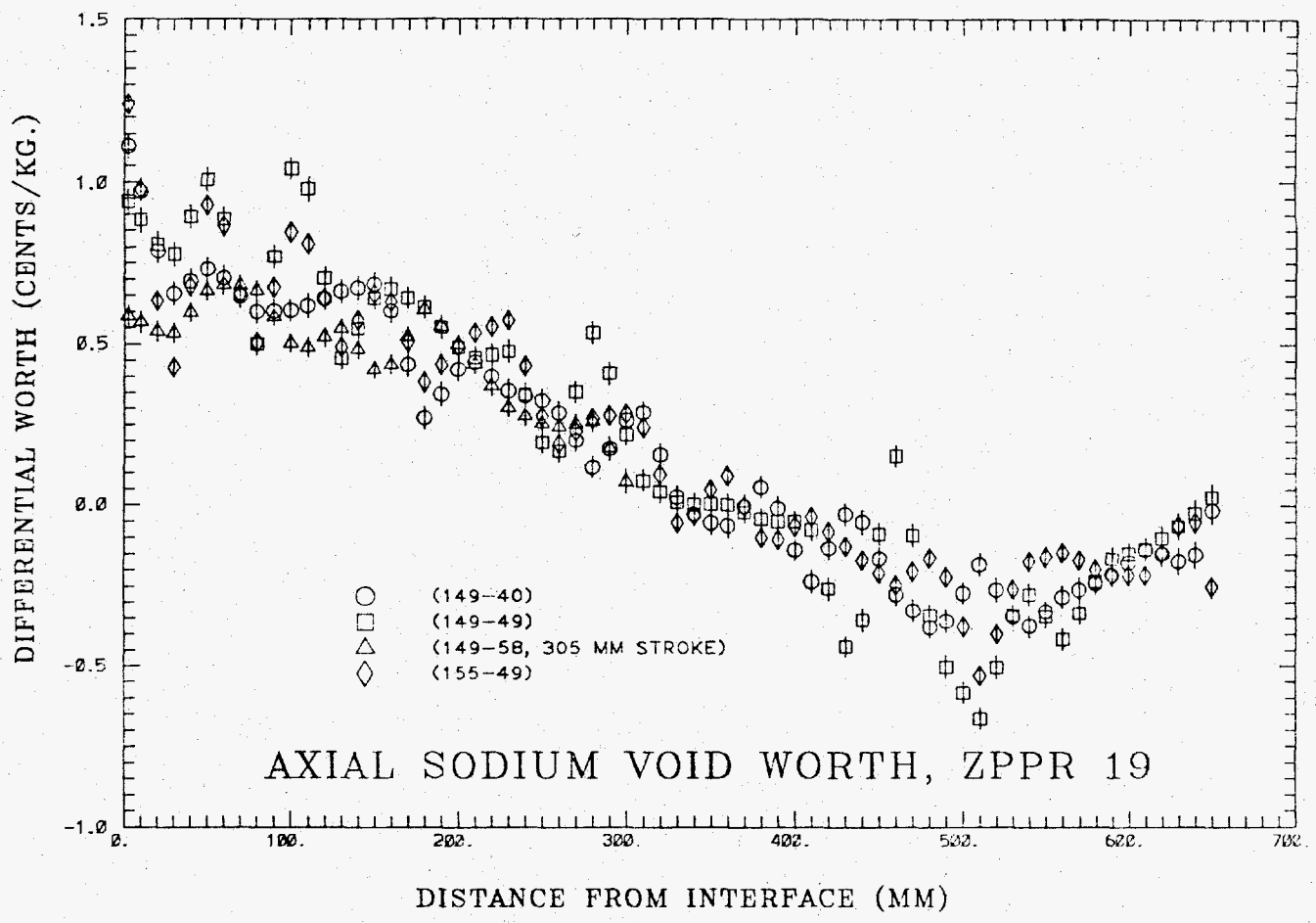

Fig. 11.2 Differential Sodium Worth Axial Profiles in ZPPR-19B

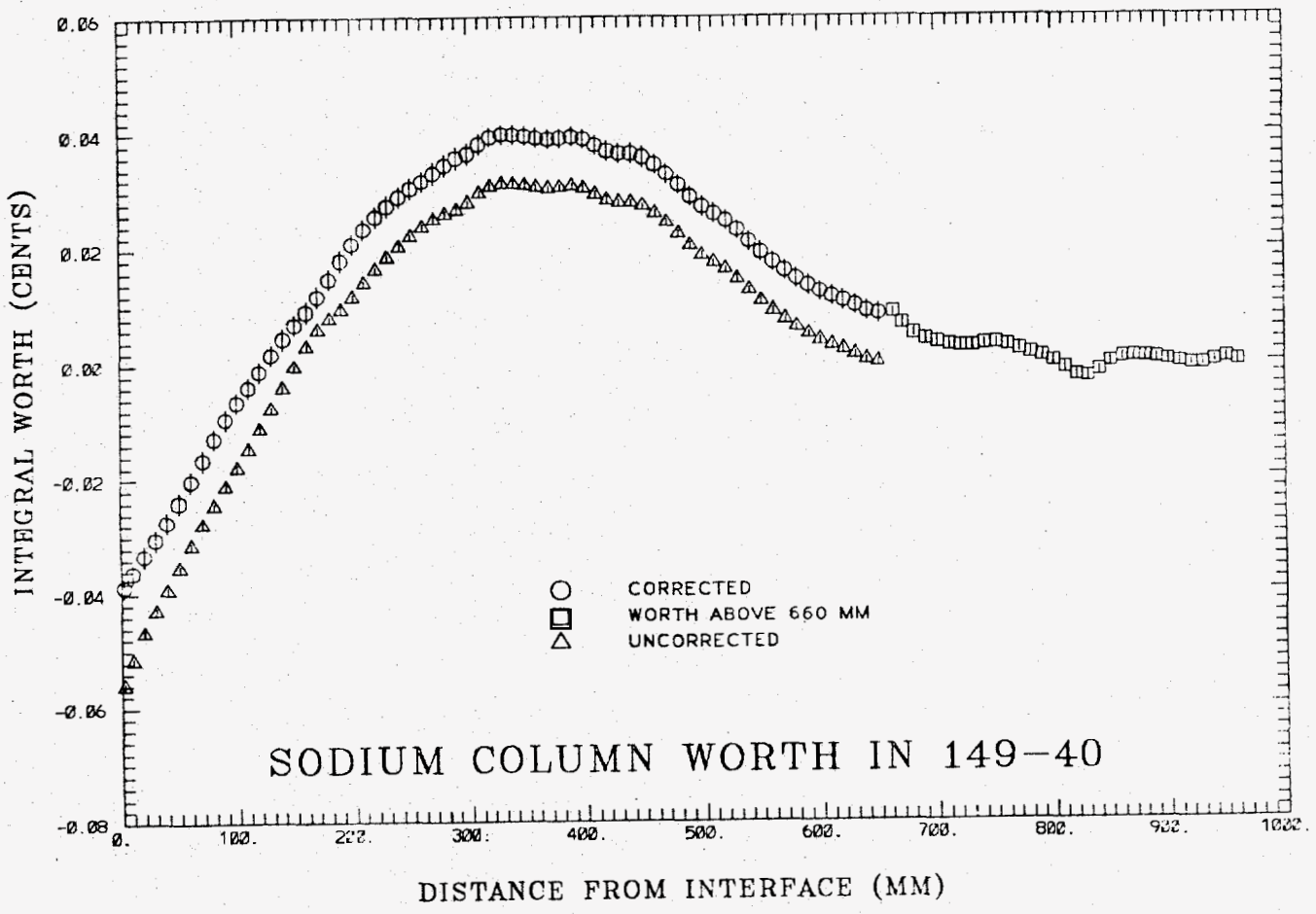

Fig. 11.3 Comparison of Corrected and Uncorrected Integral Sodium Worth Axial Profiles in ZPPR-19B

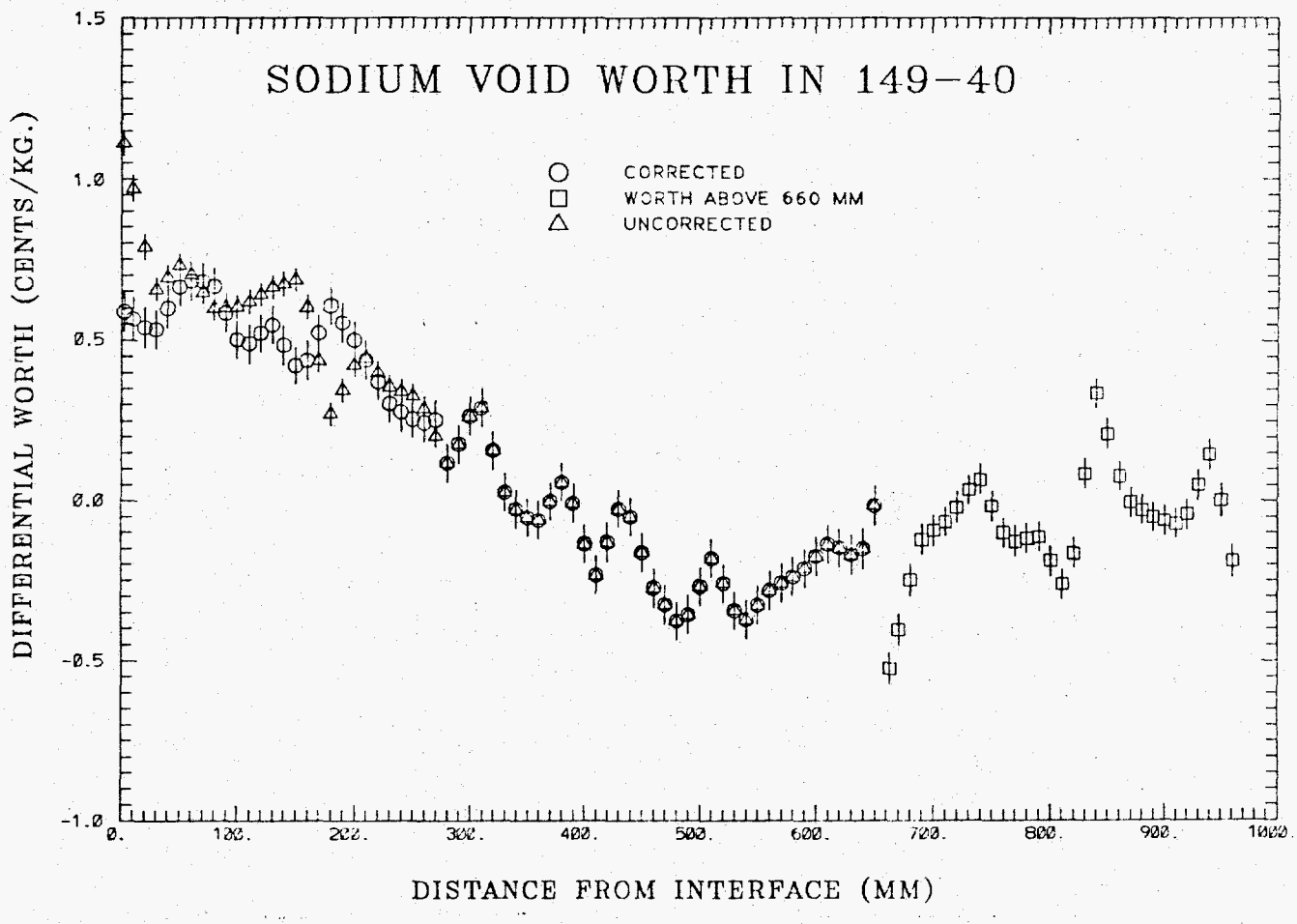

Fig. 11.4 Comparison of Corrected and Uncorrected Differential Sodium Worth Axial Profiles in ZPPR-19B

12. ON THE MODELING OF THE URANIUM FUEL IN ZPPR-18

(G. L. Grasseschi and P. J. Collins)

The axial half-height of the uranium fuel in ZPPR-18 was 1.11 cm greater than that of the plutonium fuel. To avoid using a fine node spacing in the nodal transport calculations, the xyz model for ZPPR-18 smeared the extra 1.11 cm of uranium over the first 5.08 cm node of the axial blanket (ANL-ZPR-489, p. 13). In order to test the effect of this approximation, two calculations were made using finite-difference diffusion theory (FDDT) with mesh boundaries 1.11 and 5.08 cm above the axial blanket boundary. The first FDDT calculation smeared the uranium through 5.08 cm as in the nodal calculation. The second FDDT calculation retained the uranium in the 1.11 cm region only. In the plutonium sector, the 1.11 cm region was assigned only axial blanket material.

The differences between the FDDT model and the reference model appear to be negligible for most parameters calculated in ZPPR-18:

i k-effective differed by 0.000001

ii Reaction rate distributions near the midplane and at 28 cm from the midplane differed by less than 0.1%

iii The axial reaction rate distributions in the outer core at the x-axis differed by less than 0.1%, including values in the axial blanket. (Only a very small difference in blanket compositions existed in these locations due to different piece lengths between the first 1.11 cm and the entire blanket thickness.)

Differences for a ^{235}U fission distribution in location 121-49, along the y-axis in the uranium sector, are shown in Table 12.1. A difference of 0.9% is indicated at the inner edge of the blanket which changes the source of neutrons into the blanket and reflection of neutron back to the core. Some uncertainty in these results may exist due to mesh-size effects.

Calculated control rod worths for outer ring rods at the boundary of the uranium sector may be affected by a few tenths of a percent by the simplified modeling. In ZPPR-19B the axial distribution in the outer core

of mixed uranium and plutonium drawers will also be changed but these effects will be masked by experimental statistics and other modeling approximations. Note that, on a finer scale, all ZPPR models have smeared fuel over the full lengths of the fuel column and neglected effects of the end clads.

TABLE 12.1 Comparison of ^{235}U Fission Rates in the Uranium Sector

Zone	Mesh Boundary, Distance from Midplane, cm	Mesh-average Fission Rate[a] Refined Model	Reference Model	Ratio
Core	36.80			
		11.831	11.833	0.9998
	41.49			
		10.400	10.409	0.9991
	46.18			
		9.0000	9.0204	0.9973
	50.88			
		8.2819	8.3003	0.9978
Uranium	51.99			
		8.6056	8.5258	1.0094
Axial Blanket	55.96			
		7.8712	7.8181	1.0068
	60.53			
		6.9980	6.9634	1.0050
	65.10			
		6.1448	6.1229	1.0036
	69.67			
		5.4114	5.3973	1.0060
	74.24			
		4.9089	4.8988	1.0021
Reflector	78.82			

[a]Abritrary units, both calculations normalized to the same reactor power.